

CHARACTERIZATION OF COAL-DERIVED LIQUIDS  
USING MASS SPECTROMETRY

By

GIL JAY GREENWOOD

Bachelor of Science

Oklahoma State University

Stillwater, Oklahoma

1971

Submitted to the faculty of the Graduate College  
of the Oklahoma State University  
in partial fulfillment of the requirements  
for the Degree of  
DOCTOR OF PHILOSOPHY  
May, 1977

Thesis  
1977D  
G 816c  
cop. 2



CHARACTERIZATION OF COAL-DERIVED LIQUIDS  
USING MASS SPECTROMETRY

Thesis Approved:

*Stuart E. Schupp*

Thesis Adviser

*Billy L. Gynes*

*Horacio Amotola*

*Walter R. Rude*

*Norman D. Durbin*

Dean of the Graduate College

997266

## ACKNOWLEDGMENTS

I extend appreciation and thanks to my adviser, Dr. Stuart Scheppele for his guidance, professional evaluations and friendship throughout the course of graduate school. I also wish to thank the members of my committee Dr. B. L. Crynes, Dr. H. A. Mottola, and Dr. N. Purdie. I wish to acknowledge not only the professional help but also the fellowship of Wayne Adkins, Heinze Hall, Richard Gruhlkey and Floyd Vulgamore. A special thanks to Norman Perreira for the time and assistance given to me throughout this study. I am also grateful to my fellow graduate students for information, assistance, and stimulating discussions.

My appreciation is also extended for financial support during my graduate studies to Oklahoma State University and the Energy Research and Development Administration. I also wish to thank Dow Chemical Company and Continental Oil Company for partial support.

To my wife, Meg and daughter Kristy, go my deepest gratitude for their understanding, encouragement, and love during my graduate career.

## TABLE OF CONTENTS

Chapter	Page
I. ADAPTATION OF THE TECHNIQUE OF FIELD IONIZATION TO OSU CEC 21-110B MASS SPECTROMETER . . . . .	1
Experimental Modifications . . . . .	5
Instrument Operation . . . . .	12
Results and Discussion . . . . .	16
II. SEPARATION AND ANALYSIS OF FEEDSTOCK AND UPGRADED ANTHRACENE OIL. . . . .	38
Results and Discussion . . . . .	38
Gas Chromatography in Conjunction With Electron Impact Mass Spectrometry . . . . .	42
High-Resolution Electron-Impact and Low- and Medium-Resolution Field-Ionization Mass Spectrometry . . . . .	65
Experimental . . . . .	120
A. Separation Procedures . . . . .	120
Acid Fraction - Apparatus and Materials. . .	120
Acid Fraction - Procedure. . . . .	122
Base Fraction - Apparatus and Materials. . .	122
Base Fraction - Procedure. . . . .	123
Neutral-Nitrogen Fraction - Apparatus and Materials. . . . .	124
Neutral-Nitrogen Fraction - Procedure. . . .	124
B. Instrumental. . . . .	125
REFERENCES CITED . . . . .	127
APPENDIX A - PLANS FOR COMBINED FI/EI ION SOURCE EQUIPMENT . . . .	132
APPENDIX B - HIGH RESOLUTION 70-eV MASS SPECTRAL DATA FOR ANTHRACENE OIL AND ITS FOUR UPGRADED REACTOR SAMPLES . . . . .	146
APPENDIX C - COMPUTER PROGRAM. . . . .	160

LIST OF TABLES

Table	Page
I. FI Relative Ion Abundances for Reactor Sample 1 . . . . .	23
II. Mole Percent Composition of Various Doublets in the Hydrocarbon + Ether Fractions of Anthracene Oil and Four Upgraded Samples . . . . .	25
III. FI- and EI-Relative Cross Sections (RCS). . . . .	29
IV. Weight Percents of Components in Test Mixture #1. . . . .	35
V. Raw Anthracene Oil Properties . . . . .	39
VI. Results From Separation and Elemental Analysis of Anthracene Oil and Four of its Hydrotreated Products. . . . .	41
VII. Weight Percent of Major Hydrocarbons and Ethers in Feedstock and Upgraded Anthracene Oil . . . . .	53
VIII. Comparison of Relative Abundances for Major Ions in the Mass Spectrum of Known Isomers With Molecular Weight 132 and the Mass Spectra of Peak 10 From the GC/MS of Anthracene Oil Feedstock Hydrocarbons + Ethers and Related Reactor Samples . . . . .	60
IX. Comparison of Relative Abundances for Major Ions in the Mass Spectrum of 1- and 2-Methylnaphthalenes With Peaks 16 and 17 in the GC/MS Data . . . . .	62
X. GC/MS Data for Peak Number 22 . . . . .	64
XI. Carbon Number Distribution for Hydrocarbons From Feedstock Anthracene Oil. . . . .	69
XII. Carbon Number Distribution for Ethers From Feedstock Anthracene Oil. . . . .	70
XIII. Carbon Number Distribution for Hydrocarbons From Reactor Sample 1. . . . .	71
XIV. Carbon Number Distribution for Ethers From Reactor Sample 1. . . . .	72

LIST OF TABLES (Continued)

Table	Page
XV. Carbon Number Distribution for Hydrocarbons From Reactor Sample 2. . . . .	73
XVI. Carbon Number Distribution for Ethers From Reactor Sample 2. . . . .	74
XVII. Carbon Number Distribution for Hydrocarbons From Reactor Sample 3. . . . .	75
XVIII. Carbon Number Distribution for Ethers From Reactor Sample 3. . . . .	76
XIX. Carbon Number Distribution for Hydrocarbons From Reactor Sample 4. . . . .	77
XX. Carbon Number Distribution for Ethers From Reactor Sample 4. . . . .	78
XXI. Carbon Number Distribution for the Oxygen-Containing Acids From Anthracene Oil . . . . .	87
XXII. Weight Percents of Oxygen-Containing Acids in Feedstock and Upgraded Anthracene Oil . . . . .	89
XXIII. Weight Percent of Phenols Identified in Acid Fraction From Feedstock and Hydrotreated Anthracene Oil. . . . .	91
XXIV. Carbon Number Distribution for the Nitrogen-Containing Acids and Major Neutral Nitrogens . . . . .	93
XXV. Compositional Data for the Nitrogen-Containing Compounds in the Acidic and Neutral-Nitrogen Fractions Isolated From Feedstock and Hydrotreated Anthracene Oil. . . . .	95
XXVI. Carbon Number Distribution for Bases From Anthracene Oil Feedstock . . . . .	97
XXVII. Carbon Number Distribution for Bases From Reactor Sample 1. . . . .	103
XXVIII. Carbon Number Distribution for Bases From Reactor Sample 2. . . . .	104
XXIX. Carbon Number Distribution for Bases From Reactor Sample 3. . . . .	105
XXX. Carbon Number Distribution for Bases From Reactor Sample 4. . . . .	106

LIST OF TABLES (Continued)

Table	Page
XXXI. Moles of Bases at Selected Molecular Weights Found in Feedstock and Hydrotreated Anthracene Oil . . . . .	107
XXXII. Moles of Bases for the Empirical Formulas Containing C <sub>13</sub> Found in Feedstock and Hydrotreated Anthracene Oil. . .	117
XXXIII. High-Resolution Data for Major Ions From the Feedstock and Reactor Sample Hydrocarbon plus Ether Fractions . .	147
XXXIV. High-Resolution Data for Major Ions From the Feedstock and Reactor Sample Acid Fractions . . . . .	151
XXXV. High-Resolution Data for Major Ions From the Feedstock and Reactor Sample Base Fractions . . . . .	155
XXXVI. High-Resolution Data for Major Ions From Feedstock and Reactor Sample Neutral-Nitrogen Fractions . . . . .	159



## LIST OF FIGURES

Figure	Page
1. Potential Energy of an H Atom in the Vicinity of a Metal Surface: (a) In the Absence of an Electric Field; (b) In the Presence of an Electric Field. . . . .	2
2. Dual Field Ionization/Electron Impact Ion Source (Exploded View) . . . . .	6
3. Schematic for Field Ionization Cathode Power Supply . . . . .	8
4. Emitter-Cathode Potential versus Cathode Power Supply Meter Reading . . . . .	9
5. Emitter Vacuum Lock and Gate Valve Assembly . . . . .	10
6. Emitter Probe Micrometer Assembly . . . . .	11
7. Enlarged Side View of the Razor Blade Emitter and Exit Slit .	14
8. Effect of Emitter-Cathode Distance on Relative Abundance for Acetone $m/e$ 58. . . . .	17
9. Peak Intensity as a Function of Emitter Potential for Acetone $m/e$ 58. . . . .	19
10. Effect of Blade Angle on Sensitivity for Acetone $m/e$ 58 . . .	21
11. Method of Separation. . . . .	40
12. 70-eV Electron-Impact Mass Spectrum of the Hydrocarbon + Ether Fraction From the Anthracene Oil Feedstock. . . . .	43
13. Gas Chromatogram of Feedstock Anthracene Oil Hydrocarbons plus Ether Fraction . . . . .	45
14. UV Spectrum of Phenanthrene . . . . .	47
15. UV Spectrum of Anthracene . . . . .	48
16. UV Spectrum of Anthracene:Phenanthrene Mixture. . . . .	49
17. UV Spectrum of Unknown Hydrocarbon with Mass 178. . . . .	50

LIST OF FIGURES (Continued)

Figure	Page
18. Gas Chromatogram of Reactor Sample 2 Hydrocarbon plus Ether Fraction. . . . .	52
19. Hydrogenation/Hydrogenolysis Scheme for Quinoline and Isoquinoline. . . . .	110
20. Possible Isomeric Structures Consistent With the Empirical Formula C <sub>13</sub> H <sub>9</sub> N. . . . .	115
21. Possible Hydrogenation/Hydrogenolysis Scheme for Benzo[f]-quinoline and Phenanthridine. . . . .	116
22. Recycling Chromatographic Column. . . . .	121
23. Vacuum Seal Block . . . . .	133
24. Goddard Valve to Ion-Source Housing Flange. . . . .	134
25. Vacuum Seal Spacers and FI Control Rod Spacer . . . . .	135
26. Micrometer Holder . . . . .	136
27. Emitter Rod Handle and Micrometer Table . . . . .	137
28. Razor Blade Vise and Vacuum Seal Cap. . . . .	138
29. Ion-Source Magnet Offsets . . . . .	139
30. Cathode and Repellers . . . . .	140
31. Cathode Insulator (Top) . . . . .	141
32. Cathode Insulator (Bottom). . . . .	142
33. Blade Alignment Jig . . . . .	143
34. Emitter and Emitter Control Rod Alignment Bench . . . . .	144
35. Emitter and Emitter Control Rod Alignment Bench . . . . .	145

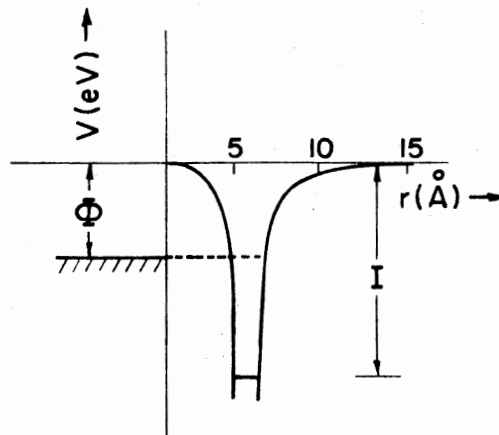
## CHAPTER I

### ADAPTATION OF THE TECHNIQUE OF FIELD IONIZATION

#### TO OSU CEC 21-110B MASS SPECTROMETER

Electric fields on the order of  $10^7$ - $10^8$  V cm<sup>-1</sup> can be used for the production of positive ions.<sup>1</sup> The ions so produced can be mass analyzed using well established methods of mass spectrometry.<sup>2</sup> This combined technique is referred to as field ionization (FI) mass spectrometry (FI/MS). The high electric fields are generated by the use of sharp metal points,<sup>1,2a,b</sup> thin metal wires,<sup>3</sup> or sharp metal edges.<sup>3c</sup> The formation of ions is explained by quantum mechanical tunnelling of electrons from the atom or molecule to the surface of the metal emitter.<sup>2,4</sup> Figure 1 illustrates the process for a hydrogen atom. In the absence of an electric field the free hydrogen atom can be considered as a potential energy trough in which the valence electron is trapped at a depth equal to its ionization energy, I (Figure 1a). The work function of the metal is represented by the letter  $\phi$ . In the presence of a high electric potential ( $V_F$ ) the potential energy diagram of the atom is deformed (Figure 1b) so that the electron of the H atom is faced in one direction with a potential barrier of finite height and width. If this barrier is small enough there is a finite probability that the electron can pass through (tunnel) the barrier and become separated from the proton. When this occurs a positive ion is formed. The formation of an ion by an electric field

(a)



(b)

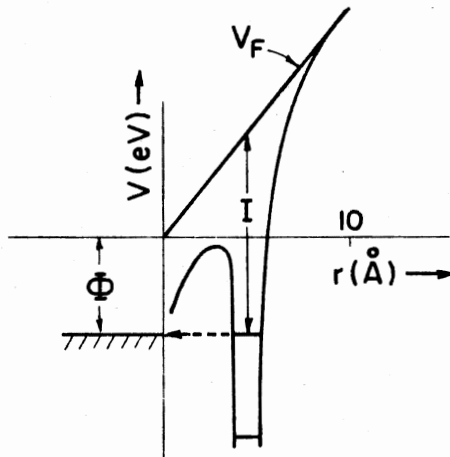


Figure 1. Potential Energy of an H Atom in the Vicinity of a Metal Surface:  
 (a) In the Absence of an Electric Field; (b) In the Presence of an Electric Field

depends upon:

- 1) the ionization potential of the atom or molecule.
- 2) the work function of the metal.
- 3) the critical distance between the molecule or atom and the metal surface.
- 4) the field strength being applied.

Equation I-1 expresses the field strength ( $F_o$ ) between the anode (emitter) and the cathode as a function of the total voltage applied

$$F_o = \frac{V_o}{r_o} K \quad (I-1)$$

to the emitter ( $V_o$ ), the radius of curvature of the emitter ( $r_o$ ) and an emitter geometry constant ( $K$ ).<sup>5</sup> The functional dependence of the emitter constant on both the distance between the emitter and cathode ( $R$ ) and upon  $r_o$  is given by equations I-2, I-3, and I-4 for tips, wires,

$$k_{\text{tip}} = \frac{2}{\ln(2R/r_o)} \quad (I-2)$$

$$k_{\text{wire}} = \frac{1}{\ln(R/r_o)} \quad (I-3)$$

$$k_{\text{blade}} = \frac{1}{\sqrt{2} (R/r_o)^{1/2}} \quad (I-4)$$

and edges (blades), respectively.<sup>5</sup> Substitution of typical values of  $10^4$  V,  $10^{-4}$  cm and 0.5 cm for  $V_o$ ,  $r_o$ , and  $R$ , respectively in equations I-2, I-3, and I-4 yields values of 21.8 MV/cm, 11.8 MV/cm, and 1.0 MV/cm for the field strength between a tip, wire, or blade emitter, respectively and the cathode. Therefore to attain a field strength from a blade equivalent to that obtained from a wire the values of  $r_o$

or R for the former must be either ca.  $10^2$  or 10 times smaller than the corresponding values of the latter.

Both the magnitude of and the fluctuations in the FI ion current as a function of time are of prime importance if FI/MS is to be used for quantitative analysis. It has been demonstrated that statistical fluctuations in the ion current could be caused by microstructure changes in the emitter as a function of time.<sup>2c,6</sup> The fluctuation in ion current  $di/i$  can be expressed as a function of the transmission, T (Equation I-5). The transmission is defined as ratio of collected ion

$$di/i \approx \frac{1}{\sqrt{T}} \quad (\text{I-5})$$

current (i) to total number of ions produced (for a given source pressure). For a given mass spectrometer the transmission can be directly related to the effective area of the emitter (A). Therefore, fluctuation in ion current is inversely proportional to the square root of the emitter area (Equation I-6).<sup>2c,6</sup>

$$di/i \approx \frac{1}{\sqrt{A}} \quad (\text{I-6})$$

Tip emitters should give the largest fluctuation in ion currents because of their small area. Attempts have been made to circumvent this problem by replacing the tip emitter with a multipoint emitter.<sup>7</sup> However, these sources can only be operated in the FI mode. This deficiency makes such an FI ion source design impractical in our applications which require routine FI and electron impact (EI) capability. Wire emitters were not considered for our initial work because of their fragile nature and the necessity for involved conditioning.<sup>8</sup> These

disadvantages were assumed to initially offset their advantages of good field strength and low ion current fluctuations. Blade emitters were chosen for our initial work because they were both commercially available and not as susceptible to rupture as are thin wires. The large surface area associated with blade emitters will minimize ion-current fluctuations (Equation I-6). However, as discussed above, the blade emitter requires an anode-cathode distance of 0.25 mm to 0.50 mm to produce a field strength sufficient to ionize most organic molecules ( $> 10^7$  V/cm).<sup>9</sup> Previous work demonstrated that this type of emitter was well suited for application of FI/MS to analysis of organic mixtures.<sup>10</sup>

#### Experimental Modifications

The combined field-ionization/electron-impact (FI/EI) ion source is shown in Figure 2. This design required modification of the electron-impact ion source for the CEC 21-110B mass spectrometer as follows.<sup>11</sup>

To permit entry of an FI emitter a 1/4 inch hole was added to the back face of the ion-source block by removal of the stainless-steel plug. A new set of repellers were machined with hemispherical openings (see Figure 30, Appendix A) to provide for 1) horizontal and vertical alignment of the emitter, 2) thermal contact for heating of the emitter, and 3) electrical contact to float the emitter at a potential determined by the ion-accelerator chassis. A counter electrode (cathode) with a 60° beveled slit was fabricated. The cathode is insulated between two insulators machined from Mikroy 750 (Ceramic Fabricators, Inc.). This assembly replaced the previous

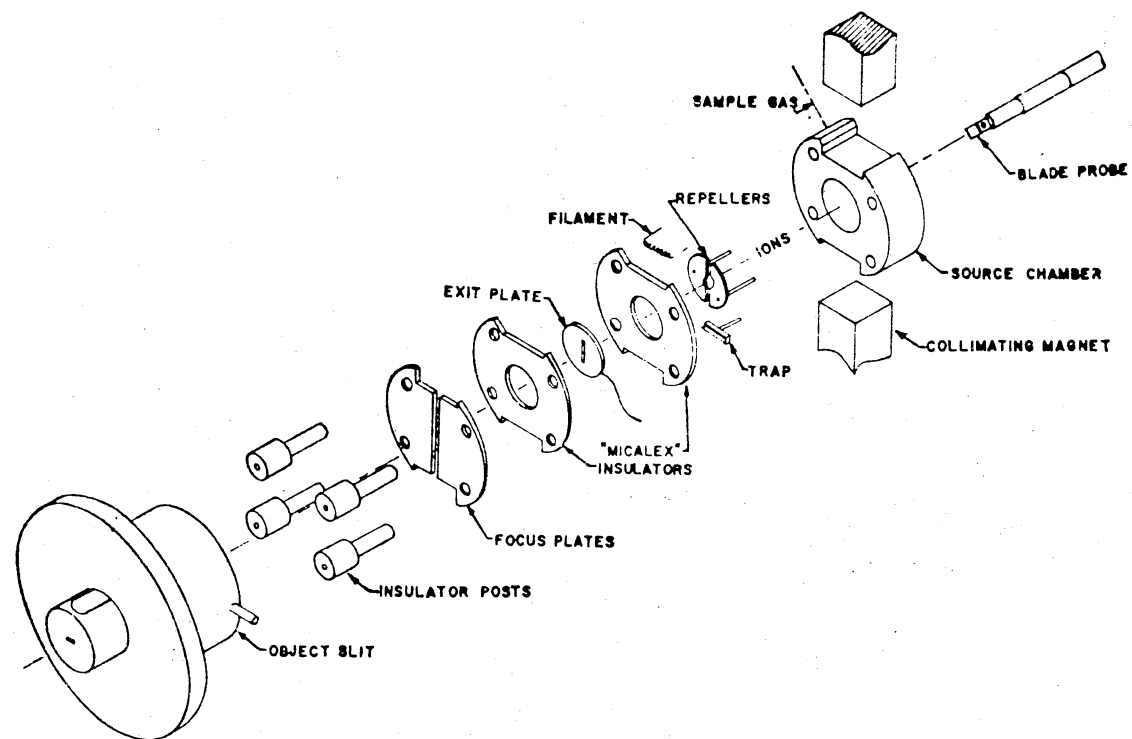


Figure 2. Dual Field Ionization/Electron Impact Ion Source (Exploded View). (From E. M. Chait, T. W. Shannon, J. W. Amy, and F. W. McLafferty, Anal. Chem., 40, 835 (1968))



ion-source exit plate as defined in the CEC 21-110B manual. The collimating magnet was offset to the side (see Figure 29, Appendix A) to permit passage of the FI probe into the ion source.

The ion accelerator chassis was modified by replacing the 5-megohm resistor in the ion-accelerating potential divider network with a 2-megohm ten-pin voltage divider in series with a 3-megohm resistor. This modification permits the application of lower voltages to the focus electrodes in the ion source for operation in the FI mode as compared with the EI mode. A 0-15 kV power supply (Figure 3) was constructed to provide a negative voltage to the cathode. The positive terminal of the power supply is referenced to the block-potential output of the ion-accelerator chassis. This design minimizes the effect of fluctuation in the voltage output of either of the power supplies on the potential difference between the anode and cathode. The microammeter in the cathode power supply (see Figure 3) is used to monitor the anode-cathode potential with respect to instrument common. The relationship between microamps of current flowing in the power supply and the anode-cathode potential is shown in Figure 4.

To permit rapid exchange of emitters a vacuum lock and gate valve assembly (Goddard Industries, Inc.) was fabricated for the ion source bell housing, see Figure 5. Construction of an emitter-probe-micrometer assembly (see Figure 6) affords horizontal adjustment (along the z axis) of the emitter by increments as small as 0.01 mm and rotational adjustment (in the xy plane) by readable increments of 1°. Finally, a bench was constructed to provide for more rapid exchange and alignment of emitters and adjustments to the FI emitter probe. Machine drawings for the bench are provided in Appendix A.

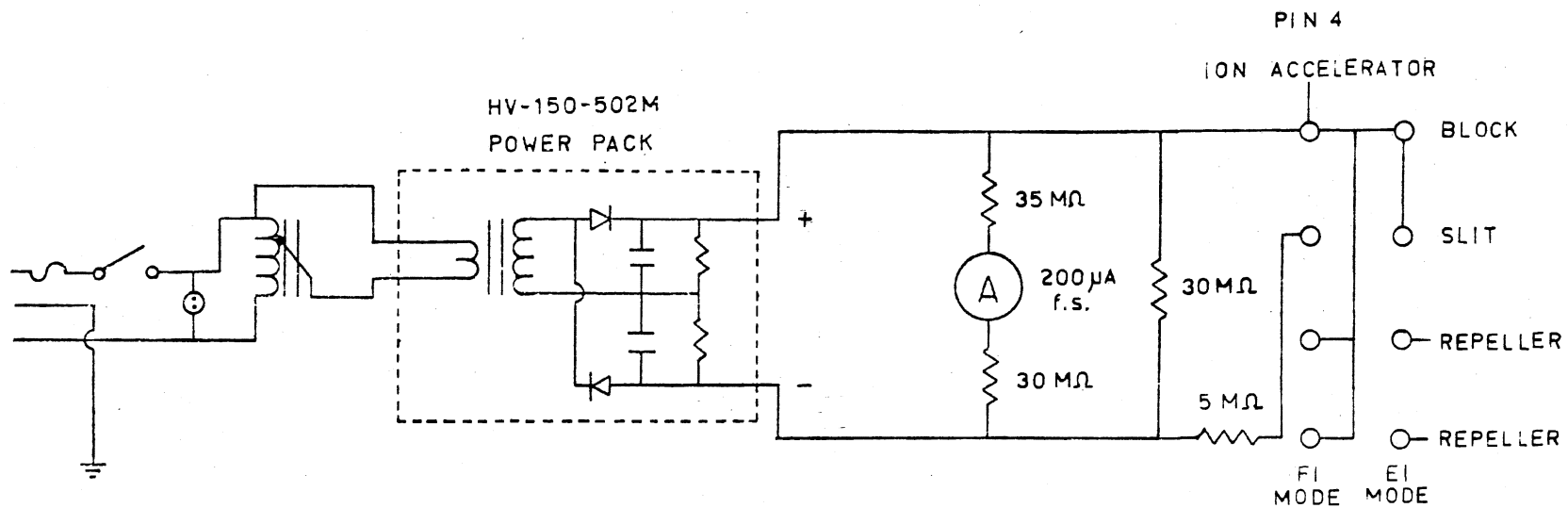


Figure 3. Schematic for Field Ionization Cathode Power Supply

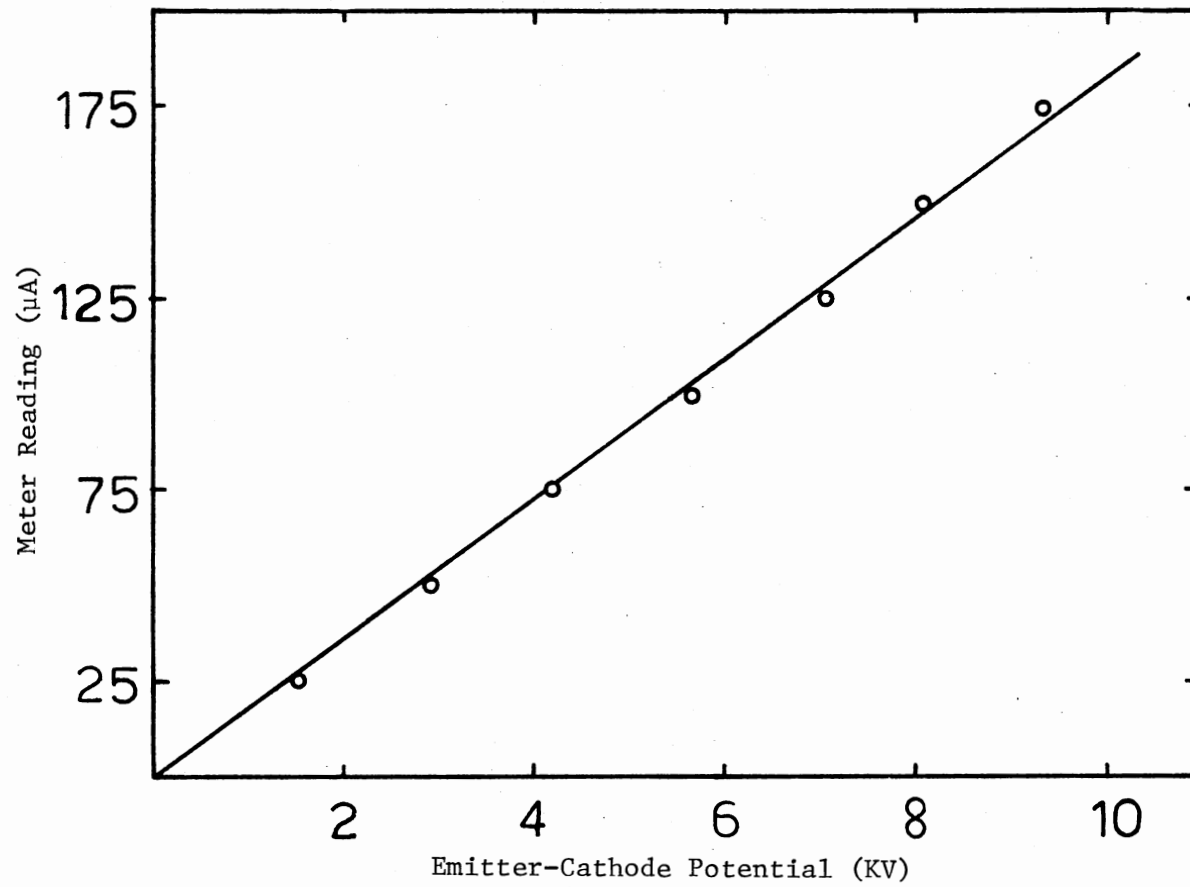


Figure 4. Emitter-Cathode Potential versus Cathode Power Supply Meter Reading

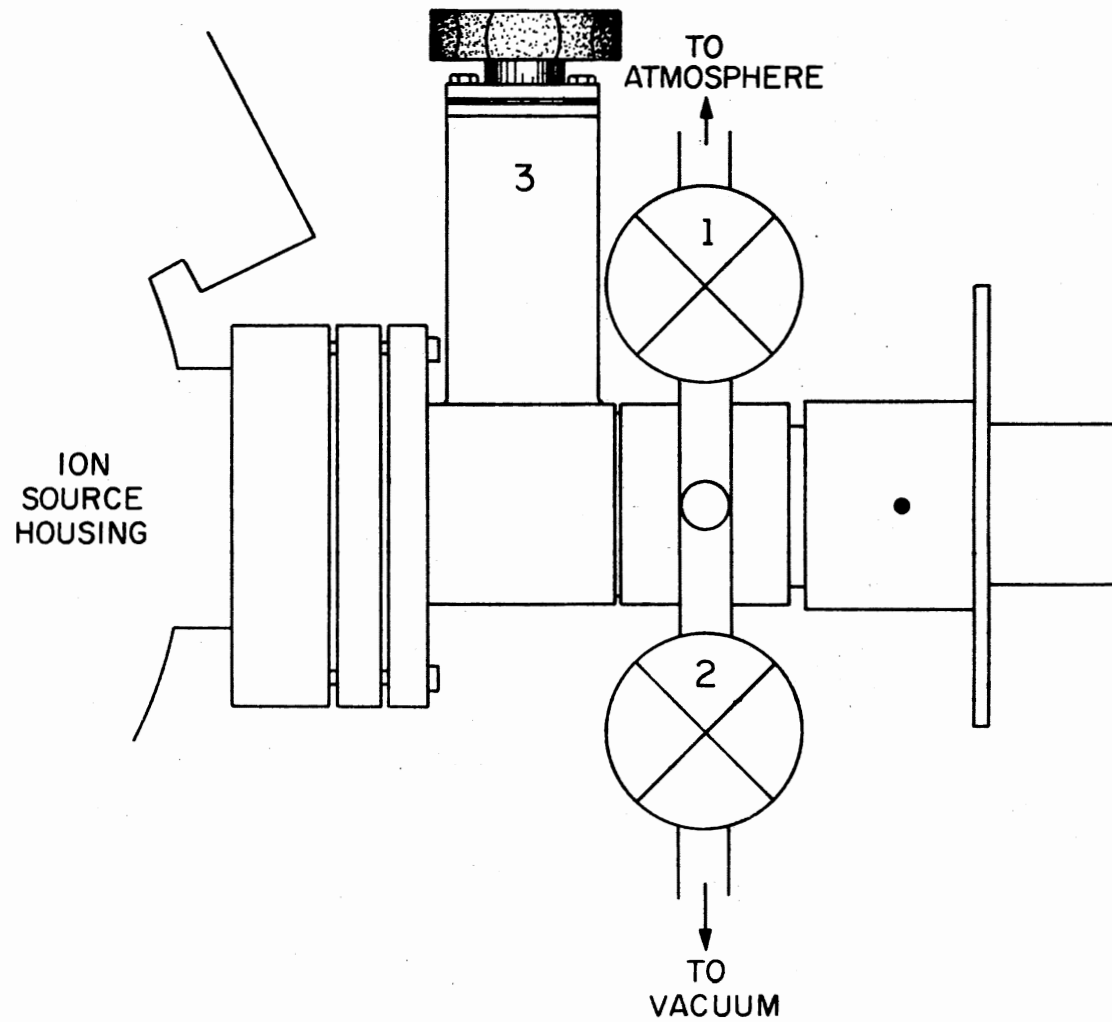


Figure 5. Emitter Vacuum Lock and Gate Valve Assembly

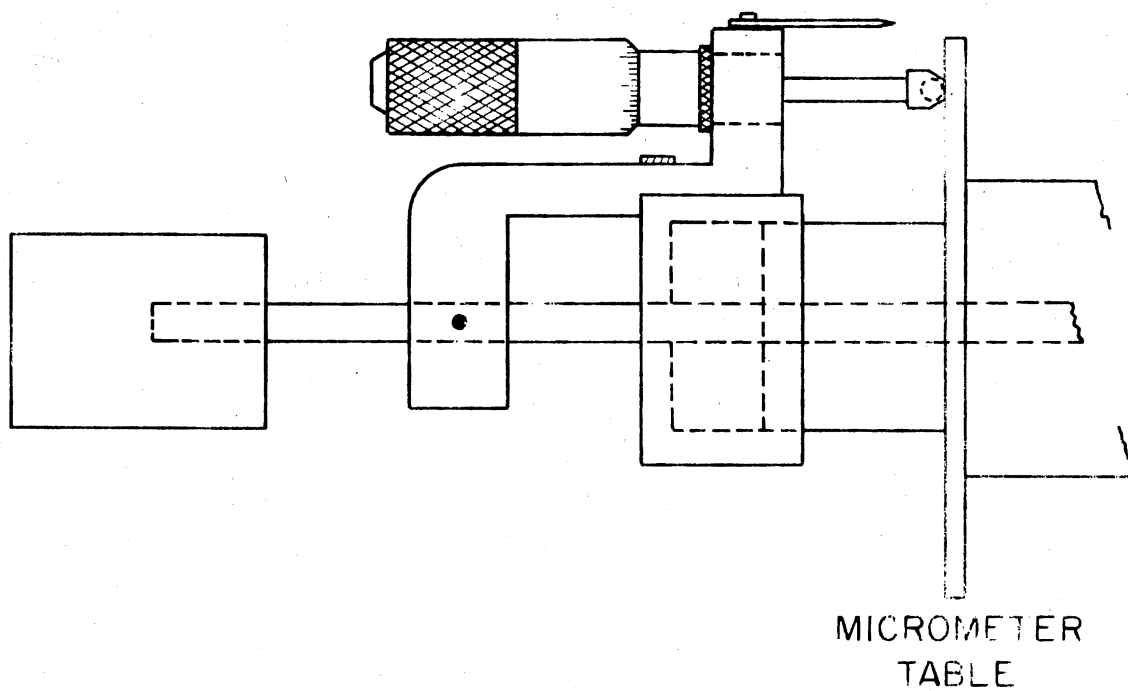


Figure 6. Emitter Probe Micrometer Assembly

## Instrument Operation

To obtain FI mass spectra an emitter must first be prepared. The work in our laboratory to date has used razor blades as emitters. Emitters (ca. 3.5 mm x 3.5 mm) are cut, using a paper cutter, from commercially obtained uncoated stainless-steel razor blades (Personna 74). The emitter is degreased by ultrasonically treating it for 1-2 minutes in a small beaker containing first toluene, and then acetone. The emitter is then air dried. The emitter-control rod containing the blade vise is inserted into the hole in the blade-alignment jig. The control rod and alignment jig are then positioned on the control-rod bench to permit insertion of the razor-blade emitter. By means of forceps the emitter is inserted into the blade vise from the side to prevent damaging the blade edge. The blade edge is positioned 0.050 of an inch from the front face of the blade vise by lining up the edge of the emitter with the second line scribed on the alignment jig. Once the emitter is centered in the blade vise the set screw is tightened. To maintain proper alignment, the emitter must be held with the forceps while the set screw is being tightened. It is important to note that even with use of the bench and alignment jig it is extremely easy to damage the edge of the emitter. After the emitter has been positioned in the blade vise the alignment jig is carefully removed and the control rod and emitter are inserted 8.8 cm into the vacuum lock. The chamber is evacuated by opening valve 2, shown in Figure 5. Next, the ion-accelerator high voltage is turned off, the tip-jack high-voltage leads on the FI power supply are moved

from the EI mode to the FI mode, and the tip-jack leads located in the ion-accelerator chassis which control the voltage supplied to the focus electrodes are moved from the EI position (ca. 6400 V) to a predetermined FI position (ca. 4600 V).

When the pressure in the vacuum lock is less than 1 micron, the gate valve between the vacuum lock and ion-source housing is opened (valve 3, Figure 5) while valve 2 is closed simultaneously. With the ion accelerator and the FI power supplies turned off the emitter is inserted into the ion source until the blade vise makes electrical contact with the repellers. Contact between repellers and the blade vise is determined by connecting the tip-jack leads from the repellers to a volt-ohm meter. Zero resistance demonstrates contact between the blade vise and the repellers. The emitter is heated in this position for ca. 15-30 minutes to remove volatiles. Removal of the volatiles is indicated by the return to a typical background ion-source pressure reading on the ion-source Bayard-Alpert gauge. Using the emitter probe micrometer assembly the distance between the emitter and the cathode is decreased in 0.05-0.1 mm increments until the edge of the razor blade extends into and is parallel with the beveled portion of the counter electrode (Figure 7). The entry and positioning are determined by slowly rotating the emitter until electrical contact is indicated by an ohm meter connected to either repeller and the cathode. Insertion of the emitter in 0.05-0.10 mm increments decreases the possibility of damaging the emitter edge. The rotation of the emitter is measured by reference degree markers inscribed on the micrometer table. It has been determined that good sensitivity coupled with prolonged emitter life is obtained by positioning the emitter so

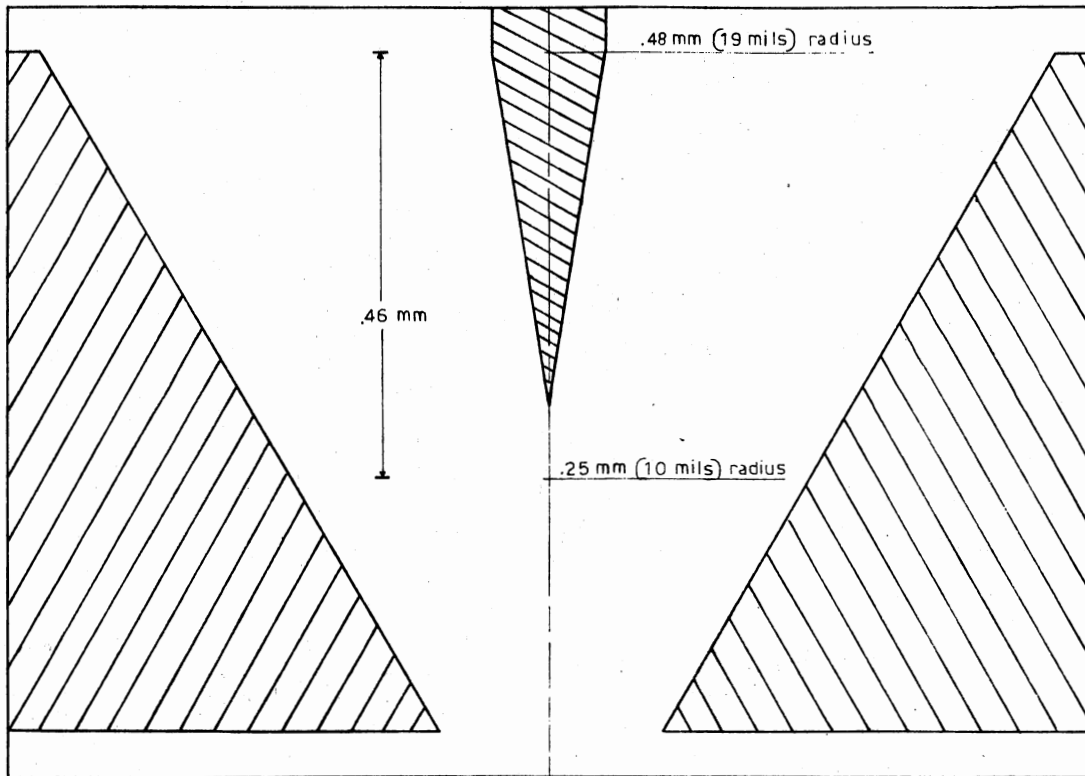


Figure 7. Enlarged Side View of the Razor Blade Emitter and Exit Slit



that an angle of 20-25° is defined by contacting one edge of the emitter with both sides of the beveled cathode slit. The emitter is then centered in the cathode. The ion-accelerator high voltage is turned on (an ion accelerator potential of either 6 or 8 kV is used). The voltage from the FI power supply is slowly increased to produce a meter reading of ca. 100  $\mu$ A. As shown in Figure 4 this corresponds to an anode (emitter)-cathode potential of 6 kV. Acetone vapor at a pressure of  $1-3 \times 10^{-5}$  torr is used to "condition" the emitter, in order to provide an ion beam for tuning the ion accelerator (output), cathode and focus potentials, and to align the emitter both horizontally and rotationally for maximum sensitivity. The term "conditioned" denotes an increase in and stabilization of the ion current obtained in this study for a specified pressure of acetone. The increase in and stabilization of the ion current are attributed to growth of semi-conducting organic materials on the emitter.<sup>2c,10d,12</sup> We have found that conditioning typically takes 5-15 minutes for our emitters and routinely produces an ion current of  $1.5-3.0 \times 10^{-12}$  amps for  $2.0 \times 10^{-5}$  torr of acetone in the ion source. In this regard, repetitive daily conditioning and routine use can lead to ion currents of  $1-3 \times 10^{-11}$  amps for  $2.0 \times 10^{-5}$  torr of acetone. This phenomenon has been noted by other authors.<sup>2c,13</sup> The ion current is maximized by adjustment of the cathode, focus, and output potentials, horizontal movement of the emitter, and rotation of the emitter while monitoring the ion intensity of the  $m/e$  58 peak for acetone on either the oscilloscope or oscillographic recorder of the mass spectrometer. Variation in types of samples analyzed or the occurrence of electrical discharges between the emitter and the

cathode may require occasional readjustment of the focus, cathode, and/or output potentials.

Operation of the mass spectrometer is switched from operation in the FI mode to operation in the EI mode as follows. Both the ion accelerator and field ionization high voltages are turned off and the tip-jacks from both the cathode and the ion accelerator are moved from the FI to the EI positions (see Figure 3). The tip-jacks in the ion accelerator are repositioned to obtain the focus potentials used for electron impact operation (i.e., typically 6300 V). After the emitter is withdrawn from the ion source the accelerator voltage and filament is turned on. In our laboratory the change from the EI mode to the FI mode or vice versa takes on the order of 1-3 minutes. If the FI probe is to be completely removed, it is pulled into the vacuum lock, the gate valve (valve 3, Figure 5) closed and the vacuum lock vented to the atmosphere (open valve 2, Figure 5). The emitter probe can then be removed from the vacuum lock.

### Results and Discussion

The optimum sensitivity, that is the number of ions detected versus the pressure of the sample in the inlet system, for the combined FI/EI source used on the OSU CEC 21-110B mass spectrometer is dependent upon: anode-cathode distance, blade angle in relation to the cathode slit, condition of the emitter edge and the anode-cathode potential. The possibility of using additional focusing lenses in the ion source to maximize sensitivity was not utilized.<sup>10a,13</sup> Figure 8 shows the effect of anode-cathode distance on the electron multiplier output recorded on the oscillographic recorder. All three curves

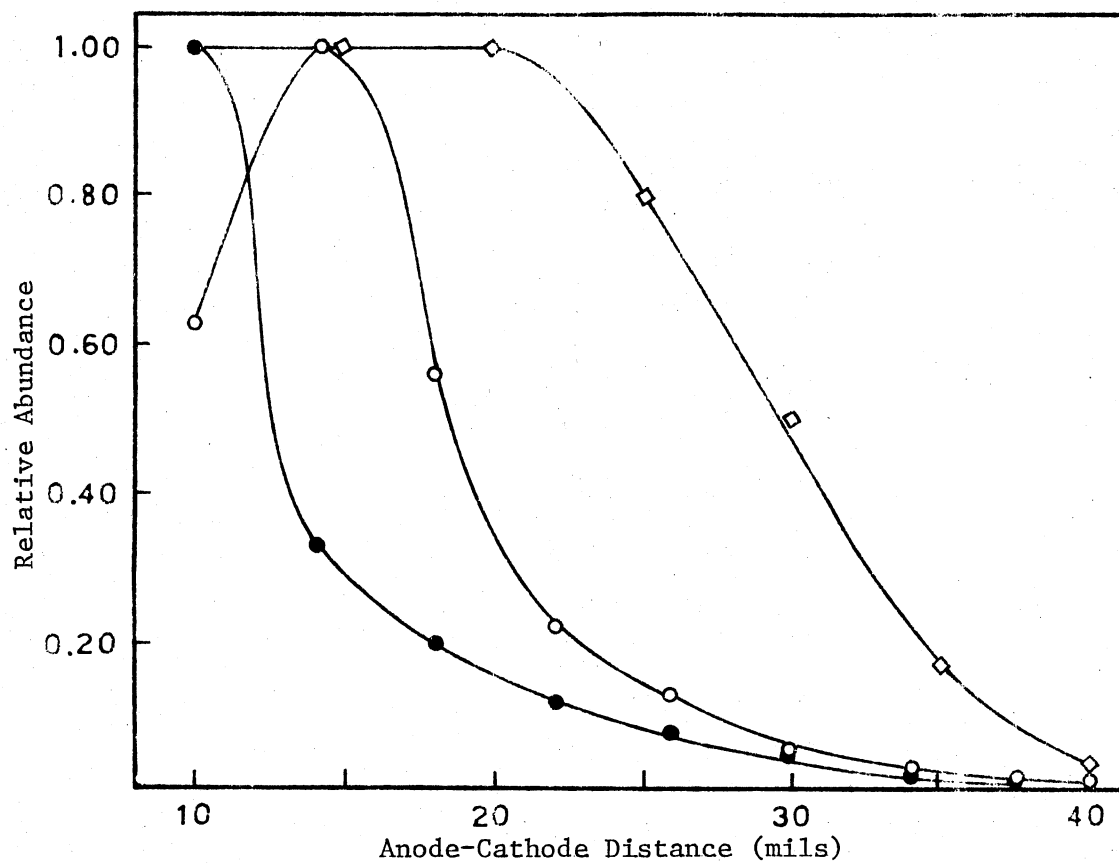


Figure 8. Effect of Emitter-Cathode Distance on Relative Abundance for Acetone  $m/e$  58: (●) Without Maximized Tuning, (○) With Maximized Tuning, (◇) Previous Work, see Reference 11a

were obtained using acetone as the ionized gas. The solid circles (Curve I) correspond to data obtained by withdrawing the emitter by 0.1 mm increments without retuning the output, focus or cathode potentials. The hollow circles (Curve II) correspond to data obtained by duplicating the previous experiment except that the ion current at the multiplier was optimized at each 0.1 mm increment. These results appear to be in contradiction with ion intensity data previously published by Chait. These latter data are shown by Curve III.<sup>11a</sup> Since experimental conditions were not published, attempts to duplicate Curve III were not pursued.<sup>11a</sup> Although the occurrence of the maximum in Curve II cannot be explained it has also been observed by Schulze et al.<sup>14</sup> They also found an inflection in the plot of ion current versus anode-cathode distance when the cathode slit was beveled at 30° and 60° with respect to the back plane of the cathode (i.e., a standard slit face is 90° with respect to the back plane of the cathode). A 60° angle of bevel produced the highest beam intensity and gave maximum curvature. This corresponds to the angle of bevel used on our combined EI/FI source cathode slit. It is important to note that Curve II in Figure 8 demonstrates that an increase (decrease) in ion intensity of approximately 40% can be realized within a distance of  $\pm 5$  mils (0.13 mm).

Figure 9 shows the relationship between peak intensity and anode-cathode potential for anode-cathode distances of 0.25 mm (10 mils) and 0.51 mm (20 mils). Acetone was used as the ionizing gas. The  $m/e$  58 ion intensity increases exponentially as the anode-cathode potential is increased from 2700 to 5500 V. This phenomenon has been previously observed.<sup>2b,c;10b</sup> The curve corresponding to an

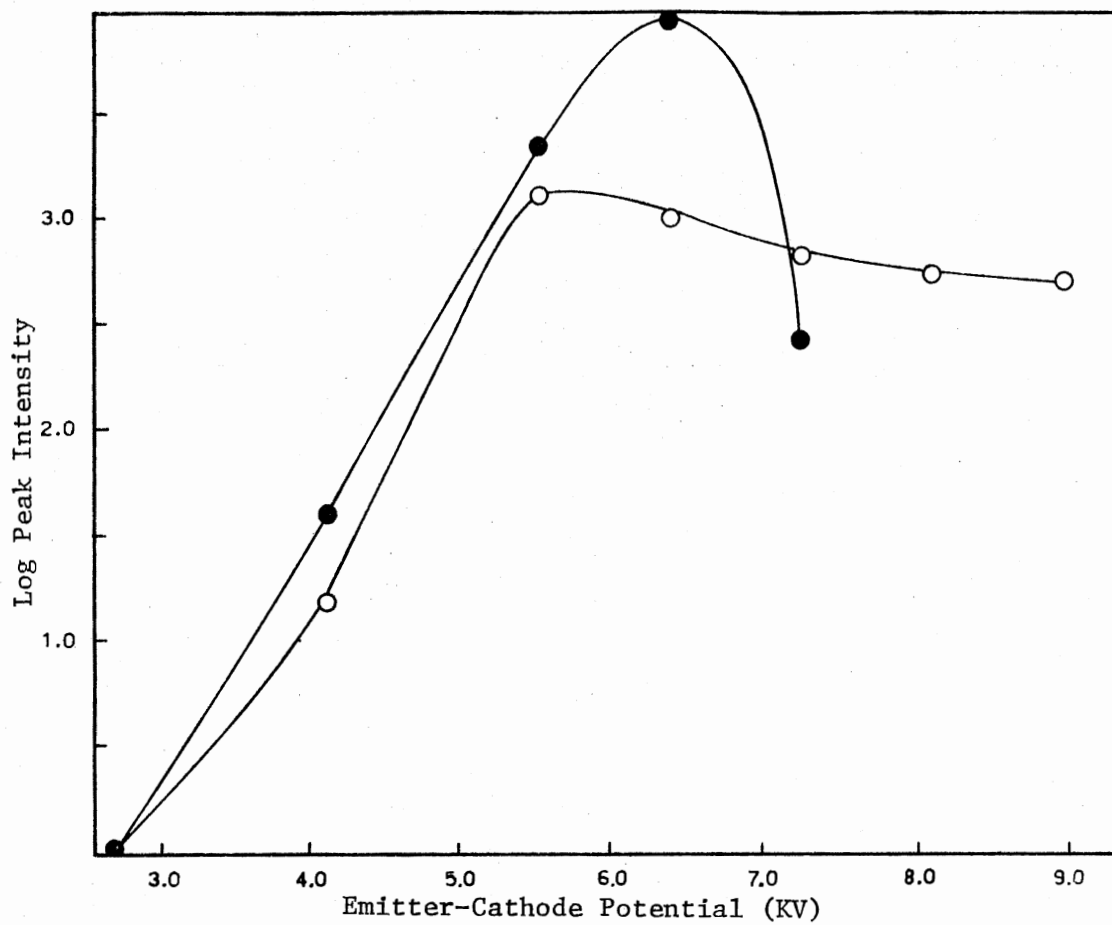


Figure 9. Peak Intensity as a Function of Emitter Potential for Acetone  $m/e$  58. Emitter-Cathode Distance: (●) 10 mils, (○) 20 mils. Ion Source Pressure ca.  $2.0 \times 10^{-5}$  torr

anode-cathode distance of 0.25 mm shows a drop by a factor of 10 in ion intensity as the anode-cathode potential is increased from approximately 6000 V to 6900 V. The decrease in ion intensity for  $m/e$  58 of acetone at these higher anode-cathode potentials is significantly less at an anode-cathode distance of 0.50 mm. However, the intensity of the  $m/e$  58 peak at optimum emitter-cathode potential is lower by an order of magnitude. A similar decrease at high field strength has been observed by Inghram and Gomer<sup>1b</sup> and Gomer<sup>2b</sup> in their studies of the FI spectra of hydrogen using tip emitters. Increasing the field strength tended to spread the profiles of ion intensity versus energy for both  $H_2^+$  and  $H^+$  and decrease the ion intensity. Broadening was indicative of ions being formed at greater distances from the tip.<sup>2b</sup> Increased fragmentation at higher field strengths was also observed.<sup>1b,2b</sup> For purposes of this study these phenomena were only noted.

The effect of emitter angle in relation to the cathode slit is one parameter which requires more attention for a blade than for wires.<sup>10c</sup> As can be seen in Figure 10, a deviation of  $1^\circ$  from the slit center was reported to cause the peak intensity to drop by 50%.<sup>11a</sup> Use of a cathode with a beveled ( $60^\circ$ ) slit permits determination of the slit center with less chance of damaging the emitter than if a standard ( $90^\circ$ ) slit was used. For example, the width of the beveled cathode slit at the point where the emitter would first be inserted is over 0.040 in. compared with 0.010-0.020 in. for previous designs.<sup>10a,11a</sup> Furthermore, by noting the angle of rotation of the emitter as it is inserted deeper into the slit (see Figure 7) the anode-cathode distance and slit center can be determined. There are

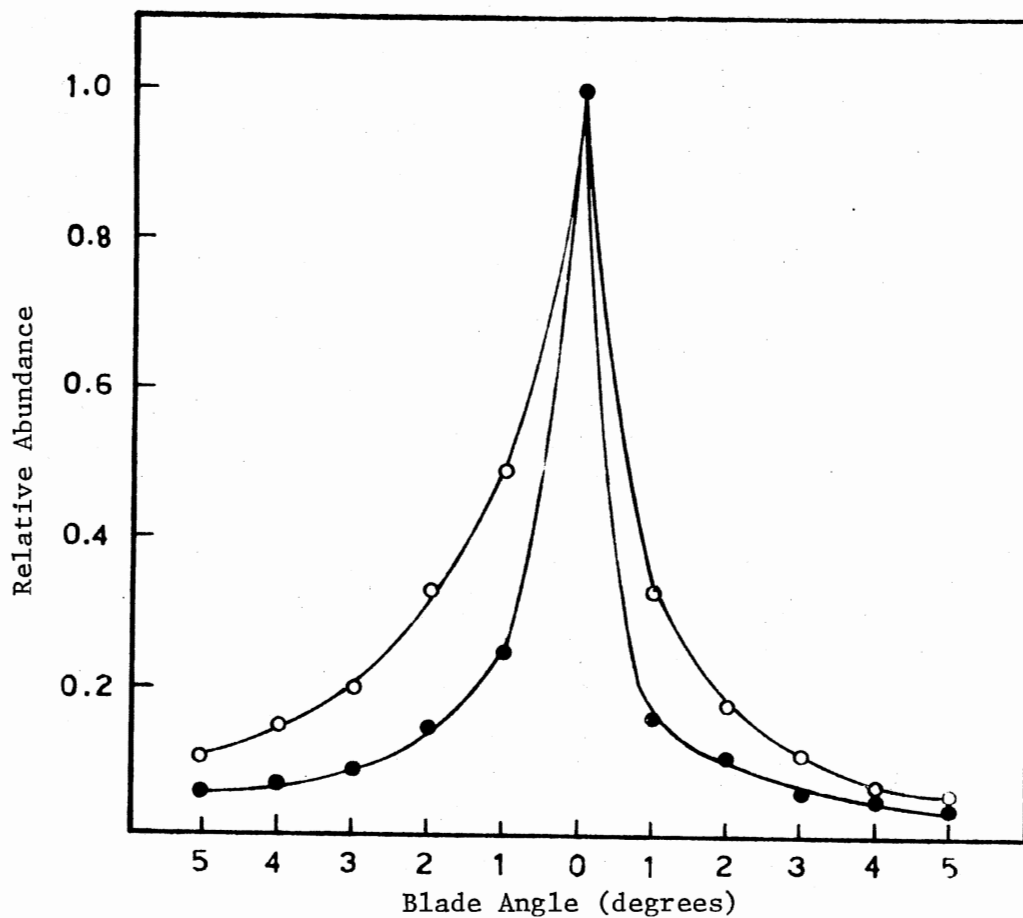


Figure 10. Effect of Blade Angle on Sensitivity for Acetone  $m/e$  58. Emitter-Cathode Distance: (●) 10 mils, (○) 30 mils. Exit Slit Width 12 mils. (From E. M. Chait, T. W. Shannon, W. O. Perry, G. E. Van Lear, and F. W. McLafferty, Int. J. Mass Spectrom. Ion Phys., 2, 141 (1969))

two major advantages of positioning the emitter in the center of the slit before the high voltage is applied. First, accidental high-voltage discharges which can decrease the radius of the blade edge are minimized since all points on the emitter edge are equidistant from the cathode. Second, the operator does not have to maximize the emitter position or handle the emitter probe with the high voltage applied.

To determine the precision in the ion abundance data obtainable from the combined FI/EI ion source, relative ion intensities from the FI mass spectra of a hydrocarbon plus ether fraction of an upgraded anthracene oil were acquired. Table I presents data obtained using two different emitters; the same emitter at two different times, and the same emitter which had been removed from, replaced, and repositioned into the ion source. The ion-source temperature was held constant at 250°C. Column 6 lists the percent standard deviations in relative ion abundances calculated using values from all three experiments. It is significant that the average percent standard deviation was < 10%. No clear trends could be seen by comparison of the data from the three experiments. Therefore, it was demonstrated that the FI ion abundances that were obtained for these hydrocarbons and ethers were independent of emitter, emitter positioning, and time.

Field-ionization mass spectra recorded with sufficient resolution to separate doublets arising from ionization of compounds possessing identical nominal masses but different exact masses constitute an important tool for characterization of mixtures. Table II presents data obtained from the medium-resolution FI mass spectra of the hydrocarbon plus ether fractions of anthracene oil and four of



TABLE I

## FI RELATIVE ION ABUNDANCES FOR REACTOR SAMPLE 1

m/e <sup>a</sup>	Relative Ion Abundances for Emitter Number				% Std. Dev. in Rel. Abd. <sup>b</sup>
	1	2	2	2 Repositioned	
118	9.17	9.60	8.75	8.00	7.68
128	70.83	72.00	70.83	72.00	0.95
132	48.33	48.80	47.50	44.40	4.19
142	33.75	35.20	35.00	34.40	1.89
146	23.33	22.00	19.58	24.00	8.75
154	58.33	54.00	58.33	56.00	3.69
156	27.50	26.40	30.00	24.80	8.04
158	37.08	37.20	40.00	40.80	4.93
166	41.67	42.00	44.58	41.20	3.57
168	55.00	56.00	61.67	56.00	5.32
170	12.08	10.40	14.58	13.60	14.43
172	14.17	12.80	14.58	14.00	5.51
174	10.83	8.00	11.67	10.40	15.40
178	100.00	100.00	100.00	100.00	0.00
180	46.25	52.00	54.17	52.00	6.64
182	62.50	68.00	70.83	72.00	6.20
186	21.67	20.00	20.00	20.00	4.90
190	10.83	11.20	10.83	12.00	4.92
192	26.25	31.20	30.42	33.20	9.66
194	17.50	17.20	18.75	17.60	3.83
196	26.67	25.20	25.83	27.60	3.96
200	7.08	7.20	7.50	9.60	15.08
202	45.00	60.00	46.25	48.00	13.86
204	24.58	22.80	25.00	24.40	3.98
206	39.58	42.00	42.50	43.60	4.05
208	20.42	18.80	20.83	20.00	4.38
210	14.58	8.80	12.50	10.00	22.52

TABLE I (Continued)

m/e <sup>a</sup>	Relative Ion Abundances for Emitter Number				% Std. Dev. in Rel. Abd. <sup>b</sup>
	1	2	2	2 Repositioned	
212	15.00	15.60	16.25	17.20	5.88
216	7.08	9.60	7.08	6.80	17.19
218	11.25	14.00	10.42	10.80	13.98
220	10.42	10.00	10.42	10.00	2.38
222	8.33	8.40	9.58	10.80	12.57
224	2.92	2.40	4.17	3.60	23.66
226	3.33	2.80	2.92	3.60	11.68
228	2.50	3.20	2.92	2.00	19.70
230	6.67	5.20	5.00	4.40	28.12
232	6.25	8.40	7.50	4.80	23.21
234	5.42	5.20	7.83	4.80	8.09
236	2.50	4.40	4.17	3.20	24.71
					Ave. 9.48

<sup>a</sup> Intensities for isotope peaks are not included for sake of brevity.

<sup>b</sup> Percent Standard Deviation represents the standard deviation divided by the average relative abundance from all four experiments.

TABLE II

MOLE PERCENT COMPOSITION OF VARIOUS DOUBLETS IN THE HYDROCARBON + ETHER  
FRACTIONS OF ANTHRACENE OIL AND FOUR UPGRADED SAMPLES

Nominal m/e	Empirical Formula	Mole Percent of Nominal Mass Peak Areas for				
		Feedstock	1	2	3	4
168	$C_{12}H_8O$	$0.53 \pm 0.02$	$0.62 \pm 0.03$	$0.58 \pm 0.03$	$0.64 \pm 0.03$	$0.57 \pm 0.04$
	$C_{13}H_{12}$	$0.47 \pm 0.02$	$0.38 \pm 0.03$	$0.42 \pm 0.03$	$0.36 \pm 0.03$	$0.43 \pm 0.04$
182	$C_{13}H_{10}O$	$0.50 \pm 0.03$	$0.31 \pm 0.02$	$0.39 \pm 0.02$	$0.29 \pm 0.01$	$0.29 \pm 0.01$
	$C_{14}H_{14}$	$0.50 \pm 0.03$	$0.69 \pm 0.02$	$0.61 \pm 0.02$	$0.71 \pm 0.01$	$0.71 \pm 0.01$
184	$C_{12}H_8S$	$0.78 \pm 0.04$	$0.29 \pm 0.04$	$0.53 \pm 0.06$	$0.13 \pm 0.15$	$0.29 \pm 0.08$
	$C_{14}H_{16}$	$0.22 \pm 0.04$	$0.71 \pm 0.04$	$0.46 \pm 0.06$	$0.86 \pm 0.15$	$0.71 \pm 0.08$
196	$C_{14}H_{12}O$	$0.70 \pm 0.07$	$0.45 \pm 0.03$	$0.51 \pm 0.03$	$0.44 \pm 0.02$	$0.45 \pm 0.02$
	$C_{15}H_{16}$	$0.30 \pm 0.07$	$0.55 \pm 0.03$	$0.49 \pm 0.03$	$0.56 \pm 0.02$	$0.55 \pm 0.02$
198	$C_{13}H_{10}S$	$0.88 \pm 0.01$	$0.27 \pm 0.09$	$0.44 \pm 0.06$	$0.07 \pm 0.00$	$0.34 \pm 0.06$
	$C_{15}H_{18}$	$0.12 \pm 0.01$	$0.73 \pm 0.09$	$0.66 \pm 0.06$	$0.93 \pm 0.00$	$0.66 \pm 0.06$
218	$C_{16}H_{10}O$	$0.59 \pm 0.04$	$0.45 \pm 0.03$	$0.49 \pm 0.02$	$0.39 \pm 0.04$	$0.49 \pm 0.06$
	$C_{17}H_{14}$	$0.41 \pm 0.04$	$0.55 \pm 0.03$	$0.51 \pm 0.02$	$0.61 \pm 0.04$	$0.51 \pm 0.06$
232	$C_{17}H_{12}O$	$0.69 \pm 0.07$	$0.25 \pm 0.04$	$0.39 \pm 0.04$	$0.21 \pm 0.02$	$0.29 \pm 0.04$
	$C_{18}H_{16}$	$0.31 \pm 0.07$	$0.75 \pm 0.04$	$0.61 \pm 0.04$	$0.79 \pm 0.02$	$0.71 \pm 0.04$

its upgraded samples. The compositional data for the samples were collected from FI ion abundances taken over a period of two weeks. Thus, it was encouraging that the percent standard deviation using this technique was generally  $\leq 10\%$ . It is important to note that mole percents at a given nominal mass are obtained from the ion intensity at that mass normalized by the sum of the ion intensities.

The accuracy of the compositional data calculated from FI ion abundances reflects, in part, the availability of sensitivity coefficient data. The dependence of sensitivity coefficients on molecular weight and structure and mixture composition has been investigated for only alkanes, alkenes, cycloalkanes, and low-molecular weight aromatic hydrocarbons.<sup>16</sup> However, characterization data for coal-derived materials<sup>17</sup> show that the available sensitivity data<sup>16,18</sup> are insufficient for routine quantitative analysis of such substances by FI/MS. Consequently, relative FI sensitivity data were determined for 61 compounds typical of those encountered in coal-derived liquids.<sup>19</sup>

Routine determinations of sample composition expressed as either weight or mole percents would normally utilize the intensity of only the molecular ion resulting from ionization of the most abundant isotope of a given component and either its gram or mole sensitivity, respectively. The mole sensitivity of a compound is the experimental intensity of the isotopically most abundant molecular ion divided by the total number of moles of the compound in the mixture used. Relative mole and relative gram sensitivities,  $s(m)_i$  and  $s(g)_i$  respectively, were determined for field ionization in this study.

Sensitivity coefficients for field ionization have been considered in terms of the probability of ionization, diffusion over the emitter surface (supply velocity), and the stability of the molecular ion with respect to fragmentation.<sup>2c</sup> Since for the 61 compounds presently studied the molecular ions accounted for > 99% of the singly charged ions, a relative mole sensitivity is related to the ionization probability and supply velocity for a compound relative to those for the reference compound, i.e., the relative cross section for field ionization. Thus, assuming other instrumental and experimental factors to be equal, reasonable estimates of the relative cross section as a function of structure and mixture composition can be obtained using either the total intensity for all or the intensity of the isotopically most abundant molecular ions of each component. The latter method was chosen to simplify data acquisition, to circumvent the difficulty in obtaining accurate estimates of peak heights for low-intensity ions, and because the intensities at  $m/e$  values formally corresponding to labelled molecular ions are not always, as a sufficiently good approximation, in the ratios of the isotopically labelled molecules.<sup>2c</sup>

For the compounds presently studied the isotopically most abundant molecular ion corresponds to ionization of the lightest isotopic molecule. Thus, the relative field ionization cross sections,  $RCS(FI)_i$ , were calculated using the weights and molecular weights of the lightest isotopic molecules for each component in a mixture,  $g_M$  and  $MW_0$  respectively. Consider a compound with a molecular formula  $C_{x_1} H_{x_2} N_{x_3} O_{x_4} S_{x_5}$  in which  $x_j$  is the number of atoms of the  $j^{th}$  element in the compound. The weight ( $g_M$ ) of the lightest isotopic molecules

of molecular weight  $MW_o$  is given by Equation I-7 where  $g_{M+1}$  and  $g_{M+2}$

$$g_M = \frac{g_T}{1 + \frac{g_{M+1}}{g_M} + \frac{g_{M+2}}{g_M}} \quad (I-7)$$

are the weights of molecules having one and two heavy isotopic atoms, respectively, and  $g_T$  is the total weight of the compound taken. Since standard methods were used in calculating the  $g_{M+1}/g_M$  and  $g_{M+2}/g_M$  ratios the mathematical formalism will not be presented here.<sup>20</sup> For the compounds presently investigated the fraction of molecules containing 0 to 2 heavy isotopes is  $\geq 0.999$ . Since the cross section is the quantity of fundamental significance, the effect of molecular structure on ionization by both an electric field and low-voltage electrons (LV/EI) is considered in terms of relative cross sections. Consequently, Table III presents relative cross sections for ionization by electric fields, RCS(FI), and by low-voltage electrons, RCS(EI). The RCS(EI) values were obtained from low-voltage EI sensitivities as follows.<sup>17a,17g,21</sup> Densities were used to convert low-voltage sensitivities reported as divisions per unit of volume into divisions per milligram.<sup>22</sup> For each compound a  $g_M$  value was computed using Equation I-7 with  $g_T = 1$  mg. For a given compound multiplication of the sensitivity in div/mg by the function  $MW_o/g_M$  yields a mole sensitivity for ionization of the isotopically most abundant molecules,  $EIS(M_o)$ , which is proportional to their cross section for ionization by electrons possessing energy eV if negligible molecular-ion fragmentation is assumed. The compound types, the available mass

TABLE III  
FI- AND EI-RELATIVE CROSS SECTIONS (RCS)

Compound	$\frac{m}{e}$ of $M^+$	FI-RCS	EI-RCS				Ave.
			Set 1	Set 2 <sup>a</sup>	Set 3	Set 4	
benzene	78	1.00	1.00 <sup>c</sup>	1.00	1.00 <sup>d</sup>	1.00	1.00
toluene	92	1.15	1.87 <sup>c</sup>	1.86	2.05 <sup>d</sup>	1.51	1.82
ethylbenzene	106	1.14	2.11 <sup>c</sup>		2.09 <sup>d</sup>	1.56	1.92
1,2-dimethylbenzene	106	1.25	3.05 <sup>c,e</sup>	2.78		2.60 <sup>e</sup>	2.81
2,3-dihydro-1 <i>H</i> -indene	118	1.24	2.87 <sup>c</sup>	2.72		3.17	2.92
1,3,5-trimethylbenzene	120	1.31	4.05 <sup>c,e</sup>			3.44 <sup>e</sup>	3.75
propylbenzene	120	1.17	2.28 <sup>c</sup>			1.62	1.95
naphthalene	128	1.45	4.52 <sup>c</sup>	5.89	6.71 <sup>d</sup>	5.16	5.57
1,2,3,4-tetrahydronaphthalene	132	1.33		2.05	4.68 <sup>d,f</sup>		3.37
2,3-dihydro-5-methyl-1 <i>H</i> -indene	132	1.28	2.54 <sup>c,e</sup>	2.38 <sup>e</sup>			2.46
1-methylnaphthalene	142	1.49	6.18 <sup>c,e</sup>		8.29 <sup>d</sup>	6.89 <sup>e</sup>	7.12
1,2-dihydroacenaphthylene	154	1.65	6.59 <sup>c</sup>	8.09		6.87	7.18
1,6-dimethylnaphthalene	156	1.72	6.91 <sup>c,e</sup>	8.00 <sup>e</sup>		9.61 <sup>e</sup>	8.17
fluorene	166	1.74	5.57 <sup>c</sup>				5.57
anthracene	178	2.16	8.97 <sup>c</sup>	12.95	9.01 <sup>d</sup>	17.76	12.17
phenanthrene	178	1.98		10.06	8.92 <sup>d</sup>		9.49
9,10-dihydroanthracene	180	1.66			8.00 <sup>d,f</sup>		8.00

TABLE III (Continued)

Compound	$\frac{m}{e}$ of $M^+$	FI-RCS	EI-RCS				Ave.
			Set 1	Set 2 <sup>a</sup>	Set 3	Set 4	
9,10-dihydrophenanthrene	180	1.77			7.97 <sup>d,f</sup>		7.97
3-methylfluorene	180	1.75	6.75 <sup>c,e</sup>				6.75
1,2,3,4-tetrahydrophenanthrene	182	1.76			7.38 <sup>d,f</sup>		7.38
1,2,3,4,5,6,7,8-octahydrophenanthrene	186	1.74			6.47 <sup>d,f</sup>		6.47
4-methylphenanthrene	192	1.86	9.56 <sup>c,e</sup>				9.56
pyrene	202	1.93	11.69 <sup>c</sup>	13.11	10.79 <sup>d</sup>		11.86
2,6-dimethylantracene	206	2.15	9.70 <sup>c,e</sup>				9.70
1,2,3,9,10,10a-hexahydropyrene	208	2.08			8.32 <sup>d,e,f</sup>		8.32
2-methylpyrene	216	2.07	12.18 <sup>c,e</sup>				12.18
chrysene	228	2.01	10.85 <sup>c</sup>				10.85
2-ethylpyrene	230	2.14	12.42 <sup>c,e</sup>				12.42
indole	117	1.78	7.84 <sup>g</sup>				7.84
quinoline	129	1.83	3.29 <sup>g</sup>				3.29
carbazole	167	2.01	13.43 <sup>g</sup>				13.43
benzo[ <i>b</i> ]thiophene	134	1.31	6.00 <sup>c</sup>	6.45			6.23
6-methylbenzo[ <i>b</i> ]thiophene	148	1.49	6.45 <sup>c,e</sup>				6.45
dibenzothiophene	184	1.78	10.56 <sup>c</sup>				10.56



TABLE III (Continued)

Compound	$\frac{m}{e}$ of $M^+$	FI-RCS	EI-RCS				Ave.
			Set 1	Set 2 <sup>a</sup>	Set 3	Set 4	
1,3-benzenediol	110	1.53			2.99 <sup>h</sup>		2.99
1-naphthalenol	144	1.66			6.61 <sup>h</sup>		6.61
dibenzofuran	168	1.69					

<sup>a</sup>See Reference 21a.

<sup>b</sup>See Reference 21b.

<sup>c</sup>See Reference 21c and 21d.

<sup>d</sup>See Reference 21f.

<sup>e</sup>Specific isomeric compound not reported.

<sup>f</sup>See Reference 21e.

<sup>g</sup>See Reference 17g.

<sup>h</sup>See Reference 17a.

spectral data, and the use of ca. 10-eV electrons in these low-voltage sensitivity determinations indicates the reasonableness of this assumption. If instrumental and experimental factors are assumed to be sensibly constant in the determination of a given set of low-voltage EI sensitivities, then division of  $EIS(M_0)$  for a given compound in the set by the  $EIS(M_0)$  value for the reference compound in the same set provides a first approximation of the  $RCS(EI)$  for a given value of the ionizing energy.

The data in Table III clearly indicate that variation in molecular structure produces corresponding effects on the cross section for ionization by either electric fields or low-voltage electrons. As observed for ionization by low-energy electrons, the cross sections for field ionization in the series benzene, naphthalene, anthracene, phenanthrene, pyrene, and chrysene depend on the size of the aromatic nucleus.<sup>21</sup> It is important to note that the trend in the  $RCS(FI)$  and in the  $RCS(EI)$  for naphthalene (1.45 and 5.57), anthracene (2.16 and 12.17); phenanthrene (1.98 and 9.49), and pyrene (1.93 and 11.86) appear to correlate with the variation in their ionization potentials,<sup>17g,23</sup> viz., 8.12, 7.55, 8.10, and 7.72 eV, respectively, relative to the ionization potential for benzene (9.24 eV).<sup>23</sup> As seen in Table III, the  $RCS(FI)$  for pyrene could be larger than the value for phenanthrene within the limits of experimental precision.

Substitution of an alkyl group for hydrogen in benzene is seen to increase both EI and FI cross sections. However, the variation in the EI- and FI-RCS values for benzene, toluene, ethylbenzene, and propylbenzene suggests that the substituent effect on the ionization cross section is not strongly dependent on the nature and size of the alkyl group. Successive replacement of hydrogens in benzene with two and

three methyl groups is seen to increase RCS(EI) and also RCS(FI) but not additively. The effect of methyl and ethyl substitution on the cross sections for FI and EI of the parent aromatic hydrocarbons tends to decrease with increasing "size" of the aromatic nucleus. For example, methyl substitution in benzene, naphthalene, fluorene, and pyrene increases the RCS(FI) and RCS(EI) by ca. 15 and 82, 3 and 28, 1 and 21, and 7 and 3 percent, respectively.

Low-voltage EI sensitivities for hydroaromatic compounds are lower than those for their aromatic precursors.<sup>21e</sup> With the exception of 1,2-dihydroacenaphthylene, RCS(EI) values were calculated for the hydroaromatics in Table III by means of equations relating hydroaromatic compound sensitivities to those of the parent aromatic compounds<sup>21e</sup> and the volume sensitivities<sup>21f</sup> and densities for the latter. For ionization by low-energy electrons and electric fields, it is interesting to note that similar cross sections relative to the parent compound are observed for 1,2,3,4-tetrahydronaphthalene (0.70 and 0.92), 9,10-dihydroanthracene (0.89 and 0.77), 9,10-dihydrophenanthrene (0.89 and 0.89), 1,2,3,4-tetrahydrophenanthrene (0.83 and 0.89), and 1,2,3,4,5,6,7,8-octahydrophenanthrene (0.73 and 0.88). The discrepancy for 1,2,3,9,10,10a-hexahydropyrene relative to pyrene (0.77 for EI and 1.08 for FI) may reflect the difficulty in determining the RCS(FI) value for the latter due to its relative insolubility.

In the structurally related series fluorene, dibenzofuran, dibenzothiophene, and carbazole, replacement of CH<sub>2</sub> by O and S is indicated to have little effect on the cross section for FI whereas substitution of NH for CH<sub>2</sub> markedly increases the cross section.

The data in Table III for 1,3-benzenediol and 1-naphthalenol show that substitution of OH for aromatic hydrogen increases both EI and FI cross sections.

The significance of these results lies in the fact that in the analysis of coal-derived liquids the specific compound types comprising the mixture may not be known. If the assumption of unit relative or extrapolated sensitivities is necessary to convert ion intensities to quantitative distributions, the present data clearly suggest, other factors being equal, that more realistic results are obtained from field ionization than from electron-impact mass spectral data.<sup>19</sup>

The accuracy for quantitative distributions obtained by using FI/MS needed to be determined. One approach was the analysis of test mixtures for which the composition was known.<sup>19</sup> Table IV presents results from the analysis of one test mixture. The components of this mixture are typical of those encountered in the hydrocarbon plus ether fraction obtained from a coal-derived liquid. Column 2 in Table IV lists the known mixture composition determined from the weights taken for the individual components. The weight percents of each component in the test mixture calculated from gas-liquid chromatography (GLC)<sup>24</sup> peak areas both excluding and including<sup>19</sup> sensitivity corrections are listed in columns 3 and 5, respectively. The percent deviation between these values and the known weight percent composition are listed in columns 4 and 6, respectively. Resolution of peaks corresponding to 1,2,3,4-tetrahydronaphthalene and benzo[*b*]thiophene, and 1-methylnaphthalene and 6-methylbenzo[*b*]thiophene could not be accomplished using the GC column and conditions employed.<sup>24</sup> However, the agreement between the weight percent

TABLE IV  
WEIGHT PERCENTS OF COMPONENTS IN TEST MIXTURE #1

Compound	Weight Percents and Percent Deviations by												
	Grams	GLC				FI				EI			
		$S_i/S_j=1^{a,b}$	% Dev	$S_i/S_j^{a,b}$	% Dev	$S_i/S_j=1^{a,c}$	% Dev	$S_i/S_j^{a,c}$	% Dev	$S_i/S_j=1^{a,b}$	% Dev	$S_i/S_j^{a,b}$	% Dev
2,3-dihydro-1H-indene	8.28	8.03	-3.0	8.25	-0.4	6.31	-23.8	7.73	-6.6	2.73	-67.0	8.90	7.5
1,3,5-trimethylbenzene	6.28	5.99	-4.6	6.20	-1.3	5.02	-20.1	5.83	-7.2	3.49	-44.4	6.35	1.1
naphthalene	4.46	5.75	28.9	4.93	10.5	4.10	-8.1	4.34	-2.7	3.12	-30.0	4.56	2.2
1,2,3,4-tetrahydronaphthalene	5.46	7.45	-14.1	9.01	3.9	4.56	-16.5	5.30	-2.9	2.12	-61.2	5.44	-0.4
benzo[b]thiophene	3.21					2.62	-18.4	3.18	-0.9	2.70	-15.9	3.39	5.6
1-methylnaphthalene	11.78	15.42	-4.4	17.13	6.2	11.25	-4.5	11.78	0.0	10.42	-11.5	12.03	2.1
6-methylbenzo[b]thiophene	4.35					4.17	-4.1	4.50	3.4	4.95	13.8	4.79	10.1
1,2-dihydroacenaphthylene	3.06	2.97	-2.9	3.17	3.6	3.32	8.5	3.16	3.3	3.71	21.2	3.10	1.3
1,6-dimethylnaphthalene	9.43	9.58	1.6	9.17	-2.8	9.94	5.4	9.15	-3.0	12.02	27.5	9.31	-1.3
1,2,3,4,5,5a-hexahydro-acenaphthylene	8.52	8.21	-3.6	8.22	-3.5	7.40	-13.1	8.72	2.3	4.65	-45.4	8.48	-0.5
fluorene	3.90	3.82	-2.1	3.93	0.8	4.25	9.0	3.91	0.3	3.51	-10.0	3.62	-7.2
dibenzofuran	3.54	3.11	-12.2	3.53	-0.3	4.06	14.7	3.78	6.8	3.44	-2.8	3.86	9.0
phenanthrene	4.05	4.54	12.1	4.14	2.2	4.95	22.2	4.02	-0.7	6.19	52.8	4.16	2.7
9,10-dihydrophenanthrene	9.11	10.04	10.2	8.44	-7.4	10.24	12.4	9.29	2.0	9.37	2.9	8.88	-2.5
dibenzothiophene	2.13	2.05	-3.8	2.31	8.5	2.42	13.6	2.25	5.6	3.42	60.6	2.21	3.8
4-methylphenanthrene	3.47	3.51	1.2	3.80	9.5	4.24	22.2	3.71	6.9	5.78	66.6	3.22	-7.2
pyrene	6.36	6.49	2.0	5.99	-5.8	7.63	20.0	6.50	2.2	11.05	73.7	5.52	-13.2
2,6-dimethylanthracene	0.63	0.68	7.9	0.37	-41.3	0.97	54.0	0.74	17.5	1.62	157.1	0.52	-17.5
chrysene	1.97	2.36	19.8	1.55	21.3	2.53	28.4	2.12	7.6	4.76	141.6	1.70	-13.7

<sup>a</sup>Uncertainty in values is ca. ± 5%.

<sup>b</sup>Average of two determinations.

<sup>c</sup>Average of three determinations.

composition determined by GLC and the known weight percent composition is reasonable. While the percent standard deviations show no clear trends the magnitude of the numbers could be taken as indicative of a first approximation to the error of this technique for analysis of mixtures. The weight percents of each component in the test mixture calculated from the FI and LV/EI ion intensities assuming unit relative-sensitivities are presented in columns 7 and 12 of Table IV, respectively. The percent deviations between these values and the calculated weight percents are listed in columns 8 and 12, respectively. Exclusion of mass spectral sensitivity corrections results in an underestimation of the weight percent for the lower-molecular-weight compounds and an overestimation of the weight percents for the higher-molecular-weight compounds. The best agreement between experimental and known weight percents is realized for compounds whose relative sensitivity most closely approximates the average relative sensitivity that would occur across each distribution. Since the variation in sensitivities is roughly related to the variation in molecular weight and since the compounds in Table IV are listed according to increasing molecular weight, the best agreement with the known weight percents is observed for compounds in the middle of the distribution. It is significant to note that the error in the compositions incurred by assuming unit-relative sensitivities is worse at all points across the distribution obtained from EI/MS than from FI/MS. Weight percents calculated using known relative gram sensitivities for both FI and LV/EI are shown in columns 9 and 13, respectively.<sup>17a,g;19,21</sup> The associated percent deviations are listed in columns 10 for FI data and 14 for LV/EI data. Inclusion of sensitivity corrections is seen to

further improve the accuracy of the weight percent composition calculated from FI ion abundances. Inclusion of sensitivities for the conversion of LV/EI ion abundances to weight percents is seen to produce excellent agreement between determined and known weight percents.

## CHAPTER II

### SEPARATION AND ANALYSIS OF FEEDSTOCK AND UPGRADED ANTHRACENE OIL

#### Results and Discussion

For our initial characterization research Dr. B. L. Crynes in the School of Chemical Engineering requested analysis on his reference coal-derived oil, raw anthracene oil. The properties of the raw anthracene oil are presented in Table V. Four samples of anthracene oil which had been upgraded using catalytic hydrogenation over a cobalt-molybdenum catalyst were also characterized. The effects of changing both the reactor temperature and pressure and the catalyst can be evaluated by comparing the characterization data for the feedstock and upgraded oils. A 20-g. sample of each of the oils was then separated according to compound class as shown in Figure 11.<sup>25</sup> This separation technique has been shown to be applicable to the separation of heavy ends from petroleum<sup>25,26</sup> and coal-derived liquids.<sup>27</sup>

The weight percents of the acidic, basic, the neutral nitrogen-containing and hydrocarbon plus ether fractions obtained from the separation and the percents of elemental sulfur and nitrogen from combustion of the feedstock and upgraded oils are presented in Table VI. The reactor conditions and catalysts are also given in Table VI.



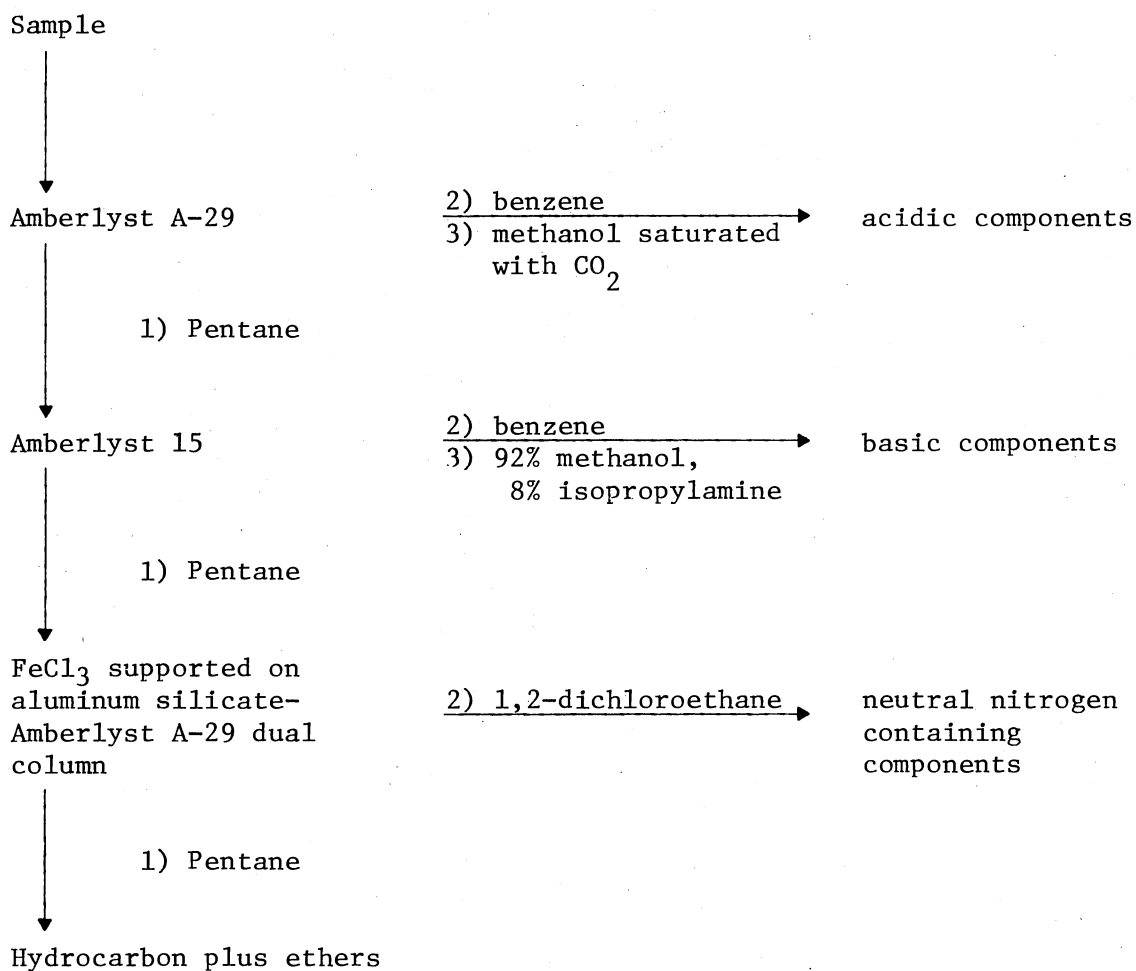
TABLE V  
RAW ANTHRACENE OIL PROPERTIES

---

Carbon	_____	90.65 wt%
Hydrogen	_____	5.76
Sulfur	_____	0.48
Nitrogen	_____	0.91
Oxygen	_____	2.2
Ash	_____	Nil
API Gravity @ 60 F	_____	-7
Initial*		193° C (380° F)
10 Vol%		232° C (450° F)
30		297° C (570° F)
50		343° C (650° F)
70		371° C (700° F)
90		435° C (815° F)

\*Normal boiling data determined from ASTM D 1160 data.

---



In each step the numbers indicate the sequence of solvents used in elution except as noted.

Figure 11. Method of Separation

TABLE VI  
RESULTS FROM SEPARATION AND ELEMENTAL ANALYSIS OF ANTHRACENE  
OIL AND FOUR OF ITS HYDROTREATED PRODUCTS

Fraction	Weight Percent in				
	Feedstock	Reactor Sample <sup>a</sup>			
		1	2	3	4
Acids	14.9	2.5	4.3	3.0	2.8
Bases	9.5	7.5	6.1	10.1	8.6
Neutral Nitrogen	1.7	1.5	1.7	1.9	0.8
Hydrocarbon + Ether	73.9	83.5	82.9	80.0	82.8
Sulfur	0.48	0.11	0.07	0.02	0.04
Nitrogen	0.91	0.62	0.69	0.54	0.67
Reactor Temperature (°F)		700	600	700	700
Reactor Pressure (psig)		1000	1000	1020	507
Reactor Catalyst		Nalco Sphericat		Harshaw HT 400	
Space Time (hr.)		1.48	2.50	0.75	0.75

<sup>a</sup>Assumes a 5% weight loss due to formation of gaseous products.

These results show that the acids are most reactive toward deheteroatomization whereas the bases and neutral nitrogen fractions appear to be reasonably resistant towards heteroatom removal. The increase in the weight percent of the hydrocarbon plus ether fractions represents the formation of hydrocarbons and/or ethers from the hydrogenolysis of compounds in the heteroatom-containing fractions. The elemental analysis indicates that the removal of sulfur-containing molecules was essentially complete. However, the elemental nitrogen analysis indicates that denitrogenation was largely ineffective.

Analysis of the hydrocarbon plus ethers, which will hereafter be referred to as the neutrals, is considered first. The 70-eV mass spectra of the feedstock anthracene oil neutrals, reproduced in Figure 12, shows the presence of little or no saturated hydrocarbons in the feedstock. This conclusion is deduced by the lack of characteristic ions at  $m/e$  values corresponding to the ionization/fragmentation of paraffins and condensed and noncondensed naphthenes.<sup>28</sup> The elemental composition of carbon and hydrogen listed in Table V also support this postulate since the weight percent carbon is indicative of a high degree of aromaticity. Similar fragmentation patterns were also observed for the neutrals obtained from separation of the upgraded oil. Therefore, separation of the neutrals into saturates and aromatics was not deemed necessary.<sup>25,29</sup>

#### Gas Chromatography in Conjunction With Electron Impact Mass Spectrometry

One approach to the characterization of components in the neutral fractions from the anthracene oil feedstock and its upgraded reactor

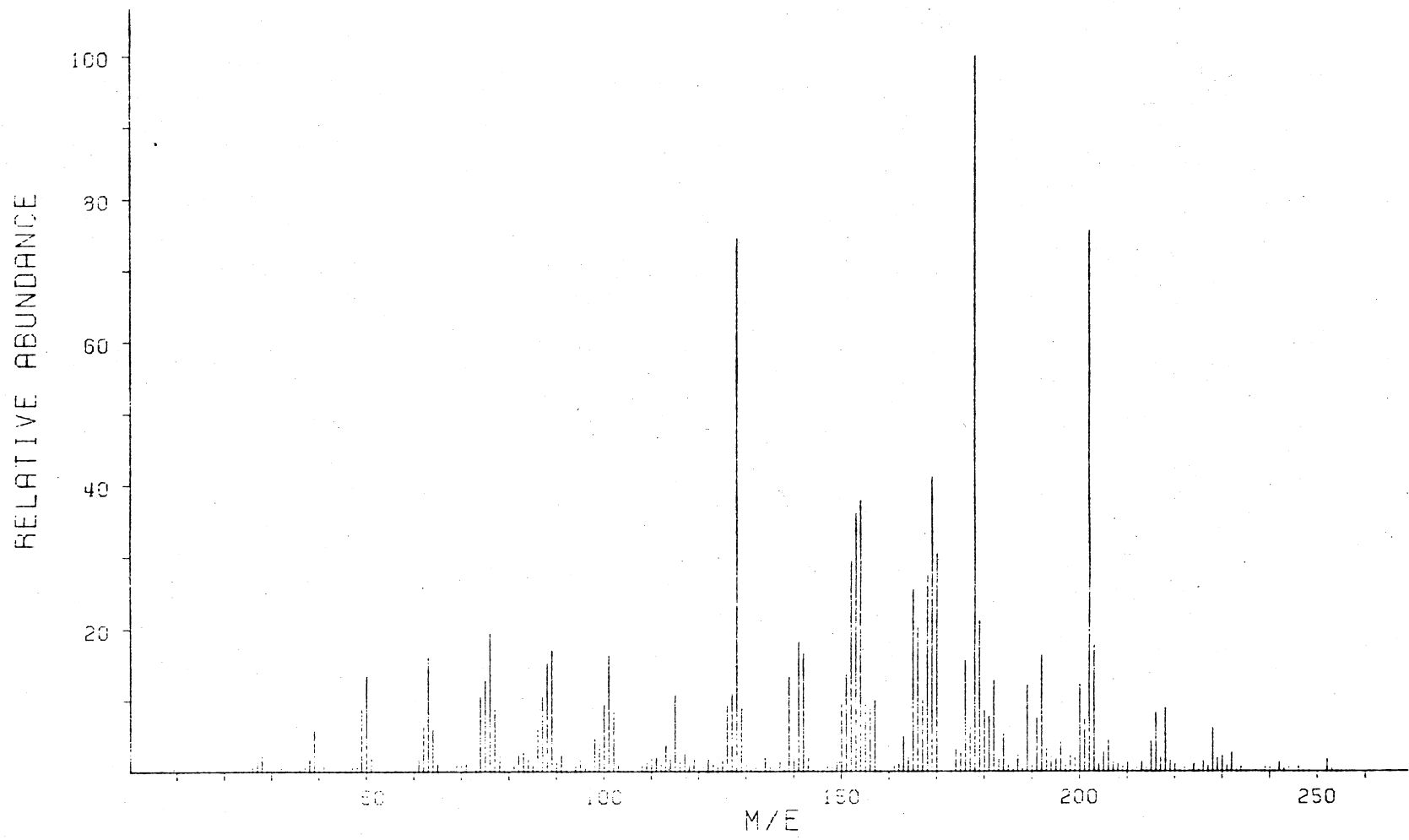


Figure 12. 70-eV Electron-Impact Mass Spectrum of the Hydrocarbon + Ether Fraction From the Anthracene Oil Feedstock

samples was the use of gas-liquid chromatography (GC) and gas-liquid chromatography coupled with mass spectrometry (GC/MS).<sup>30</sup> Figure 13 is a reproduction of the gas chromatogram for the feedstock neutrals. Although the chromatogram exhibits approximately 40 peaks, the major percentage of the sample can be accounted for by fewer than 15 peaks. GC/MS data were acquired on the column effluents in an attempt to determine the components represented by the area under each peak. The total ion current (TIC) from the mass spectrometer was also recorded as a function of time. Comparison of the TIC chromatogram and the gas chromatogram permitted proper compound peak assignments in the gas chromatogram. Since a new multiplier had just been installed on the LKB 9000 gas chromatograph/mass spectrometer the output from the electrometer was sufficient for recording of mass spectra of column effluents. Even with the lowest electron-multiplier voltage some major peaks needed for comparison of relative ion intensities were off scale. For comparison of mass spectra in which key peaks were off scale the pattern of ion  $m/e$  values and ion intensities were used. Aside from these problems, comparison of 140 mass spectra recorded during the course of two GC/MS runs with available standard API mass spectra and knowledge concerning the relative retention times of compounds known to be present in anthracene oils and coal-derived liquids permitted deduction of a number of the compounds and compound types present in the feedstock anthracene oil neutrals.<sup>31</sup> The compounds comprising the major portion of this fraction are naphthalenes and 3- and 4-ring aromatics such as acenaphthene, dibenzofuran, fluorene, phenanthrene and/or anthracene, and fluoranthene and pyrene. The component corresponding to either anthracene or

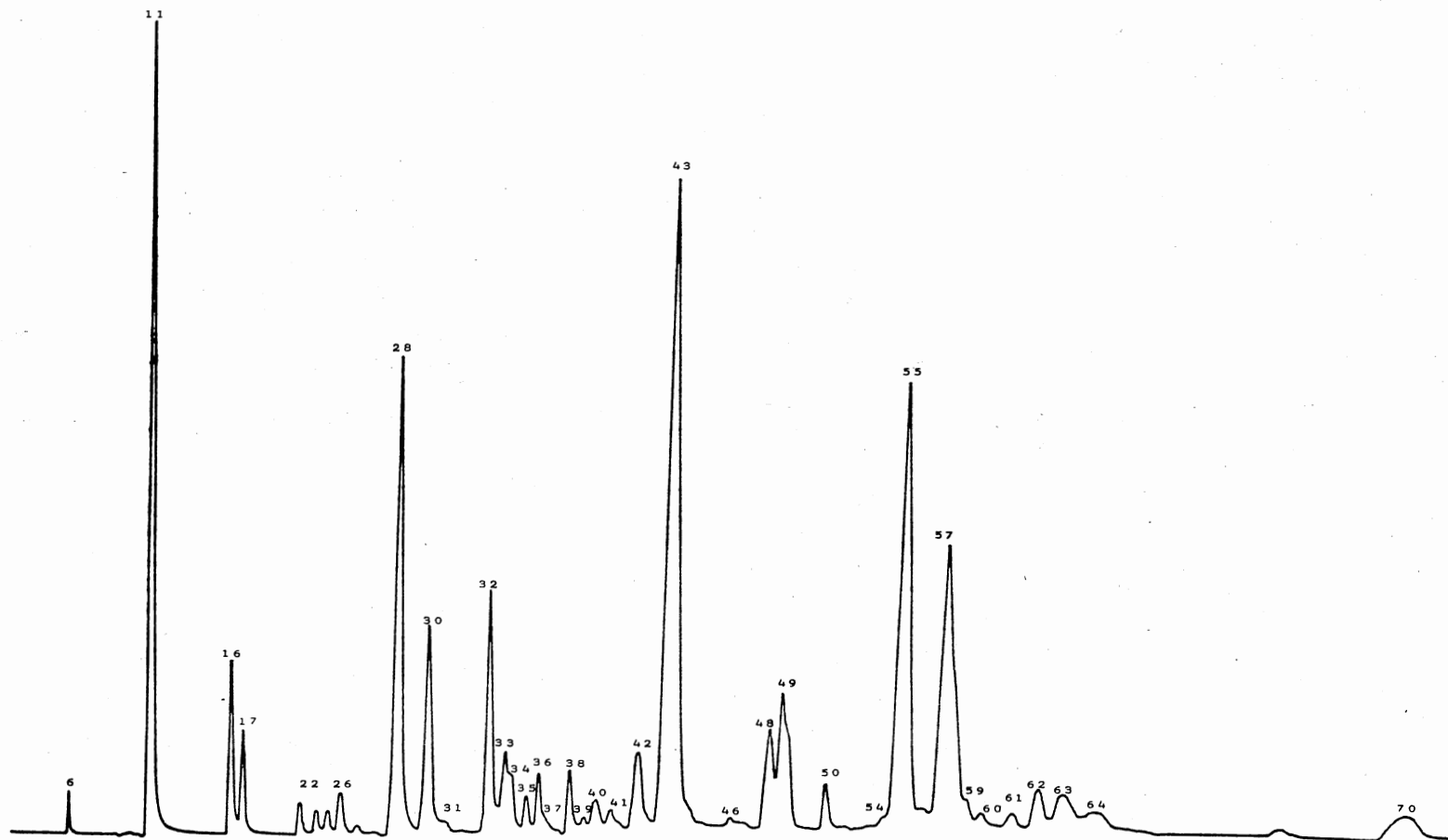


Figure 13. Gas Chromatogram of Feedstock Anthracene Oil Hydrocarbons plus Ether Fraction. Separated on 5% OV-101 on Gas Chrom Z (100/120) AW-DMSC 12' x 1/8" Glass Column; Temperature Program 5 Minutes Isothermal at 100°C Then 1°/Minute to 200°C Then Isothermal; He Flow 23 ml/min.

phenanthrene or both in the feedstock was preparatively isolated by gas chromatography. The component was identified as > 95% phenanthrene. This conclusion is based upon comparison of pure phenanthrene and anthracene standards with the hydrocarbon component using: 1) GC retention times on an OV-101 and a N,N'-bis(p-methoxybenzylidene)- $\alpha,\alpha'$ -bi-p-toluidine column, 2) ultraviolet (UV) spectroscopy and 3) melting point. Figures 14 and 15 are the UV spectra of pure (>99%) phenanthrene and anthracene samples. Since phenanthrene and anthracene exhibit  $\lambda_{\max}$  values of 251 nm and 252 nm, respectively, the unique series of absorptions observed in the spectrum of anthracene in the region from 300 nm to 385 nm were used for identification. A reasonable detectable limit for determination of anthracene in phenanthrene was found by obtaining UV spectra from standard mixtures of the two. Figure 16 shows the UV spectra of a mixture of 95.6% phenanthrene and 4.4% anthracene. At this concentration the absorbance of anthracene at 375 nm is observable and was assumed to be the lower limit for its detection in the mixture. Comparison of the spectra obtained from a solution of the hydrocarbon component(s) of mass 178, Figure 17, reveals absorbances characteristic of phenanthrene with little or no absorbance in the region of 375 nm. The melting points of anthracene, phenanthrene, and the unknown hydrocarbon were 99.5–100°C, 215.5–216°C, and 98–99°C, respectively. Assumably the anthracene has been precipitated during cooling of the liquid obtained from coal pyrolysis and, hence, the product oil should be termed phenanthrene oil.

Gas chromatographic analysis of the four reactor sample neutral fractions showed that catalytic upgrading had significantly increased



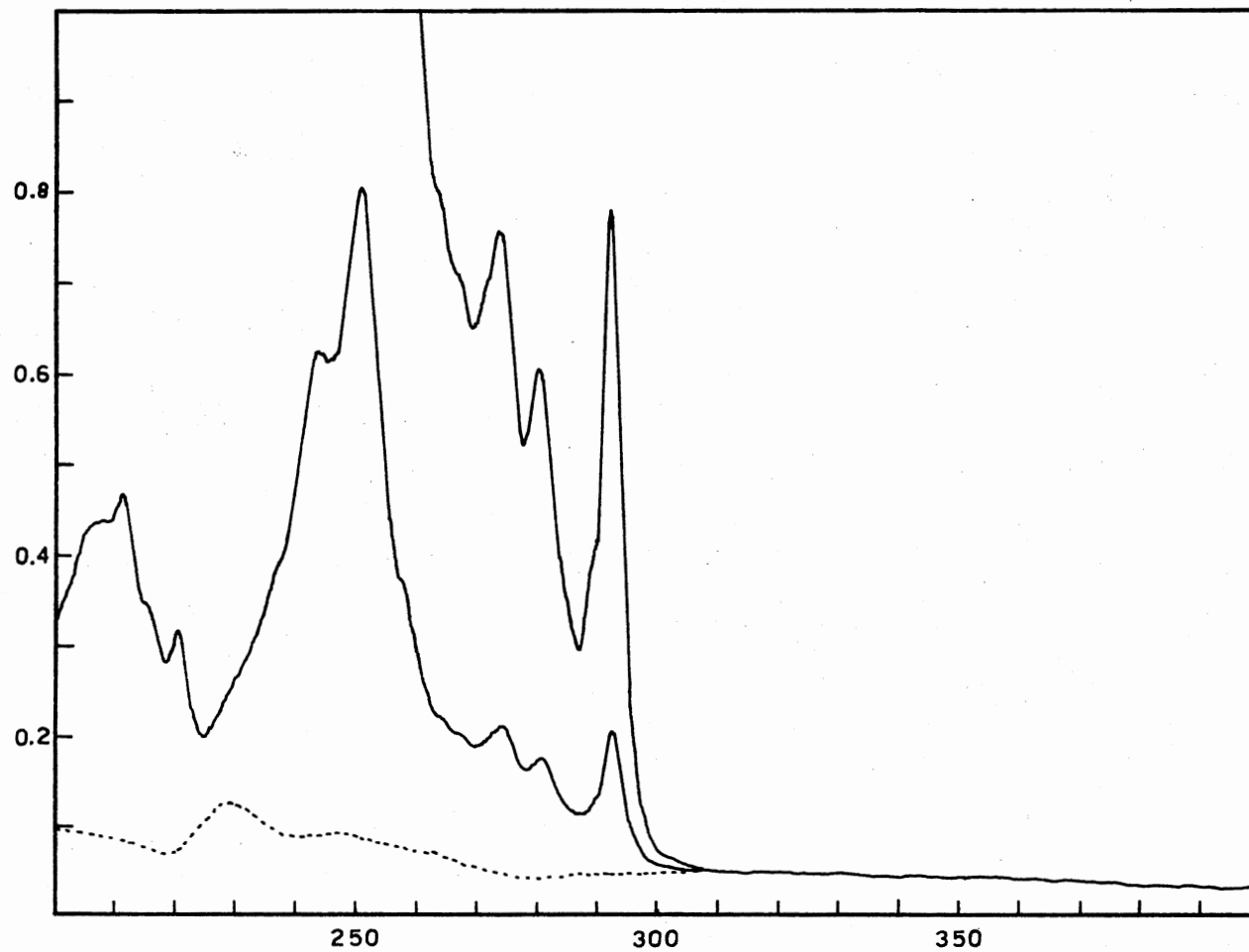


Figure 14. UV Spectrum of Phenanthrene.  $6.106 \times 10^{-4}$  M and  $1.221 \times 10^{-5}$  M  
Solutions, Solvent: n-Hexane

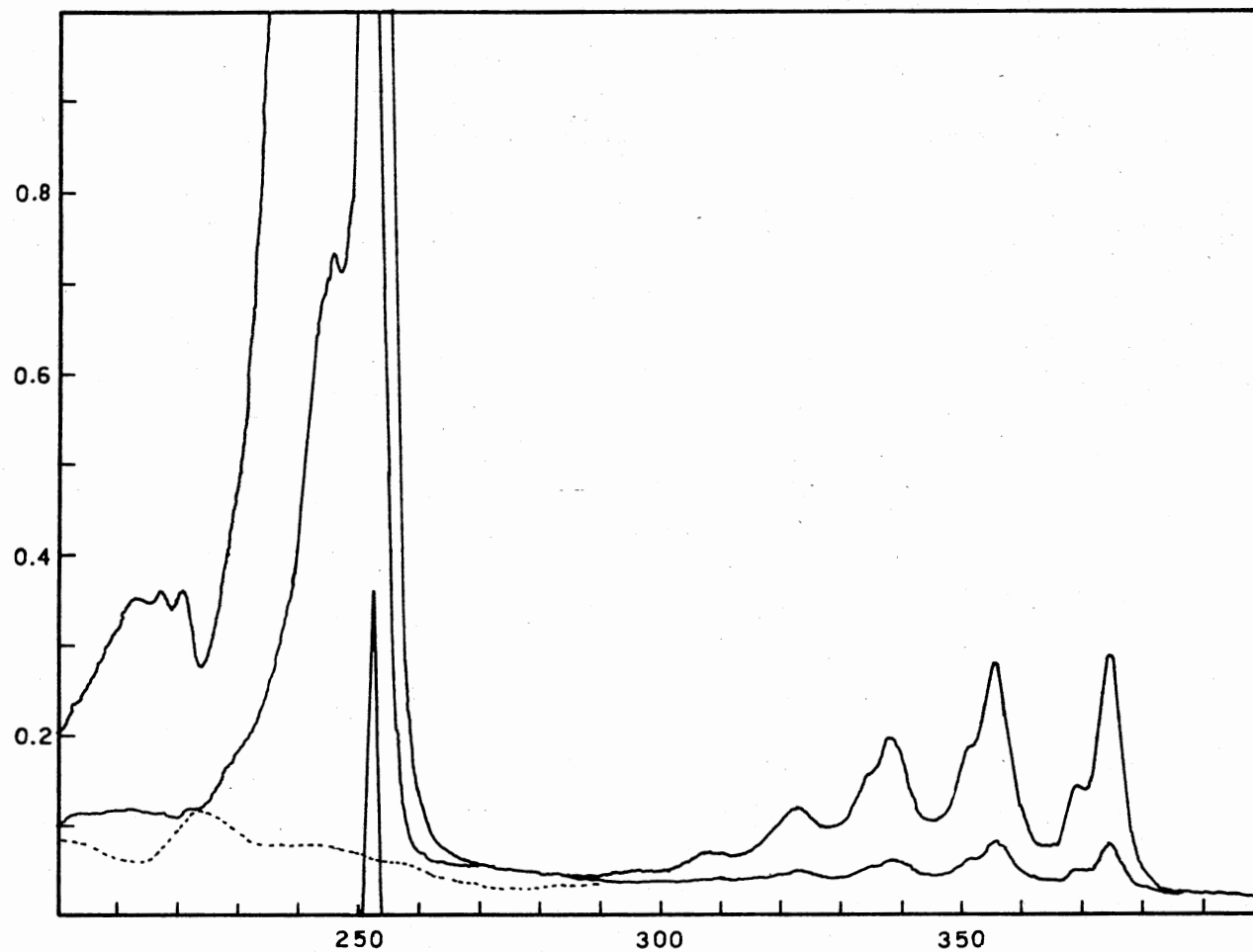


Figure 15. UV Spectrum of Anthracene.  $2.783 \times 10^{-5}$  M and  $5.566 \times 10^{-6}$  M  
Solutions, Solvent: n-Hexane

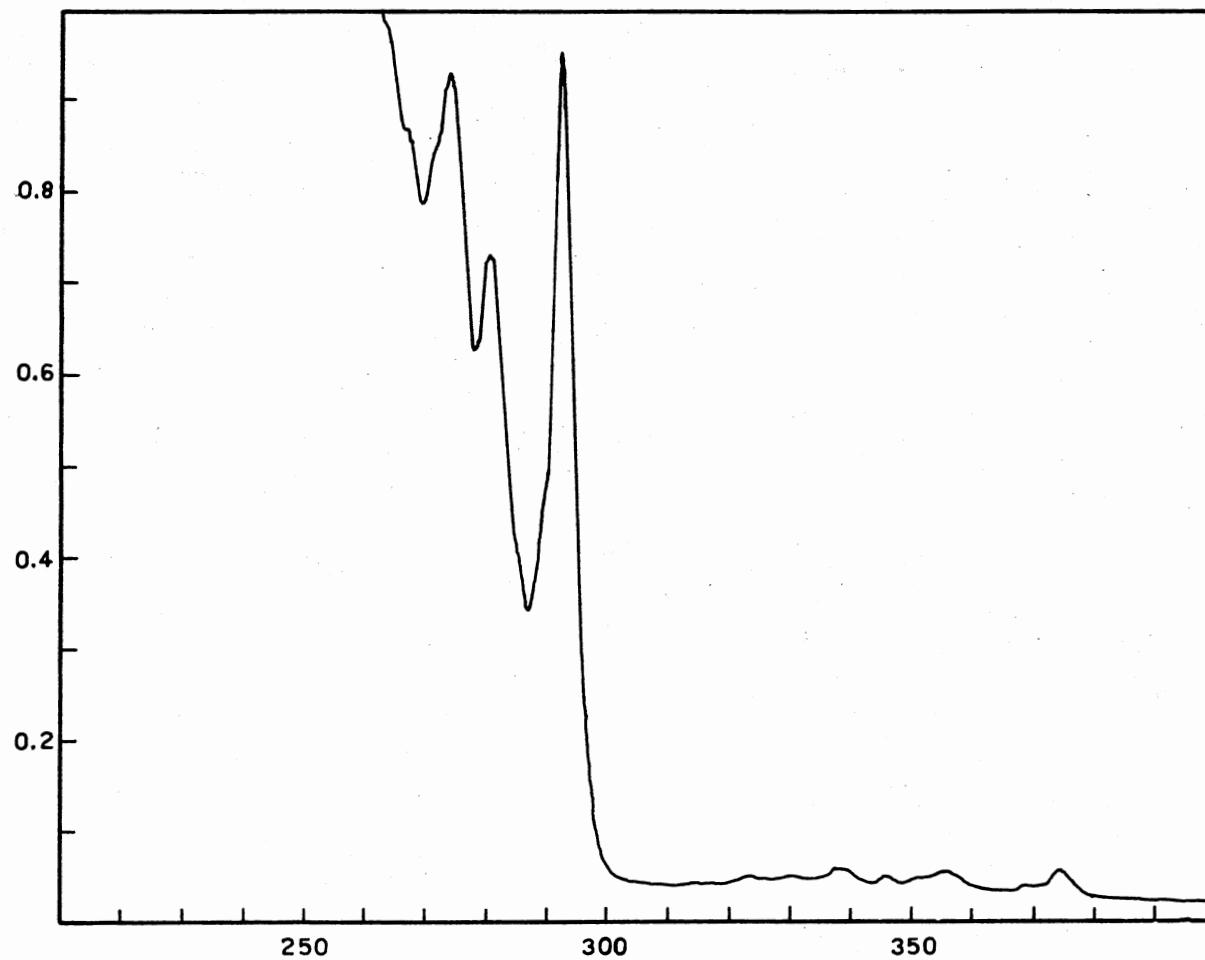


Figure 16. UV Spectrum of Anthracene:Phenanthrene Mixture.  $2.783 \times 10^{-6}$  M Anthracene and  $6.106 \times 10^{-4}$  M Phenanthrene Solution, Solvent: n-Hexane

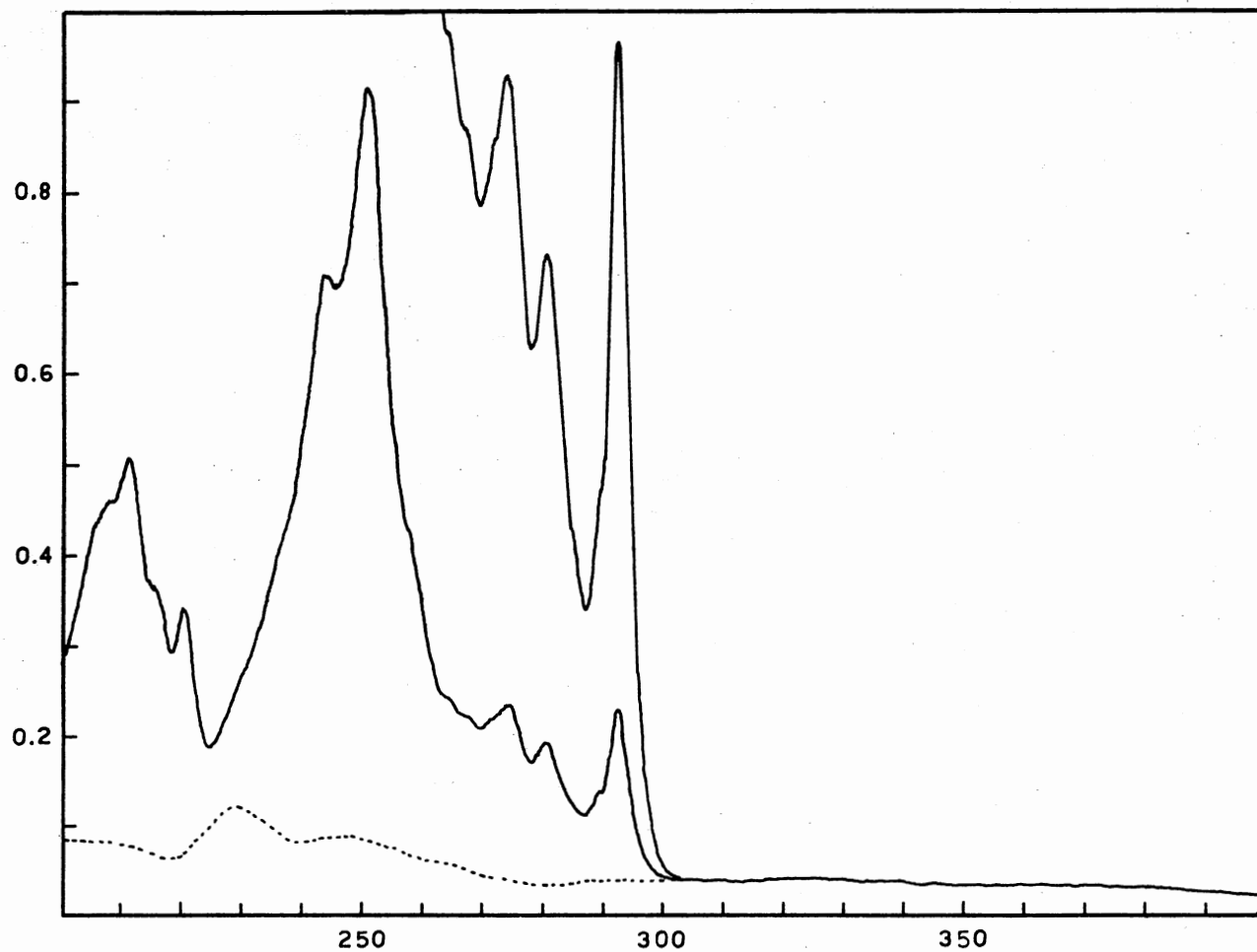


Figure 17. UV Spectrum of Unknown Hydrocarbon with Mass 178.  $4.045 \times 10^{-5}$  M and  $8.090 \times 10^{-6}$  M Solutions, Solvent: n-Hexane

the complexity of the hydrocarbons. Comparison of the gas chromatogram shown in Figure 18 for the neutral fraction from reactor sample 2 with the chromatogram in Figure 13 substantiates this conclusion.

Table VII presents the results of the GC/MS analysis of the feedstock and four upgraded hydrocarbon plus ether fractions. GC/MS analysis of these five fractions involved recording, reviewing, and comparing approximately 400 mass spectra. Data handling and compound assignments were made as previously described. The peak numbers in column 1 of Table VII correspond to the numbers above the peaks in Figures 13 and 14. Column 2 lists  $m/e$  values of ions which either can be assigned to or are consistent with "molecular ion(s)" observed in each of the mass spectra. It is important to note that we do not claim to have identified all compounds or compound types present in these five samples by GC/MS analysis. The major difficulties in interpreting the mass spectral data for the column effluents in these fractions are the presence of peaks arising from column bleed and the possibility of two or more compounds having identical or nearly identical retention times. The former phenomenon contributes to the problem of gas chromatographic column temperatures in excess of 170°C. It should be noted that identification of higher-molecular-weight components was also hampered by the unavailability of standard mass spectra. The weight percents in columns 4-8 of Table VII are on the basis of the total sample and were obtained in the following manner. The peak areas for a chromatogram were normalized assuming the relative gram flame ionization detector (FID) sensitivities to be 1.00. Although this assumption introduces some error into the analysis it was necessary because of the lack of sufficient calibration data. The

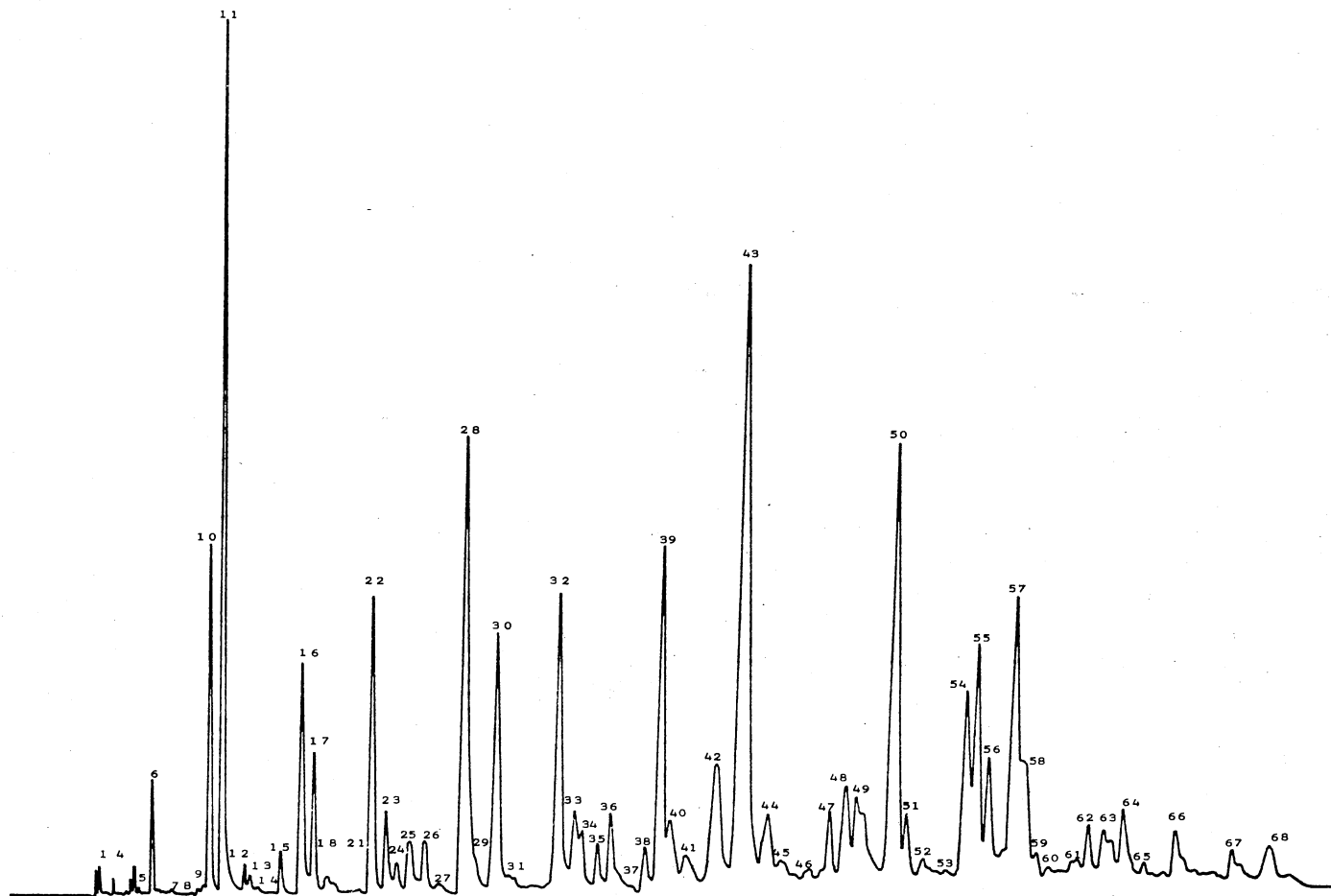


Figure 18. Gas Chromatogram of Reactor Sample 2 Hydrocarbon plus Ether Fraction. Separated on 5% OV-101 on Gas Chrom Z (100/120) AW-DMSC 12' x 1/8" Glass Column; Temperature Programmed 5 Minutes Isothermal at 100°C then 1°/Minute to 200°C Then Isothermal; He Flow 23 ml/min.

TABLE VII

WEIGHT PERCENT OF MAJOR HYDROCARBONS AND ETHERS IN  
FEEDSTOCK AND UPGRADED ANTHRACENE OIL

Peak Number	m/e of Parent Ion	Compound Assignment	Weight Percent <sup>a</sup> in				
			Anthracene Oil Feedstock	Reactor Sample			
				1	2	3	4
1		Unknown		0.22 ± 0.03	0.14	0.07	0.24
2	106	Xylene, Ethylbenzene		0.25 ± 0.07	0.05	0.22	0.14
3	116	Indene		0.20 ± 0.02	0.14	0.18	0.24
4	120	C-3-alkylated benzene		0.17 ± 0.05	0.23	0.14	0.21
5	120	C-3-alkylated benzene		0.22 ± 0.04	0.09	0.14	0.14
6	118	Indane <sup>b</sup>	0.26 ± 0.01	0.94 ± 0.17	0.79	0.90	1.06
7	138	Unknown		0.12 ± 0.01	0.14	0.11	0.16
8	132	Methylindane <sup>b</sup>		0.08 ± 0.01	0.05	0.14	0.07
9	138	Unknown		0.13 ± 0.02	0.07	0.13	0.10
10	132	Tetralin <sup>b</sup>		4.16 ± 0.26	1.84	5.34	2.82
11	128	Naphthalene <sup>b</sup>	6.05 ± 0.18	5.49 ± 0.41	4.79	2.63	5.24
12	146	Methyltetralin <sup>b</sup>		0.41 ± 0.08	0.23	0.44	0.24
13	146	Methyltetralin <sup>b</sup>		0.29 ± 0.05	0.14	0.22	0.17
14	146	Methyltetralin <sup>b</sup>		0.10 ± 0.01	0.05	0.04	0.07
15	146	Methyltetralin <sup>b</sup>		0.63 ± 0.10	0.26	0.83	0.37

TABLE VII (Continued)

Peak Number	m/e of Parent Ion	Compound Assignment	Weight Percent <sup>a</sup> in				
			Anthracene Oil Feedstock	Reactor Sample			
				1	2	3	4
16	142,146 <sup>c</sup>	Methylnaphthalene <sup>b</sup>	1.51 ± 0.05	1.88 ± 0.27	1.66	1.22	1.37
17	142	Methylnaphthalene <sup>b</sup>	0.90 ± 0.02	1.00 ± 0.07	1.14	0.66	0.82
18	160	Dimethyl- or Ethyltetralin		0.56 ± 0.08	0.23	1.17	0.37
19	160	Dimethyl- or Ethyltetralin		0.23 ± 0.05	0.12	0.04	
20		Unknown		0.16 ± 0.03	0.02	0.08	
21	160	Dimethyl- or Ethyltetralin				0.17	0.07
22	154,158 <sup>c</sup>	Biphenyl <sup>b</sup> , Tetrahydroacenaphthene <sup>b</sup>	0.38 ± 0.03	4.35 ± 0.23	2.25	5.62	2.67
23	156	Dimethyl- or Ethylnaphthalene <sup>b</sup>	0.25 ± 0.03	0.96 ± 0.06	0.65	0.66	0.86
24	156	Dimethyl- or Ethylnaphthalene <sup>b</sup>	0.29 ± 0.01	0.44 ± 0.04	0.41	0.22	0.37
25	156	Dimethyl- or Ethylnaphthalene <sup>b</sup>	0.54 ± 0.01	0.78 ± 0.03	0.75	0.77	0.69
26	156	Dimethyl- or Ethylnaphthalene <sup>b</sup>	0.11 ± 0.01	0.87 ± 0.03	0.60	0.95	0.58
27	156	Dimethyl- or Ethylnaphthalene <sup>b</sup>		0.23 ± 0.07	0.14	0.30	0.34
28	154,168 <sup>c</sup>	Acenaphthene <sup>b</sup>	5.62 ± 0.29	3.33 ± 0.44	4.84	2.30	3.88
29	168	Methylacenaphthene		0.70 ± 0.27		0.51	0.82
30	168	Dibenzofuran <sup>b</sup>	2.44 ± 0.06	2.77 ± 0.08	2.81	2.02	2.90
31		Unknown	0.14 ± 0.07		0.14		
32	166	Fluorene <sup>b</sup>	2.82 ± 0.05	3.08 ± 0.04	3.13	3.14	3.20
33	168	Methylacenaphthene	1.52 ± 0.18	0.30 ± 0.06	0.88	0.66	1.09



TABLE VII (Continued)

Peak Number	m/e of Parent Ion	Compound Assignment	Weight Percent <sup>a</sup> in				
			Anthracene Oil Feedstock	Reactor Sample			
				1	2	3	4
34	168	Methylacenaphthene	0.35 ± 0.16	1.10 ± 0.21	0.14	1.54	0.61
35	182	Dimethyl or Ethylacenaphthene	0.46 ± 0.01	0.67 ± 0.01	0.56	0.51	0.61
36	182	Methyldibenzofuran	0.71 ± 0.00	0.89 ± 0.08	0.83	0.73	0.96
37		Unknown	0.17 ± 0.20	0.18 ± 0.07			
38	180	Methylfluorene	0.75 ± 0.01	0.17 ± 0.05	0.58		
39	180	Dihydrophenanthrene	0.25 ± 0.07	3.21 ± 0.04	3.64	2.56	1.72
40	186	Octahydrophenanthrene	0.61 ± 0.04	1.97 ± 0.00	0.18	1.38	2.78
41	196,182,180	Unknowns	0.47 ± 0.18	0.55 ± 0.12	0.83	1.61	1.09
42	196,184,182	Methyltetrahydrophenanthrene, Dibenzothiophene, Tetrahydrophenanthrene	1.46 ± 0.02	3.41 ± 0.27	2.07	3.99	3.49
43	178	Phenanthrene <sup>b</sup>	14.09 ± 1.22	8.57 ± 1.01	10.58	8.86	11.29
44	192	Methylphenanthrene		1.80 ± 0.07	1.45	2.26	1.85
45	212,194	Unknowns		0.48 ± 0.33	0.14	0.18	0.05
46	204	Dihdropyrene		0.52 ± 0.16	0.46	0.47	0.31
47	196	Methyltetrahydrophenanthrene	0.10 ± 0.01	0.89 ± 0.07	1.09	1.10	0.55
48	192	Methylphenanthrene	1.65 ± 0.14	1.66 ± 0.13	1.53	2.05	1.75
49	190,192	Cyclopentaphenanthrene, Methylphenanthrene	3.58 ± 0.86	1.80 ± 0.03	2.42	2.38	1.37

TABLE VII (Continued)

Peak Number	m/e of Parent Ion	Compound Assignment	Weight Percent <sup>a</sup> in				
			Anthracene Oil Feedstock	Reactor Sample			
				1	2	3	4
50	206,208	Unknowns	0.73 ± 0.21	4.34 ± 0.26	5.94	3.94	1.99
51	204	Unknown		0.40 ± 0.02	0.30	0.22	0.41
52	208	Unknown		0.50 ± 0.10	0.41	0.37	0.14
53	208	Unknown		0.26 ± 0.02		0.37	
54	206,204	Unknowns		0.86 ± 0.14	2.68	1.10	0.69
55	202	Fluoranthene <sup>b</sup>	10.30 ± 0.39	3.93 ± 0.26	3.32	3.10	7.00
56	204,220	Unknowns		0.25	2.01	0.14	0.75
57	202	Pyrene <sup>b</sup>	7.45 ± 0.73	4.65 ± 0.39	4.15	4.70	5.48
58	218	Unknown	0.61 ± 0.04	0.39 ± 0.06	1.43		1.78
59	218	Unknown	0.62 ± 0.10	0.13 ± 0.07	0.18		0.34
60		Unknown	0.53 ± 0.14	0.06 ± 0.03	0.05		
61	220 <sup>c</sup> ,216	Unknowns		0.99 ± 0.03	0.83	1.17	0.82
62	216	Unknown	0.99 ± 0.07	0.67 ± 0.04	1.29	0.66	0.96
63	216,218	Unknowns	1.83 ± 0.26	1.47 ± 0.42	2.07	1.10	1.54
64	232,218,216	Unknowns	1.16 ± 0.12	0.75 ± 0.21	1.29	0.88	0.82
65	234,232	Unknowns		0.32 ± 0.05	0.21	0.14	0.10
66	230	Unknown		0.15 ± 0.03	0.74	0.50	0.10

TABLE VII (Continued)

Peak Number	<u>m/e</u> of Parent Ion	Compound Assignment	Weight Percent <sup>a</sup> in				
			Anthracene Oil Feedstock	Reactor Sample			
				1	2	3	4
67	246,232, 218,216	Unknowns		0.68 ± 0.05	0.27		0.51
68		Unknown			0.52		
69	228,244 <sup>c</sup>	Unknowns	0.24 ± 0.09				
70	252,244 <sup>c</sup> , 228	Unknowns	1.21 ± 0.04				

<sup>a</sup>Deviations are average deviations.

<sup>b</sup>Identification made by comparison of m/e values and intensities of ions in recorded spectra with API Project 44 mass spectra.

<sup>c</sup>Observed only in the reactor samples.

weight percents for each component(s) in the mixture were then multiplied by the weight percent of the appropriate neutral fraction in Table VI to obtain the weight percents of each component in the total oil. Since a peak could represent the presence of more than the assigned compounds, the analytical data in Table VII represent an upper limit to the weight percents of the assigned compounds or compound types. The weight percents listed for the neutral components in the feedstock and reactor sample 1 are the average of two determinations; the analytical data for reactor samples 2, 3, and 4 are based upon one analysis each.

Comparison of the weight percent data in Table VII for the feedstock neutrals and with the corresponding results for each of the reactor samples reveals a number of interesting facts. First, there has been an increase in the weight percents of compounds corresponding to both alkyl- and naphthenobenzenes. For example, appearance of peaks 4 and 5 in the upgraded neutrals is attributed to formation of benzene with three carbons exocyclic to the ring. The GC/MS analysis of the effluents corresponding to peaks 10, 12-15, and 18-19 are consistent with the formation of tetralin, methyltetralins and ethyl- and/or dimethyltetralins during upgrading of the anthracene oil. Second, the weight percents for the 2-, 3-, and 4-ring aromatics such as naphthalene, phenanthrene, and pyrene and fluoranthene have, in general, decreased. Third, the weight percents of compounds attributable to hydrogenated polynuclear aromatics have increased. If sufficient GC resolution were available, these data could provide estimates of the degree of hydrogenation occurring in each of the samples. However, the complexity of the MS data and the lack of

computer acquisition of and computer-assisted interpretation of the GC/MS data precluded such an analysis. Proton NMR was used to determine the degree of hydrogenation occurring in each of the neutral reactor fractions. Since the signals for aromatic and nonaromatic protons in each of the samples occur between 6.5-8.7  $\delta$  and 0.0-4.2  $\delta$ , respectively, the ratios of their integrated areas provided estimates of the degree of hydrogenation in each of the neutral reactor fractions. The ratios of saturate to aromatic protons are 0.292, 0.878, 0.688, 1.129, and 0.772 for the feedstock and reactor samples 1 through 4, respectively. These numbers tend to indicate that a significant amount of hydrogenation occurred in the neutral aromatic fractions and that the degree of hydrogenation relates to changes in temperature, pressure, catalyst, and space velocity.

The process of deducing molecular structure for compounds assigned in Table VII is illustrated for the mass spectra recorded for peak 10. Mass spectral data are reproduced in columns 4 and 5 in Table VIII. The highest mass peak attributable to a molecular ion occurs at  $m/e$  132. Aromatic compounds typically found in coal-derived liquids with molecular weights of 132 are tetralins, methylbenzofurans and methylindanes.<sup>17a,b,d;31,33</sup> Columns 6 through 10 in Table VIII present relative abundances for major ions in the mass spectra of representative compounds possessing molecular weight 132. It is important to note that each compound type has a different fragmentation pattern. Comparison of the measured mass spectra recorded as the component(s) comprising peak 10 eluted from the chromatographic column with the standard spectra leads to the conclusion that tetralin and not methylated indanes or methylated benzofurans contribute to determining the

TABLE VIII

COMPARISON OF RELATIVE ABUNDANCES FOR MAJOR IONS IN THE MASS SPECTRUM OF KNOWN ISOMERS WITH MOLECULAR WEIGHT 132 AND THE MASS SPECTRA OF PEAK 10 FROM THE GC/MS OF ANTHRACENE OIL FEEDSTOCK HYDROCARBONS + ETHERS AND RELATED REACTOR SAMPLES

<u>m/e</u>	Relative Intensities								
	Reactor Sample				Tetralin API #539	2-Methyl- benzofuran API #89	7-Methyl- benzofuran API #90	4-Methyl- indane API #941	1-Methyl- indane API #1103
	1 <sup>a</sup>	2 <sup>a</sup>	3	4					
133	-	-	8.3	8.3	4.4	7.9	9.8	4.1	2.9
132	-	-	52.5	66.1	42.2	78.8	100.0	39.0	27.2
131	-	-	13.3	16.5	10.9	100.0	91.5	22.6	9.0
130	-	-	2.7	4.6	1.3	7.4	6.1	1.6	1.8
118	-	-	1.7	0.9	1.2	-	-	9.7	9.8
117	-	-	15.3	17.4	12.8	-	-	100.0	100.0
116	-	-	6.2	6.4	5.1	-	-	9.6	6.7
115	-	-	13.8	15.8	10.8	0.5	-	20.1	20.4
105	-	-	11.7	11.0	9.6	1.2	1.8	2.1	0.5
104	-	-	100.0	100.0	100.0	5.5	18.1	1.8	0.5
103	-	-	9.3	9.2	8.7	13.3	19.0	2.8	1.5
102	-	-	4.0	4.6	3.5	5.3	8.4	2.2	1.7

<sup>a</sup>Base peak at m/e 104 was off scale when spectra were recorded; spectral patterns confirmed tetralin.

peak area. The lack of methylated benzofurans was also substantiated by high resolution mass spectral analysis of the reactor samples (see Appendix B, Table XXXIII).

Compound identification cannot always be accomplished by comparison of experimental and reference mass spectra. For example, Table IX gives in columns 2 and 3 the relative abundances for the major ions in the mass spectra of 1-methyl- and 2-methylnaphthalene, respectively, and in columns 4 through 13 major ions present in the mass spectra of column effluents from peaks 16 and 17 in each sample. It can be seen by comparison of the standard spectra in columns 2 and 3 that, within the limits of experimental error, it would be difficult to differentiate between 1-methyl and 2-methylnaphthalene using mass spectrometry alone. Comparison of the mass spectral data in Table IX shows that for each sample the compounds corresponding to peaks 16 and 17 produce essentially identical mass spectra. However the GC relative retention times of 1.000 and 1.070 for 2-methylnaphthalene and 1-methylnaphthalene, respectively, confirms that the former and the latter contribute to determining the area under peaks 16 and 17, respectively.

The presence of two or more compounds having essentially identical retention times complicates GC analysis. Mass analysis of the effluent can be used to both differentiate and semi-quantify inseparable components provided that they are not isomeric.<sup>34</sup> Conditions needed for this type of analysis are: 1) principal ions used for identification of one component must not appreciably contribute to those being used for identification of the other component(s) and 2) the instrumental sensitivity of each component

TABLE IX

COMPARISON OF RELATIVE ABUNDANCES FOR MAJOR IONS IN THE MASS SPECTRUM OF 1- AND 2-METHYLNAPHTHALENES WITH PEAKS 16 and 17 IN THE GC/MS DATA

<u>m/e</u>	Relative Intensities											
	1-Methyl naphthalene API #487	2-Methyl naphthalene API #855	Anthracene Oil Feedstock Peak		Reactor Sample							
			16	17	1 Peak		2 Peak		3 Peak		4 Peak	
					16 <sup>a</sup>	17	16 <sup>a</sup>	17	16 <sup>a</sup>	17	16 <sup>a</sup>	17
143	11.0	11.6	12.9	12.6	11.9	12.6	12.9	13.1	13.7	12.4	12.6	12.6
142	100.0	100.0	100.0	100.0	100.0	100.0	100.0	100.0	100.0	100.0	100.0	100.0
141	69.1	67.1	71.8	72.3	72.2	72.9	71.3	73.8	74.0	73.5	71.6	73.9
140	5.8	2.8	7.1	6.9	6.3	6.5	7.1	7.4	5.5	6.7	6.3	6.7
139	9.8	9.2	10.0	10.7	10.3	10.3	10.4	10.7	9.6	10.1	10.5	10.9
116	2.7	2.5	2.4	2.5	4.0	2.8	4.3	3.3	11.0	3.4	3.2	2.5
115	25.9	22.8	24.1	25.2	27.8	26.2	25.2	24.6	43.8	25.8	25.3	25.2
114	1.5	1.2	1.2	1.3	0.8	0.9	1.2	0.8	2.2	1.1	1.1	0.8
113	1.8	1.6	1.8	1.9	1.6	0.9	1.7	0.8	2.2	1.1	1.1	1.7

<sup>a</sup>Mass spectra indicated this peak to contain traces of compound with a molecular weight of 146.



either must be known or estimatable. This approach is illustrated using the data in Table X for peak 22 in the GC/MS of the feedstock and reactor sample 1 neutral fractions. Comparison of the data in columns 2 and 5 shows that the  $m/e$  values and the relative abundances of the ions in the mass spectra of peak 22 in the feedstock are in good agreement with those for biphenyl. The mass spectral data for the peak 22 in the reactor sample is seen to contain at least a second component in addition to biphenyl. Comparison of the data in columns 4 and 6 of Table X shows that this component can be attributed to the presence of tetrahydroacenaphthene. Assuming that the sensitivities of the two molecular ions are approximately equal for 70-eV electrons the data in column 4 leads to the conclusion that biphenyl and tetrahydroacenaphthene account for 52 and 48 weight percent of the compounds comprising peak 22, respectively. Since this peak accounts for 4.35% of reactor sample 1 the weight percents of biphenyl and tetrahydroacenaphthene are 2.26% and 2.09%, respectively. It is important to note that the sum of the weight percents of tetrahydroacenaphthene and acenaphthene in reactor sample 1 approximately equals the weight percent acenaphthene found in the feedstock. Since biphenyl could be a product resulting from heteroatom removal from such molecules as dibenzothiophene and carbazole it is significant that its weight percent increases by 600% in reactor sample 1 compared to the feedstock.

The results obtained from GC and GC/MS analysis of the hydrocarbons plus ethers of the feedstock and four hydrotreated samples are pertinent for the following four reasons. First, weight percents of well-resolved components can be compared with results from other types

TABLE X

## GC/MS DATA FOR PEAK NUMBER 22

m/e	Relative Intensities				
	Anthracene Oil Feedstock Peak 22	Reactor Sample 1 Peak 22 Normalized to Mass		Biphenyl API #613	2a,3,4,5-Tetrahydroacenaphthene API #1217
		154	158		
158			36.8		34.0
157			11.7		10.0
155	13.8	17.4	15.5	12.7	3.0
154	100.0	100.0	90.0	100.0	1.0
153	33.4	34.6	30.1	26.2	2.0
152	25.9	29.4	26.4	21.1	3.0
130	0.8		100.0	0.1	100.0
129	0.8		32.2	1.7	30.0
128	5.5		23.0	3.9	15.0
127	3.2		9.4	2.9	5.0
115	5.3		26.4	4.8	23.0

of analysis. Second, the analysis can provide important information concerning isomer distribution as a function of reactor conditions. Third, compositional data can be obtained for compounds possessing either identical exact or nominal masses. Fourth, isolation of specific compounds whose identification would be extremely difficult by mass spectrometry alone can be accomplished. The main disadvantages of GC/MS analysis of complex mixtures is the fact that the analysis can be too detailed and time consuming. Without the use of an adequate data system and reference mass spectra library this technique is not well suited for routine analysis of coal-derived liquids.

High-Resolution Electron-Impact and Low- and  
Medium-Resolution Field-Ionization  
Mass Spectrometry

Analytical data were also obtained using the technique of high-resolution 70-eV electron-impact mass spectrometry with photographic plate recording.<sup>35</sup> The magnetic field was held constant at a strength sufficient to insure that the highest-mass ion detectable in the 70-eV mass spectrum was recorded on the photographic plate.<sup>35</sup> Computer processing of the line positions measured from the photographic plates provided exact masses for various ions in each mass spectrum. The "exact" mass for a particular ion represents the average of the values found in both the feedstock and reactor samples mass spectra unless otherwise stated. A complete listing of the high-resolution 70-eV mass spectral data can be found in Table XXXIII through XXXVI in Appendix B. Exact masses are also listed for best fit

molecular formulas in these Tables. Only molecular formulas with exact masses which deviated less than  $\pm 0.005$  amu from measured values were considered. It should be noted that  $\geq 95\%$  of all the average experimental exact masses agreed with the values for the assigned molecular formulas by  $\leq 0.0025$  amu. This difference is within the standard deviation for the determination of the experimental exact mass. Compound types were then assigned consistent with the molecular formulas deduced from 70-eV electron-impact data and hydrocarbon types previously shown to be present in coal liquids.<sup>17a,b,c;31,33</sup>

Compositional data for the five neutral fractions were calculated from the ion abundances taken from the field ionization mass spectra (FI/MS) of each fraction. Weight percents for the  $i$ th component in the mixture can be calculated either with or without sensitivity corrections. These calculations use equation II-1 and II-2 where  $wt\%_i$  is the weight percent,  $H_i$  is the peak height,  $mw_i$  is the

$$wt\%_i = \left[ \frac{H_i/S_i}{\sum_{i=1}^n H_i/S_i} \right] \times 100 \quad (\text{II-1})$$

$$wt\%_i = \left[ \frac{H_i(mw_i)}{\sum_{i=1}^n H_i(mw_i)} \right] \times 100 \quad (\text{II-2})$$

molecular weight, and  $S_i$  is the relative weight sensitivity for the  $i$ th component. Equation II-2 can be used to provide a first

approximation to the weight percent of the  $i$ th component if the gram sensitivities are assumed to be equal. However, if  $S_i$  is known, equation II-1 is rigorously correct. Since relative FI sensitivities had been determined or could be estimated for compounds shown to be present in the neutral fractions, equation II-2 was used for calculation of quantitative distributions for hydrocarbons and ethers.<sup>19</sup> Computer programs were written to calculate the weight percents of compound types in each fraction. These were then converted into weight percent for the total sample by multiplying each weight percent by the appropriate weight fraction for the neutral fractions listed in Table VI. For each sample the weight percents represent the average of three FI/MS analyses. The compositional data for the neutrals from the four reactor samples were calculated from FI ion abundances obtained over a period of 10 days. It is thus encouraging to note that the percent standard deviation for compounds representing over 2 weight percent of the sample is approximately 3 percent.

The use of FI/MS at a resolution of ca. 6000 permitted separation of ion doublets arising from ionization of hydrocarbons and ethers having the same nominal mass. For example, dibenzofuran ( $C_{12}H_8O$ ) and methylacenaphthene ( $C_{13}H_{13}$ ) have a nominal mass of 168 and exact masses of 168.0575 and 168.0939, respectively. Separation of the  $C_{12}H_8O$  ion from the  $C_{13}H_{13}$  ion requires a resolution of 4600. In analyzing the neutral fractions the resolution of the mass spectrometer was set to permit separation of ions occurring at different exact and identical nominal masses so that the individual ion intensities could be measured.

The compound types assigned to the molecular formulas deduced from high resolution 70-eV electron-impact mass spectra and quantitative distributions calculated from low and medium resolution FI mass spectra for the feedstock and reactor sample neutral fractions are presented in Tables XI-XX. The Z number given in column 1 is used to catalogue the various compound types. For hydrocarbons, the number arises from the relationship  $C_n H_{2n+z}$ .

The feedstock neutral fraction analyzed by FI/MS was found to contain at least 18 compound classes. The hydrocarbon types comprising the major portion of the feedstock were 2-, 3-, and 4-ring aromatics. The carbon number distributions in Table XI are characterized by the majority of the weight percent for each series being accounted for by the parent hydrocarbon and its alkylated derivatives containing one or two carbons exocyclic to the nucleus. Since anthracene oil is the product from a high-temperature coal pyrolysis the compound types and short distributions in Table XI would be expected.<sup>17b</sup> The Z = -6 series is most reasonably comprised of benzene and its alkylated derivatives. FI analysis of the feedstock neutrals showed only trace amounts of compounds in the Z = -6 series containing 9 and 10 carbons. These compounds would be variously substituted alkylbenzenes with three or four carbons exocyclic to the benzene ring. The components of the Z = -8 series are most reasonably attributed to indanes and/or tetralins and their alkylated homologs. Components for the Z = -14 series can correspond to acenaphthene and biphenyl and their alkylated homologs. In this regard, GC/MS and GC relative-retention-time data showed the 154 mass compounds to be 94% acenaphthene and 6% biphenyl. Interpretation of

TABLE XI

## CARBON NUMBER DISTRIBUTION FOR HYDROCARBONS FROM FEEDSTOCK ANTHRACENE OIL


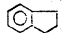
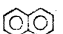
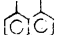

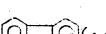
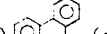
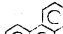
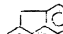
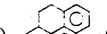



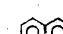

Z Number	Examples of Possible Structures for Parent Molecules	Weight Percents by FI/MS for Carbon Number											Total				
		8	9	10	11	12	13	14	15	16	17	18		19	20		
-6	 (78)	0.05	0.04														0.09
-8	 (118)	0.20	0.14	0.08													0.42
-12	 (128)			4.83	2.31	1.30	0.64	0.23	0.03								9.34
-14	 (154)  (154)					5.26	1.83	1.35	0.37	0.27	0.14	0.04					9.26
-16	 (166)  (180)						2.59	1.85	0.74	0.26	0.10	0.05					5.59
-18	 (178)							10.41	3.18	1.32	0.41	0.11					15.43
-20	 (190)  (204)									1.39	2.37	0.91	0.34	0.33			5.34
-22	 (202)  (202)										12.13	2.66	1.63	0.27	0.16		16.85
-24	 (228)												1.63	0.38	0.16		2.17
-26	 (226)													0.13	0.12	0.16	0.41
-28	 (252)															0.33	0.33
Carbon Number Totals		0.25	5.01	2.39	6.56	5.06	13.84	5.71	16.35	4.22	3.93	1.10	0.81				

TABLE XII

## CARBON NUMBER DISTRIBUTION FOR ETHERS FROM FEEDSTOCK ANTHRACENE OIL

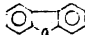
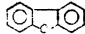
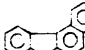
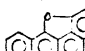
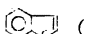
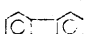
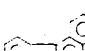
Z Number	Examples of Possible Structures for Parent Molecules	Weight Percents by FI/MS for Carbon Number											Total			
		8	9	10	11	12	13	14	15	16	17	18		19	20	
-16(O)	 (168)					2.06	1.35	0.86	0.27							4.54
-18(O)	 (208)									0.12	0.14					0.26
-22(O)	 (218)										1.30	0.75				2.05
-26(O)	 (244)												0.11			0.11
-10(S)	 (134)	0.15	0.10													0.25
-16(S)	 (184)					0.82	0.24	0.08								1.14
-22(S)	 (234)										0.16					0.16



TABLE XIII

## CARBON NUMBER DISTRIBUTION FOR HYDROCARBONS FROM REACTOR SAMPLE 1


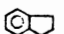
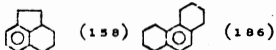
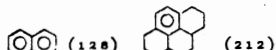

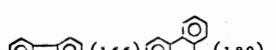
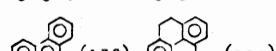
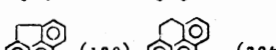
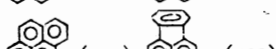
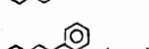
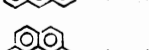
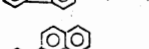
Z Number	Examples of Possible Structures for Parent Molecules	Weight Percents by FI/MS for Carbon Number												Total			
		8	9	10	11	12	13	14	15	16	17	18	19		20		
-6	 (78)		0.25	0.19	0.10	0.09											0.63
-8	 (110)		0.52	3.23	1.42	1.06	0.60	0.20									7.03
-10	 (150) (186)					2.99	1.00	1.49	0.50	0.21							6.19
-12	 (128) (212)			3.92	2.25	1.44	0.73	0.27	0.22	1.25							10.08
-14	 (154) (182)					3.51	1.44	3.33	0.90	0.55	0.29	0.14					10.16
-16	 (166) (180)						2.66	3.73	1.25	1.63	0.53	0.32	0.14				10.26
-18	 (178) (206)							7.25	2.44	3.91	1.15	0.67	0.20	0.10			15.72
-20	 (190) (204)								0.87	2.73	0.85	1.04	0.22	0.16			5.87
-22	 (202) (202)									6.13	1.28	0.92	0.29	0.28			8.90
-24	 (228)											0.51	0.18	0.16			0.85
-26	 (226)												0.25	0.15	0.11		0.51
-28	 (252)															0.10	0.10
Carbon Number Totals			0.77	7.34	3.77	9.09	6.43	16.27	6.18	16.41	4.10	3.85	1.18	0.91			

TABLE XIV

## CARBON NUMBER DISTRIBUTION FOR ETHERS FROM REACTOR SAMPLE 1

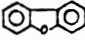
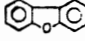


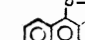
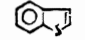
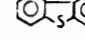
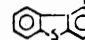
Z Number	Examples of Possible Structures for Parent Molecules	Weight Percents by FI/MS for Carbon Number											Total			
		8	9	10	11	12	13	14	15	16	17	18		19	20	
-16(O)	 (168)					2.34	1.50	0.74	0.32							4.90
-18(O)	 (208)									0.09						0.09
-22(O)	 (218)										0.72	0.35	0.17			1.24
-18(O)	 (222)										0.52	0.22				0.74
-26(O)	 (244)												0.10			0.10
-10(S)	 (134)	0.00	0.00													0.00
-16(S)	 (184)					0.11	0.08	0.00								0.19
-22(S)	 (234)											0.07				0.07

TABLE XV

## CARBON NUMBER DISTRIBUTION FOR HYDROCARBONS FROM REACTOR SAMPLE 2


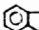
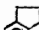
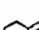
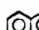
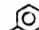



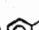
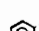

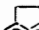
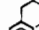
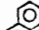




Z Number	Examples of Possible Structures for Parent Molecules	Weight Percents by FI/MS for Carbon Number											Total					
		8	9	10	11	12	13	14	15	16	17	18		19	20			
-6	 (78)		0.21	0.19	0.12	0.05											0.57	
-8	 (118)		0.41	1.84	0.95	0.65	0.52	0.22									4.59	
-10	 (138)  (186)					1.84	0.59	0.56	0.29	0.09							3.37	
-12	 (128)  (212)			4.56	2.41	1.72	0.72	0.30	0.15	0.34							10.20	
-14	 (154)  (182)					4.86	1.75	2.26	0.80	0.28	0.21	0.09					10.25	
-16	 (168)  (180)						2.91	4.84	1.57	0.24	0.37	0.11	0.09				10.13	
-18	 (178)  (206)							7.94	2.82	5.23	1.21	0.67	0.16	0.08			18.11	
-20	 (190)  (204)								0.77	4.02	1.07	0.77	0.17	0.16			6.96	
-22	 (202)  (202)									4.72	1.41	1.39	0.37	0.26			8.15	
-24	 (228)											0.69	0.26	0.20			1.15	
-26	 (226)												0.07	0.07	0.12		0.26	
-28	 (252)																0.13	0.13
Carbon Number Totals			0.62	6.59	3.48	9.12	6.49	16.12	6.40	14.92	4.27	3.79	1.12	0.95				

TABLE XVI

## CARBON NUMBER DISTRIBUTION FOR ETHERS FROM REACTOR SAMPLE 2

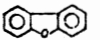
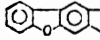
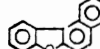
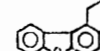
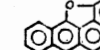
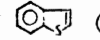
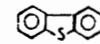
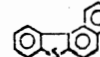
Z Number	Examples of Possible Structures for Parent Molecules	Weight Percents by FI/MS for Carbon Number												Total		
		8	9	10	11	12	13	14	15	16	17	18	19		20	
-16(O)	 (160)					2.41	1.45	0.83	0.37							5.06
-18(O)	 (208)									0.24						0.24
-22(O)	 (218)										1.03	0.50				1.53
-18(O)	 (222)									0.30	0.23					0.53
-26(O)	 (244)												0.08			0.08
-10(S)	 (134)	0.00	0.00													0.00
-16(S)	 (184)					0.36	0.08	0.00								0.44
-22(S)	 (234)										0.10					0.10

TABLE XVII

## CARBON NUMBER DISTRIBUTION FOR HYDROCARBONS FROM REACTOR SAMPLE 3



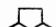
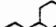
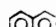

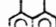




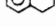
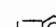
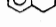





Z Number	Examples of Possible Structures for Parent Molecules	Weight Percents by FI/MS for Carbon Number											Total				
		8	9	10	11	12	13	14	15	16	17	18		19	20		
-6	 (78)		0.18	0.18	0.11	0.06											0.53
-8	 (118)		0.38	4.27	1.92	1.43	0.80	0.32									9.12
-10	 (158)  (186)					3.65	1.39	2.63	0.75	0.40							8.82
-12	 (128)  (212)			2.00	1.24	0.93	0.52	0.29	0.40	1.91							7.29
-14	 (154)  (182)					2.35	1.15	3.41	1.09	0.48	0.32	0.18					8.98
-16	 (166)  (180)						2.46	2.97	1.10	1.87	0.61	0.52	0.17	0.06			9.76
-18	 (178)  (206)							5.94	2.10	3.57	1.19	0.75	0.24	0.16			13.95
-20	 (190)  (204)								0.72	2.18	0.72	1.03	0.24	0.20			5.09
-22	 (202)  (202)									5.25	1.13	0.81	0.10	0.28			7.57
-24	 (228)											0.63	0.24	0.29			1.16
-26	 (226)											0.35	0.27	0.12			0.74
-28	 (252)														0.21		0.21
Carbon Number Totals			0.56	6.45	3.27	8.42	6.32	15.56	6.11	15.66	3.97	4.27	1.26	1.32			

TABLE XVIII

## CARBON NUMBER DISTRIBUTION FOR ETHERS FROM REACTOR SAMPLE 3


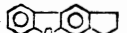


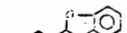
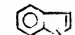


Z Number	Examples of Possible Structures for Parent Molecules	Weight Percents by FI/MS for Carbon Number												Total			
		8	9	10	11	12	13	14	15	16	17	18	19		20		
-16(O)	 (168)					2.04	1.39	0.85	0.33								4.61
-18(O)	 (208)									0.14							0.14
-22(O)	 (218)										0.46	0.27	0.12				0.85
-18(O)	 (222)									0.58	0.19						0.77
-26(O)	 (244)												0.08				0.08
-10(S)	 (134)	0.00	0.00														0.00
-16(S)	 (184)					0.05	0.03	0.00									0.08
-22(S)	 (234)										0.00						0.00

TABLE XIX

## CARBON NUMBER DISTRIBUTION FOR HYDROCARBONS FROM REACTOR SAMPLE 4


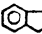
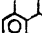
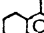
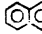
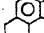
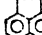
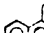

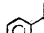

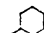
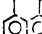
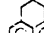
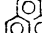
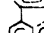
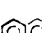
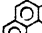
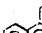
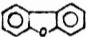
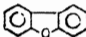
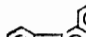

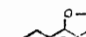

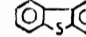

Z Number	Examples of Possible Structures for Parent Molecules	Weight Percents by FI/MS for Carbon Number												Total			
		8	9	10	11	12	13	14	15	16	17	18	19		20		
-6	 (78)		0.26	0.21	0.10												0.57
-8	 (118)		0.49	2.54	1.16	0.79	0.33	0.13									5.44
-10	 (138)  (186)					2.40	0.67	0.99	0.33	0.14							4.53
-12	 (128)  (212)			4.45	2.30	1.60	0.71	0.31	0.17	0.52							10.06
-14	 (154)  (182)					4.30	1.82	3.58	1.07	0.44	0.25	0.08					11.54
-16	 (166)  (180)						2.84	2.56	1.11	1.24	0.44	0.27	0.10	0.01			8.57
-18	 (178)  (206)								8.79	2.60	2.39	0.84	0.47	0.13	0.05		15.27
-20	 (190)  (204)									1.11	2.37	0.81	0.95	0.18	0.08		5.50
-22	 (202)  (202)										8.99	1.70	0.97	0.26	0.23		12.15
-24	 (228)												0.69	0.22	0.17		1.08
-26	 (226)												0.12	0.10	0.10		0.32
-28	 (252)															0.16	0.16
Carbon Number Totals			0.75	7.20	3.56	9.09	6.37	16.36	6.39	16.09	4.04	3.55	0.99	0.80			

TABLE XX

## CARBON NUMBER DISTRIBUTION FOR ETHERS FROM REACTOR SAMPLE 4

Z Number	Examples of Possible Structures for Parent Molecules	Weight Percents by FI/MS for Carbon Number											Total		
		8	9	10	11	12	13	14	15	16	17	18		19	20
-16(0)	 (168)					2.42	1.46	0.88	0.36						5.12
-18(0)	 (208)								0.15						0.15
-22(0)	 (218)									0.78	0.39	0.16			1.13
-18(0)	 (222)									0.41	0.16				0.57
-26(0)	 (244)											0.08			0.08
-10(S)	 (134)	0.00	0.00												0.00
-16(S)	 (184)					0.13	0.09	0.00							0.22
-22(S)	 (234)									0.02					0.02



the data for the Z = -14 series above C<sub>13</sub> is complicated by the possible presence of tetrahydrophenanthrenes. The -16 Z series is consistent with a series of fluorenes, a series of dihydrophenanthrenes commencing at C<sub>14</sub>, and beginning at C<sub>16</sub> the presence of a series of hexahdropyrenes and/or hexahydrofluoranthenes. The shape of the feedstock distribution would tend to indicate that the feedstock carbon number distribution is composed of primarily fluorene and its alkylated homologs.

As discussed previously, the first carbon number in the -18 Z series is represented by  $\geq 95\%$  phenanthrene. For this reason, it is believed the weight percents in this Z series are represented by phenanthrene and its alkylated homologs rather than anthracene and its alkylated homologs. At C<sub>16</sub> in this series tetrahydropyrene and/or tetrahydrofluoranthene are isomerically possible. However, the highly aromatic nature of the feedstock and the shape of the carbon number distribution for this series suggest that such compounds contribute minimally. Reasonable constituents in the -20 Z series are cyclopentaphenanthrenes (mass 190) and dihydropyrenes and their alkylated homologs. The presence of dihydropyrene in the feedstock is suggested but not proven by the increase in the weight percent at C<sub>16</sub> of this distribution. The -22 Z series is consistent with the presence of pyrene and/or fluoranthene. The weight percents of pyrene (mass 202) and fluoranthene (mass 202) are 5.09 and 7.04, respectively from GC/MS data. The presence of both isomers in the feedstock complicates assignment of molecular structures at C<sub>17</sub>, C<sub>18</sub>, C<sub>19</sub>, and C<sub>20</sub>. The -24 Z series are characteristic of the presence of benzoanthracenes or benzophenanthrenes. These possible molecular

structures were chosen since the nonlinear type of polynuclear aromatic molecules tend to be the predominant structural type in coal liquids.<sup>36</sup> The high-resolution data for compounds in the -26Z series is consistent with but does not prove the presence of benzo-fluoranthene in the feedstock neutrals. The -28 Z series corresponds to molecules such as benzopyrenes. The weight percents of compounds which would correspond to methylated benzopyrenes have been summed with the weight percent of the parent aromatic observed in the -28 Z series.

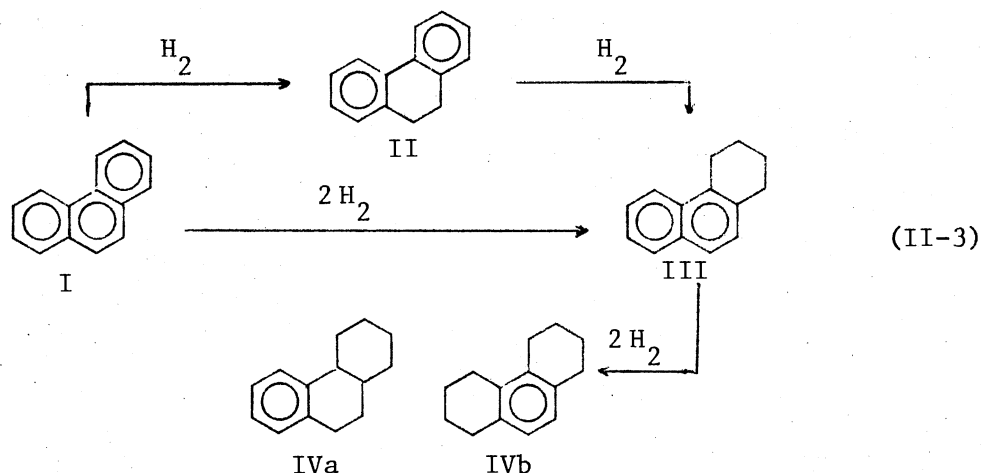
Table XII presents the carbon number distributions for the major oxygen and thio type ethers present in the feedstock neutral fraction. Molecular formulas were consistent with the presence of dibenzofurans, benzonaphthofurans, benzothiophenes, dibenzothiophenes, and benzonaphthothiophenes. The carbon number distributions, like those for the hydrocarbons, are short and the weight percents drop off rapidly after the carbon value corresponding to the parent compound.

Comparison of the carbon number distributions of the reactor sample neutral fractions with those of the feedstock revealed a number of interesting facts. First, upgrading has shifted the major portion of the hydrocarbon distribution to lower Z series. For example, the weight percent of hydrocarbons represented by compound types in Z series up to Z = -18 has increased from 40.13% in the feedstock to 60.07%, 57.22%, 58.45%, and 55.98% for reactor samples 1-4, respectively. This result suggests the occurrence of hydrogenation and hydrogenolysis of higher-molecular-weight hydrocarbons and formation of lower-molecular-weight hydrocarbons from

removal of heteroatoms. The increase in both the length of the carbon number distribution and the total weight percent in the benzene series ( $Z = -6$ ) from 0.09% in the feedstock to 0.63%, 0.57%, 0.53%, and 0.57% for reactor samples 1-4, respectively, supports these postulates. Furthermore, for each of the reactor samples the sum of the weight percents of tetralin ( $C_{10}$  in the  $-8 Z$  series) and naphthalene ( $C_{10}$  in the  $-12 Z$  series), which are 7.15, 6.40, 6.27, and 6.99 weight percent for reactor fractions 1-4, respectively, exceed the weight percent for the corresponding  $C_{10}$ 's in the feedstock, which is 4.97%. Application of similar mass balance to higher-molecular-weight compounds leads to similar results. However the percentages decrease as the size of the compound type nucleus increases.

The types of partially hydrogenated aromatics within a given series of compound types are indicative of changes in reaction conditions during upgrading. This is demonstrated by the phenanthrene series data. The column corresponding to the weight percents of  $C_{14}$  hydrocarbons in Tables XIII, XV, XVII, and XIX can be represented by the presence of phenanthrene (I) in the  $-18 Z$  series, methylfluorene and/or dihydrophenanthrene (II) in the  $-16 Z$  series, acenaphthene and/or biphenyl with two carbons exocyclic to the aromatic nucleus and/or tetrahydrophenanthrene (III) in the  $-14 Z$  series, and octahydrophenanthrene (IV) in the  $-10 Z$  series. If we assume that the weight percents of 1.85 and 1.35 in the feedstock carbon distribution are the upper limit for the weight percent of methylfluorenes and alkylated acenaphthenes and/or biphenyls in the reactor samples then the increases and decreases of weight percents for

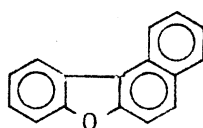
$C_{14}$  compounds in the -18, -16, -14, and -10 Z series, as a function of reactor conditions can be used to postulate the progressive hydrogenation of phenanthrene (Equation II-3). A decrease in the



reactor temperature from 700°F to 600°F (compare Tables XIII and XV) reduces the weight percent of IV from 1.49% to 0.56% and the weight percent of III from 4.84% to 3.73%. Reduction in reactor temperature increases the weight percent of II from 3.73% to 4.84%. Comparison of the data in Tables XVII and XIX shows that a decrease in hydrogen pressure from 1020 psig to 507 psig reduces the formation of IV by 1.64%, i.e., from 2.62 to 0.99. The weight percent of III remains essentially constant whereas the weight percent of II drops from 2.97% to 2.56%. As shown by the data in Tables XIII and SVIII, changing the catalyst from Nalco Sphericat to Harshaw HT 400 increases the weight percent of IV from 1.49% to 2.63%. The weight percent of III remains essentially constant, whereas the weight percent of II decreases from 3.73 to 2.97 and of I decreases from 7.25% to 5.94%. It is realized that differences in space velocity and catalyst aging between samples could also affect the product distributions. However for this discussion changes in these parameters

are assumed to have a minimal effect on the product distributions. These results are similar to those reported by Qader in his study of hydrogenation/hydrocracking of anthracene using CoS, MoS<sub>2</sub>, NiS and WS<sub>2</sub> supported on silica-alumina.<sup>37</sup> Qader found that reaction products could be explained by the hydrogenation of anthracene to form dihydro-, tetrahydro- and octahydroanthracene, which then underwent hydrocracking to form benzindanes and alkylated naphthalenes. It should be noted that the weight of C<sub>14</sub> in the naphthalene series (Z = -12) is higher in all four reactor samples than in the feedstock. It is important to note that in both Qader's model compound study and our work there was no evidence for formation of the perhydroanthracenes and perhydrophenanthrenes in the upgrading process.

The aromatic ethers were found to be resistant in both hydrogenation and hydrogenolysis. For example, as seen in Tables XII, XIV, XVI, XVIII, and XX, the total weight percent of compounds consistent with dibenzofuran in the feedstock is 4.54% and for reactor samples 1-4 the weight percents are 4.90, 5.06, 4.61 and 5.12, respectively. The increase in the weight percent for reactor sample 2 and 4 may reflect either the combined uncertainty of the separation and analysis or intramolecular cyclization of a hydroxybiphenyl. With one exception no evidence was found for partially hydrogenated aromatic ethers. The exception was the presence of compounds whose molecular formulas are consistent with benzonaphthofuran (VII) in the -6(0) Z series. High-resolution data for the



VII

reactor samples revealed the presence of compounds in the -2(0) Z series which correspond in molecular formula to the tetrahydro derivatives of the compounds in the -6(0) series. In the reactor samples 1-4 the sum of the weight percents across both the -2(0) and -6(0) Z series at C<sub>16</sub> and at C<sub>17</sub> is 1.24 and 0.57, 1.33 and 0.73, 1.04 and 0.46, and 1.19 and 0.55, respectively. The feedstock data show weight percents of 1.44 and 0.75 for these carbon numbers. Comparison of this data leads to the conclusion that appreciable deoxygenation of these compound types did not occur during the upgrading process. However, increases in the weight percents of the -2(0) Z series at C<sub>16</sub> and C<sub>17</sub> are indicative of formation of tetrahydro VII. Weight percents for C<sub>16</sub> and C<sub>17</sub> in the -2(0) Z series are 0.72 and 0.35, 0.30 and 0.23, 0.58 and 0.19 and 0.41 and 0.16, respectively for reactor samples 1-4. This compares with 0.14 and 0.00 for the weight percents at C<sub>16</sub> and C<sub>17</sub> in the feedstock. It is important to note that the carbon number distribution for the -6(0) series has increased in length in the reactor samples as compared with the feedstock.

The thiophene-type compounds were shown to be very reactive toward sulfur removal for the catalysts, temperatures and H<sub>2</sub> pressures employed during the upgrading. This is supported by the virtual absence of thiophene-type molecules in reactor samples as compared to the feedstock. No evidence was found in the reactor samples for the presence of partially hydrogenated thiophenes. This observation is consistent with desulfurization studies on benzothiophene in which formation of the partially reduced analogs was insignificant.<sup>38</sup>

High-resolution 70-eV mass spectral data were obtained for each of the 15 acidic, basic, and neutral-nitrogen-containing fractions separated from the feedstock and upgraded anthracene oil. A complete tabulation of the experimental exact masses, calculated exact masses and corresponding molecular formulas is given in Table XXXIV through XXXVI of Appendix B. The determination of and the assignment of molecular formulas to the experimental exact masses was accomplished as previously described for the feedstock and reactor sample neutral fractions.

The low-resolution FI/MS was recorded in triplicate for each of the acidic, basic and neutral-nitrogen-containing fractions. For each fraction semiquantitative distributions were calculated from FI ion abundances assuming unit-relative sensitivities. Although not valid, the assumption of unit-relative-gram sensitivities is presently required because of the absence of sufficient field-ionization sensitivity data for the compound classes encountered in these fractions. However, it should be noted that previous investigations of the FI-relative sensitivities show that the variation in their magnitude with change in molecular structure is considerably less than that observed for ionization by low-voltage electrons.<sup>19</sup> Hence, these studies and the analysis of synthetic blends suggest that the assumption of unit-relative sensitivities yields reasonable first approximations to the weight percents of the compound types present in these fractions.<sup>19</sup> Also in converting FI-ion abundances obtained for the acid fraction to weight percents, the intensity at  $m/e$  X was corrected where necessary for the isotopic contribution from the ion at mass X-1. For example, in the FI/MS of reactor sample 4

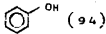
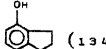
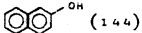
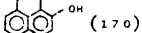
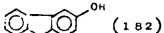
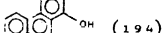
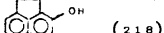
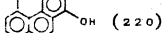
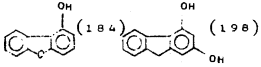
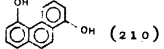
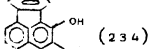
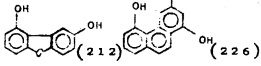
the  $C_{13}H_{11}N$  ion,  $m/e$  181, contributes ca. 35 percent of the total intensity at  $m/e$  182. Therefore, the weight percent of fluorenol (mass 182) is reduced from 0.67% to 0.45% upon correcting the intensity of the 182 ion for the contribution from the intensity of the ion at  $m/e$  181. For the base and neutral-nitrogen fractions such isotope corrections do not alter the weight percents within the limits of experimental precision. The recording of FI/MS at an instrument resolution of ca. 6500 provided the requisite ion intensity data for computing the weight percents of the compound types in the acid and base fractions possessing identical nominal but different exact masses. Quantitative distributions for the neutral-nitrogen-containing fractions were based upon the low-resolution FI/MS data owing to the absence of molecular ion multiplets.

The carbon number distribution obtained for the oxygen-containing acids in the feedstock is presented in Table XXI. Column 2 in Table XXI lists reasonable structures which are consistent with the 70-eV high-resolution data for the parent compound in each Z series. These assignments are based upon conclusion drawn from previous analysis of coal-derived materials and from our analysis of the compound types observed in the hydrocarbon fractions.<sup>17a,b,d;31,33,40</sup> The weight percents presented in the carbon number distributions refer to the total anthracene oil. The feedstock acid fraction is composed primarily of singly oxygenated compounds whose molecular formulas are consistent with phenols, indanols, naphthalenols, acenaphthenols and/or phenylphenol and fluorenols. These compound types account for respectively 34%, 4%, 9%, 12% and 10% of the feedstock oxygen-containing acids. The



TABLE XXI

## CARBON NUMBER DISTRIBUTION FOR THE OXYGEN-CONTAINING ACIDS FROM ANTHRACENE OIL

Z Number	Examples of Possible Structures for Parent Molecules	Weight Percents by FI/MS for Carbon Number													Total		
		6	7	8	9	10	11	12	13	14	15	16	17	18		19	
-6(0)	 (94)	0.91	1.46	1.06	0.33	0.15	0.03	0.06									4.00
-8(0)	 (134)				0.16	0.14	0.07	0.06	-	0.03							0.46
-12(0)	 (144)				0.31	0.34	0.18	0.10	0.10								1.03
-14(0)	 (170)								0.35	0.48	0.35	0.20	0.08	0.02			1.48
-16(0)	 (182)									0.53	0.31	0.20	0.09	0.06	0.02		1.21
-18(0)	 (194)										0.13	0.09	0.06	0.03			0.31
-22(0)	 (218)												0.08	0.03	0.03		0.14
-20(0)	 (220)												0.18	0.12	0.07	0.03	0.40
-16(O <sub>2</sub> )	 (184) (198)								1.11	1.00	0.46	0.16	0.06				2.79
-18(O <sub>2</sub> )	 (210)												0.03				0.03
-22(O <sub>2</sub> )	 (234)												0.02	0.01			0.03
-16(O <sub>3</sub> )	 (212) (226)								0.05	0.06	0.02						0.13

molecular formulas for the multioxygenated compounds are consistent with but do not necessarily prove the presence of compound types such as hydroxydibenzofurans or fluorenediols. These two series of compounds accounts for 23% of the feedstock oxygen acids.

Comparison of the mass spectra for the reactor sample acid fractions with that from the feedstock shows that the oxygen-containing acids were extremely susceptible to deoxygenation. Table XXII lists the molecular weight, molecular formula and a possible structure type for each of the 12 oxygen-containing acid series isolated from the feedstock and upgraded oils. Columns 4-8 in Table XXII list the sum of the weight percents from the carbon number distribution of each series for the feedstock and reactor samples 1-4. Comparison of the feedstock weight percents with those for the reactor samples indicates acidic oxygen functions are easily removed for the reaction conditions, space times, and catalysts employed. Changes in reactor temperature (compare columns 5 and 6) and  $H_2$  pressure (compare column 7 and 8) appear to have some effect on the degree of deoxygenation in these samples. It is important to note that except for the presence of molecular formulas consistent with dihydroxyrenol there was no evidence for existence of partially hydrogenated phenols in the feedstock or reactor samples. Thus, if oxygen removal proceeds via reduction of aromatic carbon-carbon double bonds then the hydroaromatics so produced must be more reactive than their aromatic precursors.

The degree of aliphatic substitution on the aromatic nucleus also affects the ease of deoxygenation. For example, Table XXIII presents data for the weight percents of phenol and its alkylated

TABLE XXII

WEIGHT PERCENTS OF OXYGEN-CONTAINING ACIDS IN FEEDSTOCK AND UPGRADED ANTHRACENE OIL

Molecular Weight	Parent Compound		Feedstock	Weight Percent in			
	Molecular Formula	Possible Structural Type		Reactor Samples			
				1	2	3	4
94	$C_6H_6O$	phenol	4.00	0.10	0.91	0.33	0.77
134	$C_9H_{10}O$	indanol	0.46	0.21	0.49	0.43	0.21
144	$C_{10}H_8O$	naphthalenol	1.03	0.00	0.01	0.00	0.00
170	$C_{12}H_{10}O$	acenaphthenol	1.48	0.02	0.46	0.27	0.33
182	$C_{13}H_{10}O$	fluorenol	1.21	0.03	0.46	0.35	0.27
184	$C_{12}H_8O_2$	dibenzofuranol	2.79	0.00	0.36	0.00	0.06
		fluorenediol					
194	$C_{14}H_{10}O$	phenanthrenol	0.31	0.00	0.05	0.00	0.00

TABLE XXII (Continued)

Parent Compound			Weight Percent in				
Molecular Weight	Molecular Formula	Possible Structural Type	Feedstock	Reactor Samples			
				1	2	3	4
210	$C_{14}H_{10}O_2$	phenanthrenediol	0.03	0.00	0.00	0.00	0.00
212	$C_{14}H_{10}O_3$	phenanthrenetriol	0.13	0.00	0.00	0.00	0.00
218	$C_{16}H_{10}O$	fluoranthenol	0.14	0.00	0.06	0.06	0.04
220	$C_{16}H_{12}O$	dihydropyrenol	0.40	0.00	0.17	0.13	0.19
234	$C_{16}H_{10}O_2$	fluoranthenediol	0.03	0.00	0.00	0.00	0.00
Reactor Temperature (°F)				700	600	700	700
Reactor Pressure (psig)				1000	1000	1020	507
Space Time (hrs.)				1.48	2.50	0.75	0.75
Catalyst				Nalco	Sphericat 474	Harshaw 400	HT

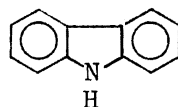
TABLE XXIII

WEIGHT PERCENT OF PHENOLS IDENTIFIED IN ACID FRACTION FROM  
FEEDSTOCK AND HYDROTREATED ANTHRACENE OIL

Example of Structural Type	Molecular Weight	Feedstock	Weight Percent in			
			Reactor Sample			
			1	2	3	4
Phenol	94	0.91	0.00	0.10	0.04	0.11
Methylphenol	108	1.46	0.00	0.23	0.08	0.21
Dimethylphenol	122	1.06	0.00	0.28	0.08	0.23
Trimethylphenol	136	0.33	0.01	0.15	0.06	0.13
Tetramethylphenol	150	0.15	0.03	0.07	0.04	0.06
Pentamethylphenol	164	0.03	0.03	0.05	0.03	0.04
Ethylpentamethylphenol	178	0.06	0.02	0.03	0.02	0.03
Reactor Temperature (°F)			700	600	700	700
Reactor Pressure (psig)			1000	1000	1020	507
Space Time (hrs.)			1.48	2.50	0.75	0.75
Catalyst			Nalco Sphericat 474		Harshaw HT 400	

homologs both in the feedstock and each of the four reactor samples. The degree of substitution on the phenol nucleus in Table XXI is listed in terms of methyl substituents. It is realized that this assumption is an oversimplification of possible isomeric forms at mass 122, 136, 150, 164, and 178 and is not meant to imply that only methylated phenols were found in anthracene oil. Comparison of the weight percents for phenols in the reactor samples with the weight percents of the feedstock show that as the amount of alkyl substitution is increased the extent of deoxygenation significantly decreases.

A major constituent of the acidic and neutral-nitrogen-containing fractions are compounds which contain a carbazole (IX) nucleus.

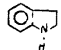
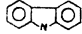
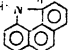
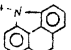
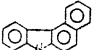

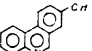
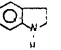
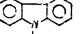
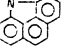
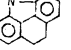
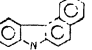


IX

The carbon number distributions for the carbazoles in both the acidic and neutral-nitrogen-containing fractions are presented in Table XXIV. The weight percents are referred to the total sample. The major acidic nitrogen-containing-compounds are carbazole, its methylated and dimethyl and/or ethylated homologs and benzocarbazole and its methylated derivative. Both high-resolution 70-eV EI and FI mass spectrometry indicated the presence of molecules containing C, H, N and O in the feedstock acid fraction. The molecular formulas assigned from the 70-eV high-resolution data are consistent with but do not prove the existence of hydroxyazanaphthalenes and

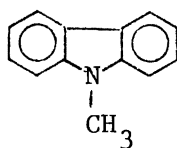
TABLE XXIV

CARBON NUMBER DISTRIBUTION FOR THE NITROGEN-CONTAINING ACIDS  
AND MAJOR NEUTRAL NITROGENS

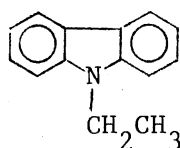
Z Number	Examples of Possible Structures for Parent Molecules	Weight Percents by FI/MS for Carbon Number										Total								
		9	10	11	12	13	14	15	16	17	18		19							
	Acid Fraction																			
-7		0.11																		0.11
-15					0.67	0.15	0.06													0.88
-19									0.16	0.02										0.18
-17									0.08	0.03										0.11
-21													0.25	0.05						0.30
-11(NO)		0.21	0.27																	0.48
-17(NO)						0.06	0.06													0.12
	Neutral-Nitrogens Fraction																			
-7		0.01	0.03	0.01	0.01															0.06
-15					0.32	0.29	0.21	0.08	0.02											0.92
-19									0.03	0.02	0.01	0.01	0.01							0.07
-17									0.03	0.02	0.02	0.01								0.08
-21													0.02	0.02						

hydroxyazaphenanthrenes. It should be noted this type of molecule accounted for ca. 4.0% of the acid fraction.

The neutral-nitrogen-containing fractions consisted primarily of molecules which were consistent with the presence of alkylated carbazoles and are also summarized in Table XXII. The presence of carbazole in the neutral-nitrogen-containing fraction suggests incomplete removal in the first step of the separation scheme (Figure 9). This is explained by the weakly acidic nature of carbazole which could lead to incomplete retention on the Amberlyst A-29 anion exchange resin. The weight percents of 0.29 and 0.21 at  $C_{13}$  and  $C_{14}$  in the neutral-nitrogen carbazole series suggest that compounds such as N-methylcarbazole (X), methylated X, and N-ethylcarbazole (XI) are contributing to the total carbazoles possessing



X



XI

1 and/or 2 carbons in the alkyl substituent(s).

Table XV presents a comparison of the weight percents for the total of each Z series for the feedstock and each of the four reactor samples. The data show that molecules consistent with a carbazole skeleton appear to be effectively resistant toward denitrogenation. The increase in the weight percents of carbazoles in reactor sample 3 compared with the feedstock from 1.80% to 1.93% can be attributed to either errors inherent in the separation and analysis<sup>25</sup> or coupling of nitrogen hydrogenolysis products to produce carbazoles<sup>41</sup> or both.



TABLE XXV

COMPOSITIONAL DATA FOR THE NITROGEN-CONTAINING COMPOUNDS IN THE ACIDIC AND NEUTRAL-NITROGEN FRACTIONS ISOLATED FROM FEEDSTOCK AND HYDROTREATED ANTHRACENE OIL

For Each Series									
Parent Compound				Weight Percent					
Molecular Weight	Empirical Formula	Possible Structural Type	Maximum Number of Alkylated Homologs <sup>a</sup>	Feedstock	Reactor Sample				
					1	2	3	4	
117	C <sub>8</sub> H <sub>7</sub> N	indole	1	0.11	0.03	0.10	0.10	0.11	
167	C <sub>12</sub> H <sub>9</sub> N	carbazole	2 (4)	1.80	1.61	1.36	1.93	1.58	
191	C <sub>14</sub> H <sub>9</sub> N	benzocarbazole	1 (3)	0.25	0.20	0.07	0.08	0.05	
193	C <sub>14</sub> H <sub>11</sub> N	dihydrobenzocarbazole	1 (3)	0.19	0.19	0.23	0.38	0.14	
217	C <sub>16</sub> H <sub>11</sub> N	naphthylindanole	1 (2)	0.35	0.30	0.14	0.14	0.12	
145	C <sub>9</sub> H <sub>7</sub> NO	hydroxyazanaphthalene	2	0.48	0.02	0.14	0.02	0.00	
195	C <sub>13</sub> H <sub>9</sub> NO	hydroxyazaphenanthrene	1	0.12	0.00	0.01	0.18	0.01	
Reactor Temperature (°F)					700	600	700	700	
Reactor Pressure (psig)					1000	1000	1020	507	
Space Time (hrs.)					1.48	2.50	0.75	0.75	
Catalyst					Nalco Sphercat 474		Harshaw HT 400		

<sup>a</sup> Numbers in parenthesis indicate maximum number of alkylated homologs found in neutral nitrogen fraction.

Compounds which contained both N and O in the acid fraction appeared reactive toward nitrogen and/or oxygen removal. There was no evidence for partially hydrogenated molecules containing both N and O.


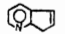

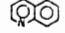


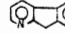
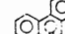

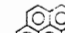



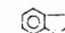
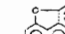

For the basic fraction from the feedstock anthracene oil, Table XVI presents for each series the Z value, possible structures for parent molecules, and the weight percents as a function of carbon number. Molecular formulas deduced from experimental exact masses are tabulated in Table XXXV of Appendix B. The interpretation of the data is formulated in terms of structural types chosen on the basis of previous analysis of materials derived from coal,<sup>17a,b,d;31,33</sup> heavy ends from petroleum,<sup>42</sup> and analogous structures to those assigned to the hydrocarbon + ether fraction. For pragmatic reasons alkyl substituents are, in general, expressed in terms of the required number of methyl groups. Although this approach is clearly an oversimplification and is undoubtedly incorrect, the present results are consistent with previous observations that in coal-derived liquids alkyl groups bound to aromatic nuclei contain only a few carbons.<sup>17b,d;33c</sup>

The -5 Z series is comprised of only two members whose molecular weights and formulas are consistent with pyridines possessing 3 and 4 methyl groups, respectively, or equivalent combinations of methyl, ethyl, propyl, and butyl groups. The absence of pyridine and methyl- and dimethylpyridines is consistent with the boiling-point range of the feedstock anthracene oil, i.e., 174-435°C at 1 atm.

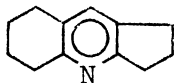
In the -9 Z series, azaindene (XII) is a reasonable candidate structure at molecular weight 117. It is interesting to note that no alkylated homologs of XII are observed. It does not appear simple to

TABLE XXVI

## CARBON NUMBER DISTRIBUTION FOR BASES FROM ANTHRACENE OIL FEEDSTOCK

Z Number	Examples of Possible Structures for Parent Molecules	Weight Percents by FI/MS for Carbon Number													Total		
		7	8	9	10	11	12	13	14	15	16	17	18	19			
-5	 (79)		0.04	0.02													0.06
-9	 (117)		0.03				0.02	0.03									0.07
-7	 (119)		0.10	0.20	0.07	0.06	0.02										0.45
-11	 (129)			0.85	0.60	0.41	0.18	0.10	0.05	0.02	0.01						2.22
-13	 (155)  (155)					0.12	0.14	0.25	0.12	0.03	0.01						0.67
-15	 (167)						0.43	0.29	0.10	0.05	0.02	0.01					0.90
-17	 (179)							1.45	0.77	0.34	0.11	0.04	0.01				2.72
-19	 (191)								0.10	0.18	0.13	0.08	0.04	0.01			0.54
-21	 (203)  (203)									0.89	0.32	0.14	0.05	0.02			1.42
-23	 (229)											0.28	0.07	0.02			0.37
-27	 (253)															0.03	0.03
-11(NO)	 (169)					0.05	0.05	0.03	0.02	0.01							0.16
-19(NO)	 (195)							0.02	0.02	0.01	0.01						0.06
-21(20)	 (219)									0.01	0.04						0.05

assign structures to the compounds at masses 173 and 187. The observed molecular formulas would seemingly require hydroaromatic nitrogen-containing compounds. A reasonable compound type which is consistent with the high-resolution data at these masses is naphthopyridines such as XIII. In view of the process used to prepare



XIII

anthracene oil, it is important to note that these compounds account for only 0.4% of the base fraction.

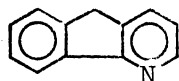
The presence of azaindane (XIV) reasonably accounts for the weight percent in the  $C_8$  series (mass 119) in the -7 Z series. The increase in weight percent at  $C_9$  could be explained by the presence of either methylated azaindanes or tetrahydroazanaphthalenes (XV) or both. Although the data prohibit drawing any real conclusions, the weight percents from  $C_9$  through  $C_{12}$  in this series seem most reasonably represented by XIV and XV containing one through four carbon atoms exocyclic to the ring.

The Z = -11 series is the second most abundant one, accounting for ca. 23.5% of the total anthracene-oil base fraction. The distribution of weight percents progressively decreases across this series. The parent compound(s) in this series is (are) most likely quinoline (and isoquinoline). The series would then be comprised of 8 homologous member compounds containing 0 through 8 carbons exocyclic to the quinoline and/or isoquinoline nucleus. The present data

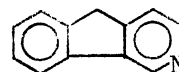
cannot exclude the possibility that 1- and/or 2-naphthalenamine (MW 143) and variously alkylated homologs also contribute to the weight percents above  $C_{10}$  in this series.

For the  $Z = +1$  series azaacenaphthene (XVI) and phenylpyridine (XVII) reasonably account for the weight percent at mass 155. It should be noted that the increase in the weight percent at  $C_{13}$  in this series suggests the presence of tetrahydroazaanthracene (XVII) and/or tetrahydroazaphenanthrene (XVIII). The series would then probably contain alkylated derivatives of XVII and/or XVIII at masses 197, 211, and 225.

The  $-15 Z$  series accounts for 10% of the total base fraction. The member of this series at mass 167 is consistent with either carbazole or azafluorenes (XIX and XX) and accounts for 4.49% of the

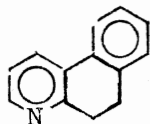


XIX

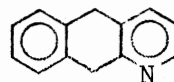


XX

base fraction. Although the nitrogen in XIX is by definition classified as nonbasic,<sup>43</sup> it is adsorbed on Amberlyst A-29 ion exchange resin<sup>25</sup> and, hence, appears in the acid fraction. It is thus reasonable to conclude that the  $C_{12}H_9N$  components in the base fraction are predominantly XX rather than XIX. The weight at mass 181 can be accounted for by compounds such as methyl-substituted azafluorenes, dihydroazaphenanthrenes (XXI) and dihydroazaanthracene (XXII). The present



XXI

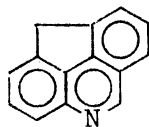


XXII

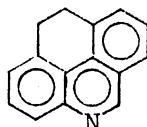
data are insufficient to determine the contributions of methylated azafluorenes and compounds such as XXI and XXII to the weight percent at mass 181 (carbon number 13). It is important to note that mass 167 and 181 comprise 80.0% of this fraction.

The -17 Z series molecular-weight distribution is the most abundant, one contributing ca. 28.8% of the total weight of the base fraction. The empirical formulas and molecular weights are consistent with the presence of 3-ring nitrogen-containing aromatics possessing up to 5 methyl substituents. In anthracene oil the aromatic hydrocarbon possessing the formula  $C_{14}H_{10}$  has been shown to be phenanthrene rather than anthracene; our data show that phenanthrene accounts for at least 95% of the GC component corresponding to the  $C_{14}H_{10}$  hydrocarbon. By analogy to the  $C_{14}H_{10}$  hydrocarbon, azaphenanthrenes and their variously alkylated homologs possessing 1 through 5 carbons exocyclic to the aromatic nucleus would constitute the Series 7 molecular-weight distribution. It is important to note that 94% of the weight of Series 7 is comprised of compounds containing 1 or 2 methyl groups or 1 ethyl group. Finally these data cannot exclude the possibility that the distribution of weight percents in this series for compounds possessing molecular weights between 193 and 249 derives contributions from phenanthrenamines and their alkylated homologs.

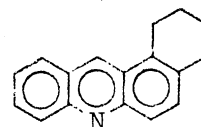
The molecular formulas at molecular weights 191, 205, and 233 for the -19 Z series are consistent with, but do not prove, the presence of cyclopentazaphenanthrene (XXIII), dihydroazapyrene (XXIV), and tetrahydrobenz[a]acridine (XXV), respectively. Representative structures for the



XXIII



XXIV



XXV

nitrogen analogs of the parent hydrocarbons are shown. Consequently, the available data are insufficient to further classify the mass 191 subseries. For example, the weight percent at mass 219 amu could represent contributions, which cannot be determined, from XXIII containing two exocyclic carbons and from methylated XXIV.

The Z = -21 series is the third most abundant one and accounts for ca. 14.6% of the base fraction. In the absence of other data, the distribution of weight percents across this series cannot be well defined in terms of its constituent compounds because the weight a) at mass 203 can represent unknown contributions from compounds such as azafluoranthenes and azapyrenes and b) at mass 217 can derive contributions from compounds such as benzoazafluorenes and benzocarbazoles in addition to methylated homologs of compounds of mass 203 amu.

The molecular formulas at mass 229, 243, and 257 and comprising the Z = -23 series were consistent with the presence of compounds such

as benz[a]acridine (XXVI), variously singly methylated XXVI, and variously doubly methylated and/or singly ethylated XXVI, respectively. The -27 Z series corresponds to molecules such as azabenzopyrenes.

Three series of structural formula types containing both N and O were detected in the base fraction. Representative structures for the parent compounds in the Z = -11(NO), -19(NO), and -21(NO) series and consistent with the experimental molecular formulas are shown in Table XXVI. It should be noted that azaromatic compounds substituted with a hydroxyl group are possible. The presence of such compounds in the basic fraction cannot be eliminated because this acid/base character in nonaqueous ion-exchange chromatography is unknown. Determination of the functional groups would be difficult using infrared spectroscopy because of the low concentration of these compounds in this fraction.

The weight percent distributions for the hydrotreated base fractions in Table XXVII-XXX show that the complexity of the bases is significantly increased upon hydrotreating anthracene oil. The maximum in the total carbon number distribution has been shifted to a lower Z value indicating extensive reaction with hydrogen. The number of carbons exocyclic to the aromatic nucleus for the lower Z series has also increased. The increased complexity makes interpretation of the hydrogenation/hydrogenolysis of the bases during the upgrading process more difficult. For simplicity, examples using only data pertinent to the hydrogenation/hydrogenolysis of quinoline and/or isoquinoline and azaphenanthrene-type molecules will be discussed.

For the reactant and product bases comprising the 129-135, 143-149, and 157-163 molecular-weight series Table XXXI presents mole data referred to 100 g. of feedstock anthracene-oil. Since in these



TABLE XXVII

## CARBON NUMBER DISTRIBUTION FOR BASES FROM REACTOR SAMPLE 1

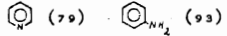
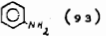
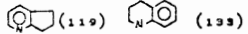

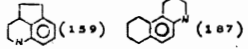
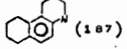
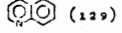
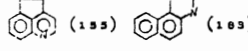
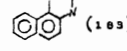

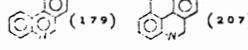
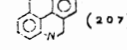
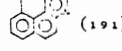
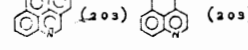
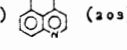
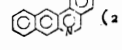
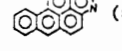
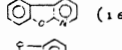
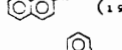
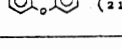
Z Number	Examples of Possible Structures for Parent Molecules	Weight Percents by FI/MS for Carbon Number													Total		
		6	7	8	9	10	11	12	13	14	15	16	17	18		19	
-5	 (79)  (93)	0.03	0.08	0.20	0.24	0.10	0.05	0.02	0.01								0.73
-7	 (119)  (133)			0.00	0.15	0.30	0.29	0.16	0.06	0.05	0.02						1.03
-9	 (159)  (167)						0.01	0.04	0.88	0.33	0.11	0.04	0.02				1.43
-11	 (129)				0.05	0.09	0.12	0.09	0.06	0.03	0.04	0.03	0.04	0.02			0.57
-13	 (185)  (183)						0.01	0.04	0.33	0.26	0.04	0.06	0.03				0.77
-15	 (167)							0.01	0.08	0.10	0.19	0.12	0.10	0.05			0.65
-17	 (179)  (207)								0.25	0.25	0.18	0.10	0.10	0.03	0.03		0.94
-19	 (191)									0.01	0.10	0.07	0.22	0.07	0.02		0.49
-21	 (203)  (203)										0.20	0.10	0.08	0.02	0.02		0.42
-23	 (229)											0.03	0.01	0.02			0.06
-27	 (233)													0.02			0.02
-11(NO)	 (169)						0.00	0.03	0.06	0.04	0.03						0.16
-19(NO)	 (195)									0.00	0.01	0.01	0.01				0.03
-21(20)	 (219)											0.01	0.00				0.07

TABLE XXVIII

## CARBON NUMBER DISTRIBUTION FOR BASES FROM REACTOR SAMPLE 2

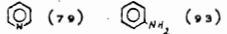
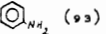
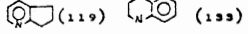
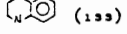
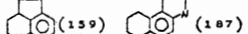
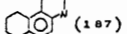
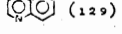
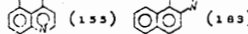
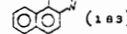
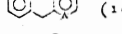
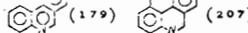
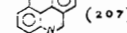

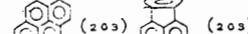

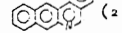
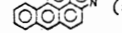


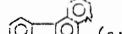
Z Number	Examples of Possible Structures for Parent Molecules	Weight Percents by FI/MS for Carbon Number														Total	
		6	7	8	9	10	11	12	13	14	15	16	17	18	19		
-5	 (79)  (93)	0.01	0.03	0.12	0.12	0.05	0.02	0.01	0.01								0.37
-7	 (119)  (133)			0.00	0.23	0.22	0.19	0.11	0.06	0.02	0.02	0.01	0.01				0.87
-9	 (159)  (187)							0.13	0.03	0.55	0.24	0.11	0.05	0.02		1.13	
-11	 (129)			0.03	0.05	0.07	0.05	0.04	0.02	0.07	0.05	0.05	0.03			0.46	
-13	 (153)  (183)							0.01	0.02	0.25	0.17	0.11	0.04	0.03		0.63	
-15	 (167)								0.08	0.12	0.09	0.22	0.15	0.13	0.06	0.02	0.87
-17	 (179)  (207)									0.19	0.15	0.11	0.08	0.12	0.05	0.04	0.74
-19	 (191)										0.01	0.05	0.04	0.15	0.07	0.03	0.35
-21	 (203)  (203)											0.04	0.05	0.05	0.02	0.03	0.19
-23	 (229)												0.02	0.02	0.02		0.06
-27	 (253)														0.02		0.02
-11(10)	 (169)						0.00	0.02	0.03	0.02	0.02						0.09
-19(10)	 (193)										0.00	0.01	0.02	0.02			0.05
-21(20)	 (219)												0.01	0.00			0.01

TABLE XXIX

## CARBON NUMBER DISTRIBUTION FOR BASES FROM REACTOR SAMPLE 3

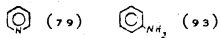
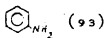
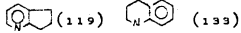
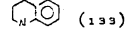
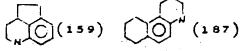
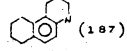
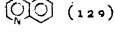
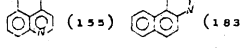
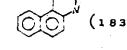
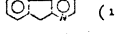
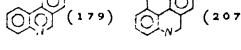
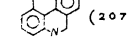
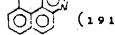
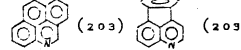
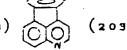
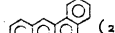

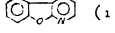

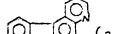
Z Number	Examples of Possible Structures for Parent Molecules	Weight Percents by FI/MS for Carbon Number													Total		
		6	7	8	9	10	11	12	13	14	15	16	17	18		19	
-5	 (79)  (93)	0.05	0.12	0.37	0.41	0.20	0.11	0.04									1.30
-7	 (119)  (133)				0.09	0.24	0.32	0.22	0.23	0.09	0.05	0.02					1.26
-9	 (159)  (187)						0.01	0.04	1.15	0.48	0.19	0.08	0.04				1.99
-11	 (129)				0.01	0.03	0.07	0.09	0.08	0.04	0.05	0.05	0.10				0.52
-13	 (155)  (183)							0.03	0.39	0.37	0.26	0.12	0.07				1.24
-15	 (167)							0.02	0.16	0.20	0.28	0.19	0.19	0.08			1.12
-17	 (179)  (207)								0.16	0.24	0.20	0.17	0.15	0.05	0.04		1.01
-19	 (191)									0.03	0.11	0.11	0.31	0.10	0.04		0.70
-21	 (203)  (203)										0.20	0.11	0.06	0.01	0.03		0.41
-23	 (229)												0.02	0.01	0.02		0.05
-27	 (253)														0.03		0.03
-11(NO)	 (169)						0.00	0.02	0.04	0.05	0.04						0.15
-19(NO)	 (193)									0.00	0.00	0.01	0.01				0.02
-21(20)	 (219)												0.00	0.00			0.00

TABLE XXX

## CARBON NUMBER DISTRIBUTION FOR BASES FROM REACTOR SAMPLE 4

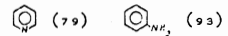
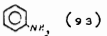
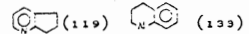

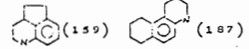
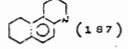

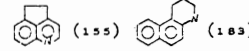
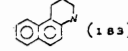
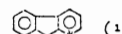
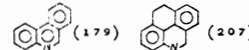
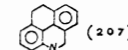
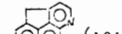
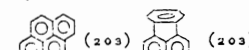
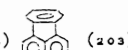
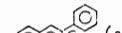

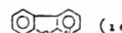

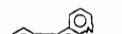
Z Number	Examples of Possible Structures for Parent Molecules	Weight Percents by FI/MS for Carbon Number														Total	
		6	7	8	9	10	11	12	13	14	15	16	17	18	19		
-5	 (79)  (93)	0.00	0.06	0.14	0.19	0.08	0.04	0.02									0.53
-7	 (119)  (133)			0.00	0.17	0.28	0.20	0.10	0.07	0.03	0.01						0.86
-9	 (159)  (187)						0.01	0.03	0.45	0.13	0.04	0.02				0.68	
-11	 (129)				0.06	0.15	0.22	0.15	0.10	0.04	0.03	0.02	0.02			0.79	
-13	 (155)  (183)						0.01	0.07	0.50	0.30	0.15	0.06	0.03			1.12	
-15	 (167)							0.21	0.47	0.28	0.17	0.09				1.22	
-17	 (179)  (207)								0.66	0.52	0.27	0.16	0.09	0.03		1.73	
-19	 (191)									0.03	0.02	0.10	0.27	0.04	0.02	0.48	
-21	 (203)  (203)										0.34	0.16	0.09	0.04	0.01	0.64	
-23	 (229)											0.04	0.03	0.02		0.09	
-27	 (253)													0.02		0.02	
-11(NO)	 (169)						0.00	0.03	0.05	0.04	0.03					0.15	
-19(NO)	 (195)								0.00	0.00	0.01	0.07				0.08	
-21(20)	 (219)										0.00	0.00				0.00	

TABLE XXXI

MOLES OF BASES AT SELECTED MOLECULAR WEIGHTS FOUND IN  
FEEDSTOCK AND HYDROTREATED ANTHRACENE OIL

Nominal Mass	Molecular Formula	Feedstock	Moles x 10 <sup>3</sup> Present in			
			Reactor Samples			
			1	2	3	4
129	C <sub>9</sub> H <sub>7</sub> N	6.60	0.39	0.23	0.08	0.46
133	C <sub>9</sub> H <sub>11</sub> N	0.15	1.10	1.70	0.68	1.20
135	C <sub>9</sub> H <sub>13</sub> N	0.15	1.80	0.89	3.00	1.40
TOTAL		6.90	3.29	2.82	3.76	3.06
143	C <sub>10</sub> H <sub>9</sub> N	4.10	0.63	0.35	0.21	1.00
147	C <sub>10</sub> H <sub>13</sub> N	0.41	2.00	1.50	1.60	1.90
149	C <sub>10</sub> H <sub>14</sub> N	-	0.67	0.33	1.30	0.20
TOTAL		4.51	3.30	2.28	3.11	3.10
157	C <sub>11</sub> H <sub>11</sub> N	2.60	0.76	0.45	0.45	1.30
161	C <sub>11</sub> H <sub>15</sub> N	0.37	1.80	1.20	2.00	1.20
163	C <sub>11</sub> H <sub>17</sub> N	-	0.35	0.12	0.67	0.25
TOTAL		3.97	2.91	1.77	3.12	2.85
Reactor Temperature (°F)			700	600	700	700
Reactor Pressure (psig)			1000	1000	1020	507
Space Time (hrs.)			1.48	2.50	0.75	0.75
Catalyst			Nalco Sphericat 474		Harshaw HT 400	

hydrotreating experiments total mass balance data were not accumulated, we were forced to make a reasonable assumption concerning the weight percent per 100 g. of feedstock appearing as reactor vent-gas. It was assumed that the fraction lost as volatiles was 5%.

The data in rows 1, 5, and 9 of Table XXXI show a reduction in the moles of compounds possessing molecular weights 129, 143, and 157. This observation follows even if such compounds are produced from higher-molecular-weight compounds during the hydrotreating of the anthracene oil. In both feedstock and reactor samples the moles at mass 143 and at mass 157 may derive some contribution from naphthalenamines and their singly methylated homologs, respectively. The moles of basic compounds at masses 133 and 135, 147 and 149, and 161 and 163 are markedly larger in the reactor samples than in the feedstock. Since alkylated XIV contribute negligibly to the composition of the feedstock bases (see previous discussion and Table XXIV), it seems reasonable to postulate that such compounds are likewise unimportant in determining the moles of compounds present at masses 133, 147, and 161 in the reactor base fractions. This situation reflects one problem arising from characterization data developed according to compound class. Both quinoline (XXVIIa) and isoquinoline (XXVIIb) can contribute to the moles at mass 129 in the feedstock. Thus, in the reactor samples the moles at mass a) 133 indicate contributions from 1,2,3,4-tetrahydroquinoline (XVa), 5,6,7,8-tetrahydroquinoline (XVb), 1,2,3,4-tetrahydroisoquinoline (XVc), and 5,6,7,8-tetrahydroisoquinoline (XVd) and b) 135 could derive contributions from hexahydro-XXVIIa and hexahydro-XXVIIb. However, considerations of aromaticity suggest that hexahydro-XXVIIa and -XXVIIb correspond to 2-propylaniline (XXVIII),

3-phenylpropylamine (XXXII), 2-ethylbenzylamine (XXIX) and 2-(2-methylphenyl)ethylamine (XXXIII). However, as discussed below, the presence of XXXII, XXXIX, and XXXIII is quite unlikely.

As shown in Figure 19, quinoline is proposed to undergo catalytic addition of two moles of hydrogen producing tetrahydroquinolines XVa and XVb. The XVa then reacts with hydrogen via the hydrogenolysis of the N-C bonds producing XXVII and XXXII. Hydrogenolysis of the C-N bond in both XXVII and XXXII produces propylbenzene (XXXI). On the basis of bond energy considerations hydrogenolysis of the aliphatic C-N bond in XVa and in XXXII producing XXVIII and XXXI should be more facile than hydrogenolysis of the aromatic C-N bond in XVa and in XXVIII producing XXXII and XXXI, respectively. This consideration would suggest that 2-propylaniline (XXVIII) is the major contributor to the moles at mass 135 in the reactor bases. The reaction sequence in Figure 14 is supported by previous kinetic studies of the reaction of quinoline with  $H_2$  catalyzed by a cobalt-molybdenum (CoMo) catalyst<sup>44</sup> and detailed product studies of the hydrogenation/hydrogenolysis of quinoline and isoquinoline using a molybdenum sulfide ( $MoS_2$ ) catalyst.<sup>45</sup> It is of interest to note that in the reaction of quinoline with  $MoS_2$ , XXXa and XXVIII account for 27.5% of the product mixture.<sup>45</sup> Hydrocarbons recovered included benzene, cyclohexane, and their methylated, ethylated, and n-propylated homologs.<sup>45</sup> Denitrogenation is reasonably considered by these authors as arising from further reaction of XXVIII or XXXII. The failure to observe decahydroquinoline in the reactor samples is consistent with the observation that this compound accounts for only 2.9% of the products obtained from the  $MoS_2$ -catalyzed hydrogenation/hydrogenolysis of quinoline.

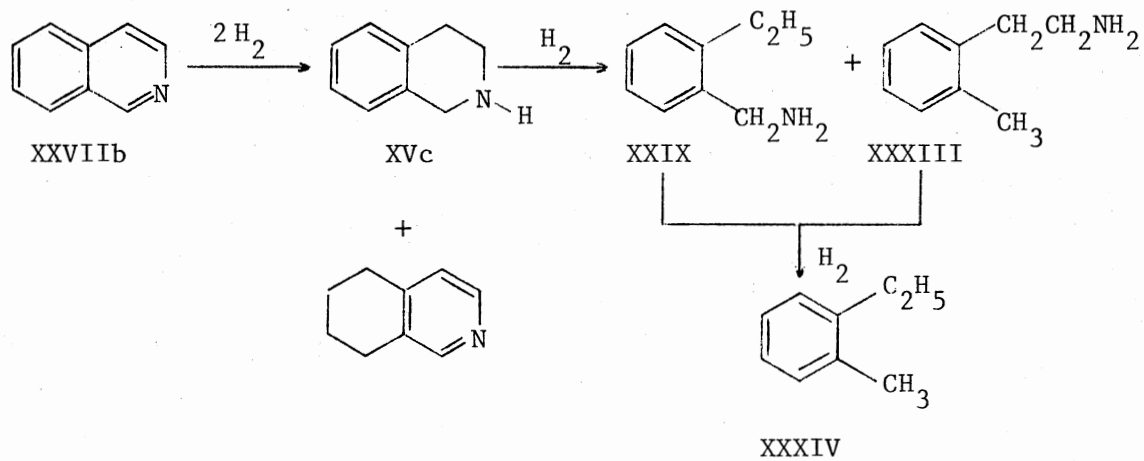
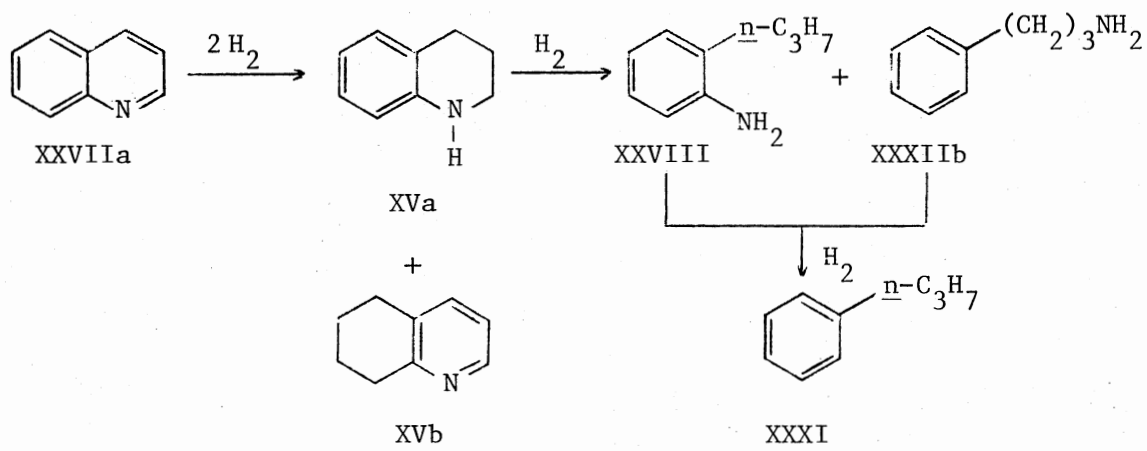


Figure 19. Hydrogenation/Hydrogenolysis Scheme for Quinoline and Isoquinoline



The MoS<sub>2</sub>-catalyzed reaction of hydrogen and isoquinoline (XXVIIb) was also investigated. The only nitrogen compounds observed corresponded to reaction of 3 and 4 moles of H<sub>2</sub> with XXVIIb.<sup>45</sup> Tetrahydroisoquinolines resulting from reduction of both the benzene and pyridine rings were observed. As shown in Figure 19 hydrogenolysis of the N-C bond in the tetrahydroisoquinoline (XVc) resulting from reduction of the pyridine ring would produce 2-ethylbenzylamine (XXIX). Since XXIX contains a benzylic NH<sub>2</sub> group, its hydrogenolysis (denitrogenation) to 2-ethylmethylbenzene XXXIII should be facile. In fact, XXXIII accounts for 45.7% of the MoS<sub>2</sub>-catalyzed reaction of XXVIIb with H<sub>2</sub>. As noted above, the NH<sub>2</sub> group in the product XXVIII resulting from ring opening of quinoline is aromatic and, hence, would be expected to undergo hydrogenolysis less readily.

For purposes of the present discussion only, we initially assume that the conversion of higher-molecular-weight compounds to XXVa,b,c,d, XXVIII, XXXII, XXIV, and XXXIII during the upgrading of raw anthracene-oil was negligible. This assumption permits estimation of the percentage of moles of quinoline and/or isoquinoline denitrogenated under the experimental conditions and catalysts listed in Table XXXI. For reactor samples 1 through 4 the mole percents of quinoline and/or isoquinoline recovered are 0.39, 0.23, 0.08, and 0.46, respectively. However, this result is clearly misleading because it does not consider the fact that XXXa,b,c,d, XXVIII, XXXII, XXIX, and XXXIII in Figure 19 are less reactive than either quinoline or isoquinoline. Consequently, a more representative measure of azanaphthalene denitrogenation is obtained by dividing the sum of the moles at masses 129, 133, and 135 in each reactor sample by the number of moles at mass 129 in the

feedstock. Expressed as percentages the values are 51.5, 42.4, 57.6, and 47.0 for reactor samples 1 through 4, respectively. These results suggest that the catalysts, temperatures, hydrogen pressures, and space times employed in these experiments produced only about a 50% denitrogenation of the quinoline and/or isoquinoline on a mole basis. These percentages also indicate that the extent of nitrogen removal from XXVIIa and from XXVIIb was similar for both the Nalco Sphericat 474 and the Harshaw HT 400 catalysts. Although the space times were not the same for the four reactor samples, the percentages for reactor samples 1 and 2 (51.5 and 42.4) and for reactor samples 3 and 4 (57.6 and 42.0) would suggest that reduction in both temperature and hydrogen pressure, respectively, increased the extent of denitrogenation. Two reasonable explanations for this untenable conclusion can be advanced. First, hydrogenation/hydrogenolysis of higher-molecular-weight compounds contributes to the moles of XXVIIa,b, XVa,b,c,d, XXVIII, XXXII, XXIX, and XXXIII. Conceivably the rates for such hydrogenation/hydrogenolysis reactions exhibit a somewhat greater dependence upon temperature and  $H_2$  pressure than do the primary hydrogenation/hydrogenolysis reactions in Figure 14. Second, the moles recovered at masses 129, 133, and 135 could reflect a dependence of catalyst aging upon reaction conditions and the feed rate of the raw anthracene oil. Clearly, the experimental results could reflect the combination of both factors.

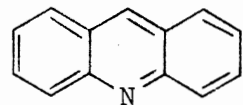
The reaction schemes in Figure 19 can be extended to the hydrogenation/hydrogenolysis of singly and doubly methylated quinoline and/or isoquinoline by giving proper consideration to the effect of the methyl substituent(s) on reactivity and product distributions. Methyl

substitution on either the benzene or pyridine ring increases the difficulty of hydrogenating that ring.<sup>46</sup> However, for quinolines substituted with only a few methyl groups hydrogenation in general occurs in the pyridine ring. Generalizations are somewhat difficult because out of the percentage of the total of both rings reduced the percentage reduction of the pyridine ring appears to be dependent upon the pattern of methyl substitution. Analysis of the moles at masses 143-149 and 157-163 is also complicated by the possible presence of a) naphthalenamines and their methylated homologs in the feedstock and reactor samples and b) basic nitrogen-containing compounds in the upgraded coal liquids produced from reaction of these compounds with  $H_2$ . If we assume that the 143 molecular-weight series represents essentially methylated quinolines and/or isoquinolines then the sums of the moles at masses 143, 147, and 149 in the reactor samples divided by the number of moles at mass 143 in the feedstock multiplied by 100 are 80.5, 53.7, 73.6, and 75.6, respectively. The corresponding values for the mass 157 series are 112, 69.2, 119, and 108 respectively. Consistent with the results for the quinoline/isoquinoline series, these percentages indicate that more reduction apparently occurs at lower temperatures and pressures. Although these percentages are subject to some uncertainty, the data for the three quinoline/isoquinoline series (masses 129-135, 143-149, and 157-163) are mutually consistent and most reasonably suggest the synthesis of their constituents or other isomeric compounds from compounds of higher molecular weight.

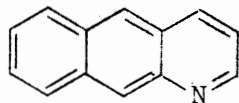
Interpretation of the hydrogenation/hydrogenolysis of the aromatic bases in the feedstock which have molecular weights greater

than 157 is complicated by ions at a given exact mass which may represent molecular ions produced by ionization of a number of isomeric compounds. For example, Figure 20 presents the eight possible isomers for molecular formula  $C_{13}H_9N$ , which was deduced from the exact mass of the ions having mass 179.0737 in the base fraction. These structures correspond to acridine (XXXV), benzoquinolines (XXXVI), benzoisoquinolines (XXXVII) and phenanthridine (XXXVIII). Application of the mechanism proposed for hydrogenation/hydrogenolysis of the quinoline/isoquinoline series to the hydrogenation/hydrogenolysis of the three-ring aromatics in Figure 20 would lead to the predicted formation of over 36 possible products. For example, mechanisms for the hydrogenation/hydrogenolysis of benzo[*f*]quinoline (XXXVIb) and phenanthridine (XXXVIII) are presented in Figure 21. Hydrogenation of XXXVIb and XXXVIII could produce hydrogenated products at masses 181, 183, 187, and 193. Hydrogenolysis of C-N bonds in the hydroazaaromatics produces aromatic amines at masses 183, 185, and 189. Therefore, a detailed understanding of the hydrogenation/hydrogenolysis of these 3-ring azaaromatic bases cannot be achieved without more detailed compositional data for the feedstock and reactor sample base fractions at masses 179, 181, 183, 185, 187, 189, and 192. However, comparison of the weight percent data at each of these masses in the feedstock with the corresponding data for each of the reactor samples provides some insight concerning nitrogen removal from the compound types listed in Figure 20.

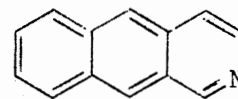
Table XXXII lists molecular formulas and number of millimoles for compounds having molecular weights 179, 181, 183, 185, 187, 189, and 193 for both the feedstock and upgraded samples. Medium resolution



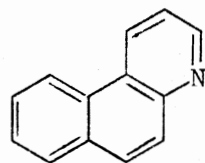
XXXV



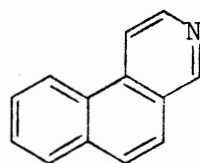
XXXVIa



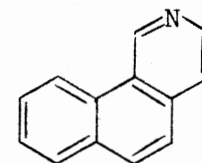
XXXVIIa



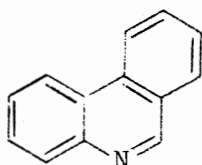
XXXVIb



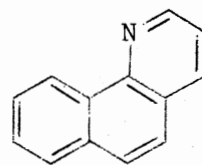
XXXVIIb



XXXIIc



XXXVIII



XXXVIc

Figure 20. Possible Isomeric Structures Consistent With the Empirical Formula  $C_{13}H_9N$

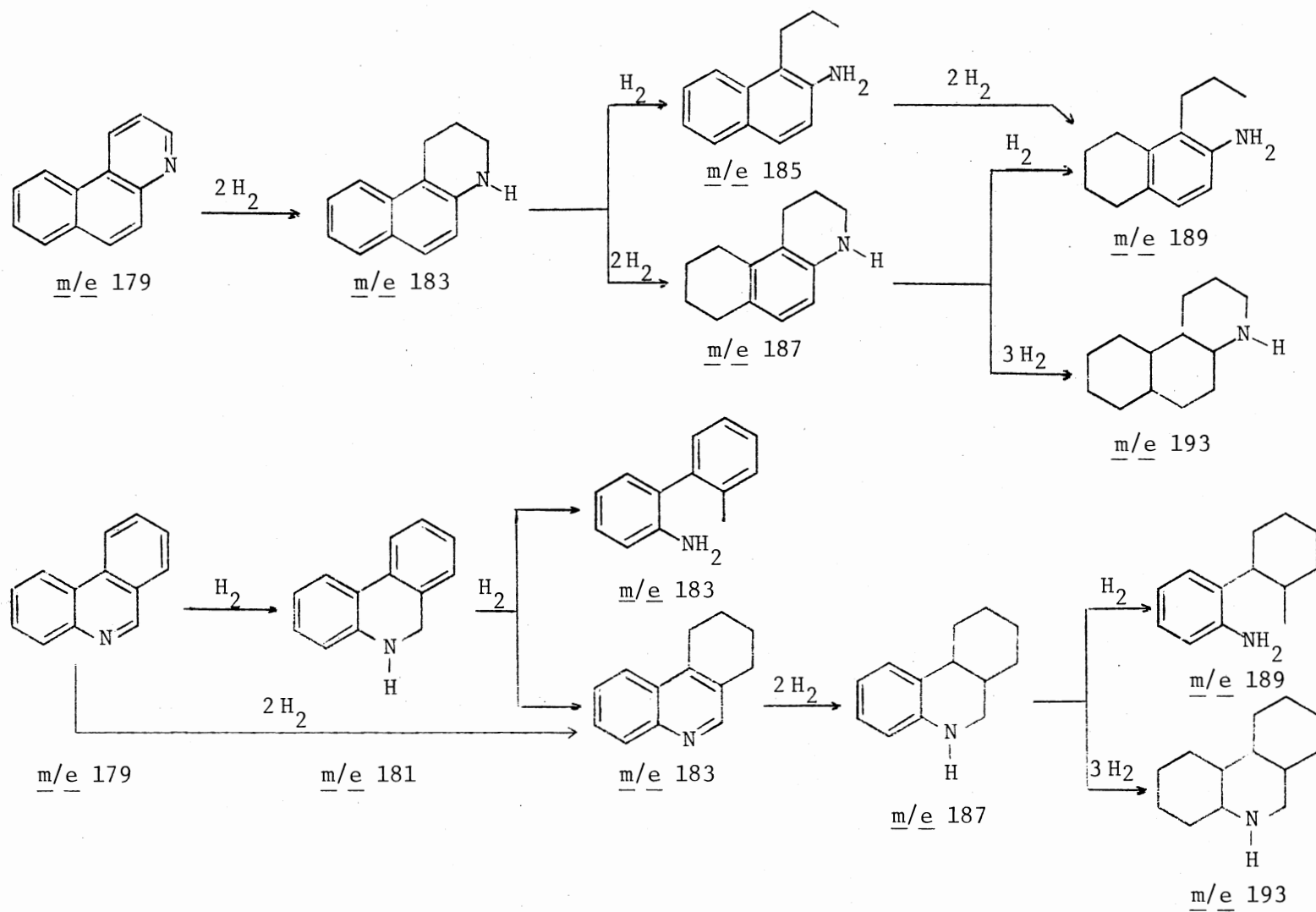


Figure 21. Possible Hydrogenation/Hydrogenolysis Scheme for Benzo[f]quinoline and Phenanthridine

TABLE XXXII

MOLES OF BASES FOR THE EMPIRICAL FORMULAS CONTAINING C<sub>13</sub> FOUND  
IN FEEDSTOCK AND HYDROTREATED ANTHRACENE OIL

Nominal Mass	Molecular Formula	Moles x 10 <sup>3</sup> Present in				
		Feedstock	Reactor Samples			
			1	2	3	4
179	C <sub>13</sub> H <sub>9</sub> N	8.12	1.38	1.06	0.87	3.68
181	C <sub>13</sub> H <sub>11</sub> N	1.62	0.46	0.65	0.88	2.61
183	C <sub>13</sub> H <sub>13</sub> N	1.36	1.30	1.35	2.13	2.75
185	C <sub>13</sub> H <sub>15</sub> N	0.56	0.31	0.24	0.41	0.51
187	C <sub>13</sub> H <sub>17</sub> N	0.11	4.68	2.95	6.14	2.41
189	C <sub>13</sub> H <sub>19</sub> N	0.00	0.67	0.34	1.23	0.39
193	C <sub>13</sub> H <sub>23</sub> N	0.00	0.07	0.53	0.39	0.00
TOTAL		11.77	8.87	7.12	12.05	12.35
Reactor Temperature (°F)			700	600	700	700
Reactor Pressure (psig)			1000	1000	1020	507
Reactor Catalyst			Nalco Sphericat 474	Harshaw HT 400		
Space Time (hr.)			1.48	2.50	0.75	0.75

FI/MS was used to separate the multiplet at mass 193 (see Appendix B, Table XXXV). For the purposes of this discussion only the weight percent corresponding to the perhydroaza aromatic base occurring at mass 193 is listed in Table XXXII. The data in Table XXXII reveal the number of millimoles of  $C_{13}H_9N$  compounds (mass 179) decreases from 8.12 millimoles in the feedstock to 1.38, 1.06, 0.87, and 3.68 millimoles in reactor samples 1-4, respectively. The decrease in the number of millimoles of compounds possessing mass 179 between reactor sample 3 and reactor sample 4 reflects an increase in hydrogen pressure from 507 psig for the latter to 1020 psig for the former. Although the difference in the millimoles of mass 179 compounds in passing from reactor sample 1 to reactor sample 2 does not reflect the decrease in reactor temperature, it should be noted that the space times for the former were shorter than the latter. The number of millimoles at mass 181 is less in reactor samples 1, 2, and 3 than in the feedstock. The millimoles of mass 181 compounds is seen to be increased in reactor sample 4. It should be noted that reactor sample 4 was obtained at approximately one-half the hydrogen pressure of the other reactor samples and at shorter space times than used for reactor samples 1 and 2. The increase at mass 181 in reactor sample 4 could reflect formation of dihydro-XXXV through XXXVIII. The number of millimoles at mass 183 for the feedstock and reactor sample 1 and 2 remained essentially constant. However, a change in catalyst increases the number of millimoles at mass 183 from 1.36 in the feedstock to 2.13 and 2.75 millimoles in reactor samples 3 and 4, respectively. The millimoles of mass 187 compounds are 4.68, 2.95, 6.14, and 2.41 in reactor samples 1 through 4, respectively, compared to 0.11 in the



feedstock. This increase can be attributed to the formation of 3-ring octahydroaza aromatic compounds (see Figure 21). Comparison of reactor sample 2 and 1 and 3 and 4 shows that temperature and pressure increase the millimoles of compounds at mass 187. Comparison of the millimoles of  $C_{13}H_{17}N$  in reactor sample 3 and reactor sample 1 indicates that the rate of formation and/or destruction of these compounds exhibits a greater dependence on catalyst than on space time.

Compounds at mass 189 are postulated to be formed by ring opening of the azahydroaromatics of mass 187 (see Figure 21). Hydrogenation of the azahydroaromatics of mass 187 would account for the formation of the perhydroazanaphthenes of mass 193. The net yields of mass 187 and 193 compounds would appear from the data in Table XXXII to be dependent upon temperature, pressure, catalyst, and space time.

Summation of the millimoles of compounds at masses 179, 181, 183, 185, 187, 189, and 193 for the feedstock and four reactor samples can be used to provide information concerning the degree of hydrogenolysis. The total number of millimoles for this series in reactor sample 3 and 4 has remained the same as the feedstock within the experimental error of the separation. This shows that although there has been significant hydrogenation of compounds in this series, significant denitrogenation was not realized. In contrast, the millimole sums for reactor sample 1 and 2 are 8.87 and 7.12, respectively, compared to the value of 11.77 for the feedstock. This result suggests a catalyst and possible space time dependence upon denitrogenation of compounds in this series.

## Experimental

### A. Separation Procedures

Acid Fraction - Apparatus and Materials. The chromatographic column is illustrated in Figure 22. The column is 1.4 cm in diameter (i.d.) and 119 cm in length. The temperature of the resin is controlled by circulating water through the outside jacket. The recycling arrangement permits continuous elution of the sample without use of large quantities of solvent or regulation of the reflux rate.

Amberlyst A-29 anion-exchange resin (Rohm and Haas, Inc.) was activated as follows. Methanolic HCl solution was prepared by mixing 10 volumes of concentrated HCl with 90 volumes of absolute methanol. Methanolic potassium hydroxide solution was prepared by adding 90 ml of methanol to 10 grams of potassium hydroxide. A volume of the resin was placed in a column, washed with a volume of methanolic HCl solution equivalent to 6 times the volume of resin taken, and rinsed with deionized water until the washings were neutral. Activation was accomplished by eluting the resin first with a volume of the methanolic potassium hydroxide equivalent to 6 times the volume of the resin taken and second with deionized water until the eluent was neutral. The resin was then removed from the column, placed in a Soxhlet extractor, and extracted for 24 hours with each of the following solvents: methanol, benzene, and pentane. After the pentane extraction the resin was vacuum dried.

n-Pentane (99 percent) was purified by flash distillation and by percolation through activated silica gel; benzene and methanol (reagent grade) were flash distilled.

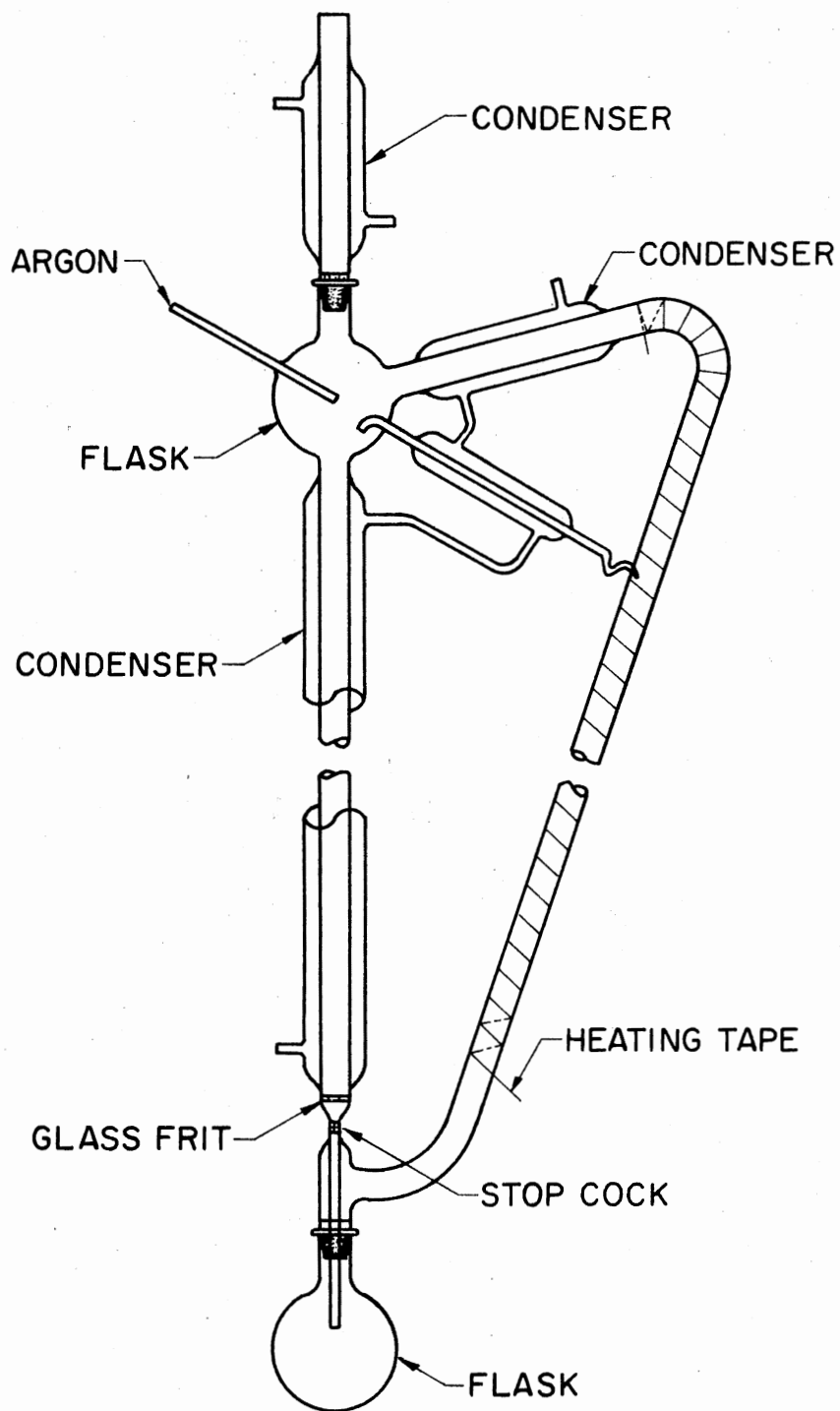


Figure 22. Recycling Chromatographic Column

Acid Fraction - Procedure. The column in Figure 22 was filled with pentane and a slurry of ion-exchange resin (150 ml) in pentane was then added. A vibrator was used to settle and pack the resin. The resin bed was then extracted with recycled pentane under an argon atmosphere for 5-10 hrs.

A weighed sample (ca. 20 g.) of anthracene oil was quantitatively transferred to the column containing the ion-exchange resin. The rate of pentane elution was 6-10 drops per minute. Elution of nonacidic material required approximately 48 hours. After elution of the nonacidic material the acids were removed as follows. Benzene was substituted for pentane as the eluent and elution continued for 24 hours. Elution with benzene removes very weakly acidic material such as carbazoles. The flask at the bottom of the column (see Figure 17) was then replaced by one containing absolute methanol. The flow of argon to the column was stopped and a glass tube with a fritted end was inserted through the top condenser of the chromatographic column so that gaseous  $\text{CO}_2$  could be bubbled into the methanol in the upper solvent reservoir. The methanol saturated with  $\text{CO}_2$  was then used to elute the strong acids from the anion exchange resin. Removal of strong acids required elution with  $\text{CO}_2$ -saturated methanol for approximately 24 hours. The solvent was removed from the sample with a roto-evaporator and room temperature water bath (ca.  $25^\circ\text{C}$ ) until a constant sample weight ( $\pm 0.02$  g.) was achieved. The materials removed from the resin bed using benzene and methanol/ $\text{CO}_2$  were combined to yield a total acid fraction.

Base Fraction - Apparatus and Materials. The chromatography column used for the separation is illustrated in Figure 22. Amberlyst

15 (Rohm and Haas, Inc.) was activated as follows. A volume of the resin was placed in a column and the resin washed with a volume of methanolic potassium hydroxide equivalent to 6 times the volume of resin taken. The rate of adding the methanolic potassium hydroxide solution was controlled by the heat generated by the discharging of the resin. The resin was then washed with deionized water until the washings were neutral. Activation was then accomplished by washing with a volume of methanolic HCl solution equivalent to 6 times the volume of resin taken. Again, the rate of adding the methanolic HCl solution was controlled by the exothermicity of reaction. The resin was then washed with deionized water until the washings were neutral, removed from the column and placed in a Soxhlet extractor, and extracted for 24 hours using each of the following solvents: methanol, benzene, and pentane. After the pentane extraction, the resin was vacuum dried. Reagent-grade isopropylamine was used as received.

Base Fraction - Procedure. The column in Figure 22 was filled with pentane and a slurry of ion-exchange resin (ca. 150 ml) in pentane was then added. A vibrator was used to settle and pack the resin. Extraction with recycled pentane under an argon atmosphere for 5-10 hours was used to remove oxygen and any remaining impurities adsorbed on the resin. The pentane solubles minus the acid components obtained from the previous separation were introduced onto the ion-exchange resin as previously described. The elution of non-basic material was identical to that described in the procedure for removal of the nonacidic components. Pentane elution of the nonbasic material required approximately 48 hours.

The bases were removed by first eluting the resin bed with benzene for 24 hours. The resin was then slowly discharged by eluting with 500 ml of an 8 vol.-% isopropylamine in methanol solution. The exothermicity from discharging the ion-exchange resin requires a decreased flow of isopropylamine/methanol eluent by approximately one-half and increased water flow through the chromatographic column jacket. The benzene and methanol/isopropylamine eluates were then combined and the solvent removed with a roto-evaporator and a room temperature water bath until a constant sample weight ( $\pm 0.02$  g.) was achieved. This material represents the bases.

Neutral-Nitrogen Fraction - Apparatus and Materials. The chromatography column used in this step of the separation procedure is shown in Figure 22. The column is 1.8 cm (i.d.) in diameter and 119 cm in length. A methanolic-ferric chloride solution was prepared by mixing 10 grams of ferric chloride hexahydrate with 90 ml of methanol. The methanolic-ferric chloride solution was then slurried with Attapulugus clay (LVM, 60/80 mesh, Engelhard Minerals and Chemicals) for one hour. The excess methanolic-ferric chloride solution was removed from the clay by filtering. After washing several times with pentane, the ferric chloride coated clay was extracted in a Soxhlet apparatus for 48 hours with pentane to remove residual nonadsorbed entrained metallic salt. The coated Attapulugus clay was then vacuum dried. Reagent-grade 1,2-dichloroethane was purified by percolation through activated silica gel.

Neutral-Nitrogen Fraction - Procedure. The column in Figure 22 was filled with pentane and a slurry of Amberlyst A-29 (ca. 100-125 ml) in pentane was then added so that the column was half filled. A

vibrator was used to settle and pack the resin. A small glass wool plug was then positioned on top of the ion-exchange resin bed. A slurry of pentane and ferric chloride-Attapulugus clay (100-125 ml) was then added until the column was filled. A vibrator was used to settle and pack the clay. The packed column was then extracted with recycled pentane under an argon atmosphere for 5-10 hours.

A weighed sample (ca. 10 g.) of anthracene oil minus the acids and the bases was dissolved in pentane and quantitatively transferred to the packed column. The hydrocarbon plus ethers were removed by elution with pentane for 12 hrs under an argon atmosphere. The colored complexes which remained were desorbed from the Attapulugus clay by elution with 1,2-dichloroethane. The eluted complexes were broken upon contact with the anion-exchange resin. The metal salt was retained on the resin while the free compounds were eluted with the solvent. The pentane was removed from the hydrocarbon plus ether fraction and 1,2-dichloroethane from the neutral-nitrogen fraction using a roto-evaporator until a constant sample weight ( $\pm 0.01$  g) was obtained.

#### B. Instrumental

All field-ionization (FI) and 70-eV high-resolution electron-impact mass spectra were obtained on a CEC 21-110B double-focusing mass spectrometer using a modified combination FI/EI ion source and standard electron-impact ion source, respectively.<sup>11</sup> Emitters were prepared as previously described (see Experimental Operation, Chapter I). Emitters were conditioned and spectra were obtained with an emitter (accelerating) potential of ca. 6.8 kV and a counter-electrode potential of -300 to -500 V. High-resolution 70-eV mass spectra were

recorded on photographic plates (Ilford Q-2) with perfluorokerosene as an internal standard. Exact masses were obtained by manual reading of the position of the lines recorded on the photographic plates followed by computer processing of the line position data. Samples were introduced into the ion source (270°C) via the all-glass inlet system (300°C).

An LKB 9000P combination mass spectrometer/gas chromatograph was used for GC/MS analysis. A 5% OV-101 on Gas Chrom Z AW-DMSC (100/120) glass column (12' x 1/8") was used for GC separation. The temperature program used was: 5 minutes at 100°C, then the temperature was increased at a rate of 1°/minute linear rise until the temperature reached 200°C. The column was then maintained at isothermal until analysis was complete. Sample size was 0.2 µl. Major components were identified by comparing the mass spectra of the column effluent with standard mass spectra published by API Project 44. Quantitative gas chromatographic data were obtained by fitting the above-mentioned column to a Hewlett-Packard 5750 gas chromatograph equipped with flame-ionization detectors. Quantitative GC data was also verified by using a Perkin-Elmer 3990 gas chromatograph. Peak areas were calculated using the product of the peak height and peak width at half height. The GC peak areas for a chromatogram were then normalized, assuming unit relative sensitivities, to provide weight percent compositions. The computer program used for calculation of weight percents from the mass spectral peak intensities is given in Appendix C.



REFERENCES CITED

1. (a) E. W. Muller, Ergeb. Exakt. Naturw., 27, 290 (1953);  
(b) M. G. Inghram and R. Gomer, J. Chem. Phys., 22, 1279 (1954).
2. (a) E. W. Muller, Adv. Electronics Electron Phys., 13, 83 (1960);  
(b) R. Gomer, "Field Emission and Field Ionization", Harvard University Press, Cambridge, 1961; (c) H. D. Beckey, "Field Ionization Mass Spectrometry", Pergamon Press, Oxford, 1971.
3. (a) A. J. B. Robertson, B. W. Viney, and M. Warrington, Brit. J. Appl. Physics, 14, 278 (1963); (b) H. D. Beckey, Z. Instrumentenk., 71, 51 (1963).
4. (a) H. D. Beckey, Angew. Chem. Internat. Edit., 8, 623 (1969);  
(b) A. J. B. Robertson, J. Scient. Inst. (J. Physics E.), 7, 321 (1974).
5. H. D. Beckey, H. Krone, and F. W. Roellgen, J. Scient. Inst. (J. Physics E.), Series 2, 1, 118 (1968).
6. H. D. Beckey and D. Schuette, Z. Instrumentenk., 68, 302 (1960).
7. (a) M. Anbar and W. H. Aberth, Anal. Chem., 46, 59A (1974);  
(b) M. Anbar and G. A. St. John, Anal. Chem., 48, 198 (1976).
8. (a) H. D. Beckey, A. Hendricks, E. Hilt, M. D. Migahed, H. R. Schulten, and H. U. Winkler, Messentechnik, 79, 196 (1971);  
(b) D. F. Barofsky and E. Barofsky, Int. J. Mass Spectrom. Ion Phys., 14, 3 (1974).
9. J. Block, Adv. Mass Spectrom., 4, 791 (1968).
10. (a) A. J. B. Robertson and B. W. Viney, Advances Mass Spectrom., 3, 23 (1963); (b) P. A. Blenkinsop, B. E. Job, D. F. Brailsford, C. M. Cross, and A. J. B. Robertson, Int. J. Mass Spectrom. Ion Phys., 1, 421 (1968); (c) H. D. Beckey, S. Blocking, M. D. Migahed, E. Octerbeck, and H. R. Schulten, Int. J. Mass Spectrom. Ion Phys., 8, 169 (1972);  
(d) P. J. Derrick and A. J. B. Robertson, Int. J. Mass Spectrom. Ion Phys., 10, 315 (1972).

11. (a) E. M. Chait, T. W. Shannon, W. O. Perry, G. E. Van Lear, and F. W. McLafferty, Int. J. Mass Spectrom. Ion Phys., 2, 141 (1969); (b) Internal Report of the Continental Oil Company, Research and Development Department, Ponca City, Oklahoma, Report No. 1007-4-1-73, authored by H. M. Curtis.
12. M. D. Migahed and H. D. Beckey, Int. J. Mass Spectrom. Ion Phys., 7, 1 (1971).
13. H. D. Beckey, H. Heising, H. Hey, and H. G. Metzinger, Adv. Mass Spectrom., 4, 817 (1968).
14. (a) C. F. Giese, Rev. Sci. Inst., 30, 260 (1959); (b) H. D. Beckey, Adv. Mass Spectrom. 2, 1 (1963); (c) W. A. Schmidt, Z. Naturforsch., 19a, 318 (1964).
15. P. Schulze, B. R. Simoneit, and A. R. Burlingam, Int. J. Mass Spectrom. Ion Phys., 2, 183 (1969).
16. (a) K. G. Hippe and H. D. Beckey, Erdoel Kohle, Erdgas, Petrochem., 24, 620 (1961); (b) M. Ryska, M. Kuras, and J. Mostecky, Int. J. Mass Spectrom. Ion Phys., 16, 257 (1975).
17. (a) A. G. Sharkey, Jr., G. Wood, J. L. Shultz, I. Wender, and R. A. Friedel, Fuel, 38, 315 (1959); (b) A. G. Sharkey, Jr., J. L. Shultz, and R. A. Friedel, Fuel, 41, 359 (1962); (c) A. G. Sharkey, Jr., J. L. Shultz, and R. A. Friedel, "Advances in Coal Spectrometry, Mass Spectrometry", Washington, U.S. Department of the Interior, Bureau of Mines, 1963; (d) J. L. Shultz, R. A. Friedel, and A. G. Sharkey, Jr., "Mass Spectrometric Analysis of Coal-Tar Distillates and Residues", Washington, U.S. Department of the Interior, Bureau of Mines, RI 7000 (1967); (e) T. Kessler, R. Raymond, and A. G. Sharkey, Jr., Fuel, 48, 179 (1969); (f) T. Aczel, J. Q. Foster, and J. H. Karhmer, Preprints, Div. Fuel Chem., Am. Chem. Soc., 13(1), 8 (1969); (g) T. Aczel and H. E. Lumpkin, 19th Annual Conference on Mass Spectrometry and Allied Topics, Atlanta, GA, 1971, p. 328; (h) J. L. Shultz, T. Kessler, R. A. Friedel, and A. G. Sharkey, Jr., Fuel, 51, 242 (1972); (i) H. Pichler and H. Herlan, Erdoel Kohle, Erdgas, Petrochem., 26, 401 (1973); (j) S. E. Scheppele, G. J. Greenwood, and B. L. Crynes, 23rd Annual Conference on Mass Spectrometry and Allied Topics, Houston, Texas, 1975, p. 226; (k) T. Aczel and H. E. Lumpkin, 23rd Annual Conference on Mass Spectrometry and Allied Topics, Houston, Texas, 1975, p. 228; (l) G. P. Sturm, P. W. Woodward, J. W. Vogh, S. A. Holmes, and J. E. Dooley, Energy Research and Development Administration, Washington, BERC RI-75/12 (1975); (m) P. W. Woodward, G. P. Sturm, Jr., J. W. Vogh, S. A. Holmes, and J. E. Dooley, Energy Research and Development Admin., Washington, BERC RI-76/2 (1976).

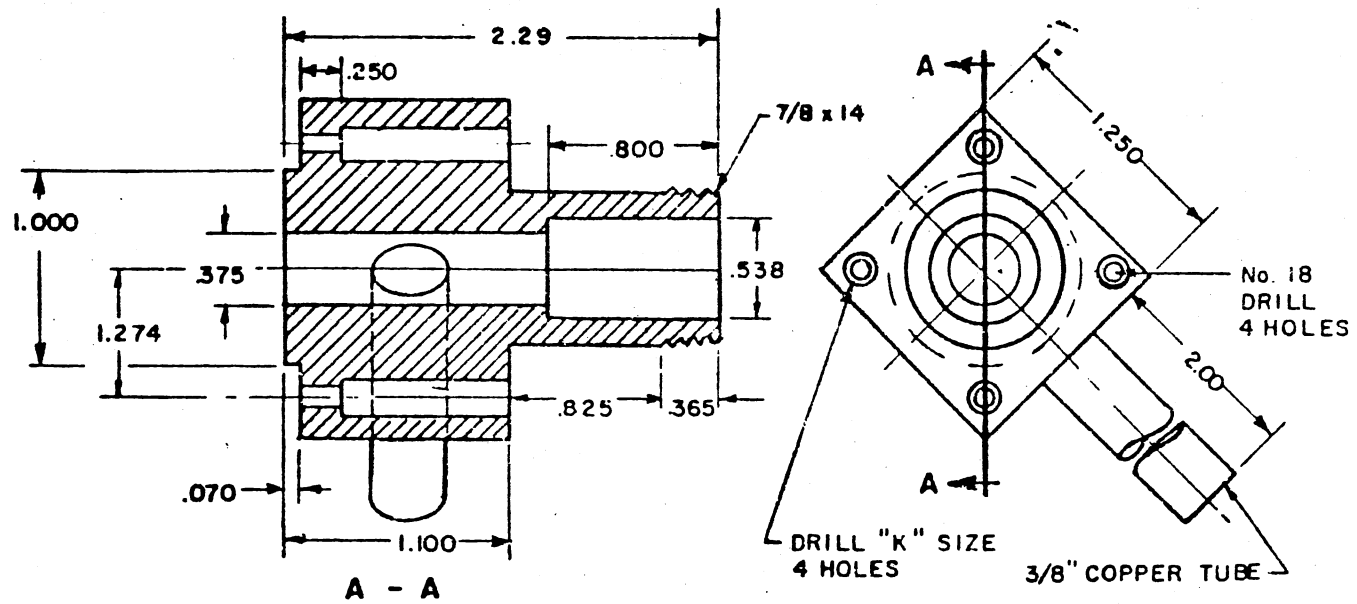
18. (a) M. Kuras, M. Ryska, and J. Mostecky, Anal. Chem., 48, 196 (1976); (b) D. Severin, H. H. Oelert, and G. Bergmann, Erdoel Kohle, Erdgas, Petrochem., 25, 514 (1972).
19. S. E. Scheppele, P. L. Grizzle, G. J. Greenwood, T. D. Marriott, and N. B. Perreira, Anal. Chem., 48, 2105 (1976).
20. J. H. Beynon, "Mass Spectrometry and Its Applications to Organic Chemistry", Elsevier Publishing Co., New York, New York, 1960, Chapter 8.
21. (a) H. E. Lumpkin, Anal. Chem., 30, 321 (1958); (b) G. L. Kerns, N. C. Maranowski, and G. F. Crable, Anal. Chem., 31, 1646 (1959); (c) H. E. Lumpkin and T. Aczel, Anal. Chem., 36, 181 (1964); (d) Private communication from T. Aczel; (e) J. L. Shultz, A. G. Sharkey, Jr., and R. A. Brown, Anal. Chem., 44, 1486 (1972); (f) Private communication from J. L. Shultz and A. G. Sharkey, Jr.
22. (a) American Petroleum Institute Project 44; (b) H. G. Davis and S. Gottlieb, Fuel, 42, 37 (1963).
23. J. L. Franklin, J. G. Dillard, H. M. Rosenstock, J. T. Herron, K. Draxl, and F. H. Field, Nat. Stand. Ref. Data Ser., Nat. Bur. Stand., No. 26 (1969) and references cited therein.
24. Gas chromatograms were obtained on a Perkin-Elmer 3920 instrument with a helium gas flow rate of 23 ml/min. Separations utilized a 5% OV-101 on Gas Chrom Z AW-OMSC (100/120) glass column (12' x 1/8").
25. D. M. Jewell, J. H. Weber, J. W. Bunger, H. Plancher, and D. R. Latham, Anal. Chem., 44, 1391 (1972) and references therein.
26. (a) D. M. Jewell, E. W. Albaugh, B. E. Davis, and R. G. Ruberto, Ind. Eng. Chem., Fundam., 13, 278 (1974); (b) J. F. McKay, P. J. Amend, P. M. Harnsberger, T. E. Cogswell, and D. R. Latham, Preprints, Div. Fuel Chem., Am. Chem. Soc. (Henry H. Storch Award Symposium), 21(7), 52 (1976).
27. R. G. Ruberto and D. M. Jewell, Paper presented in part at National Science Foundation Workshop, "Analytical Needs of the Future as Applied to Coal Liquefaction", Greenup, Kentucky, August 21-23, 1974; and at the Symposium "Supplemental Fuels From Coal: New Analytical Needs," 27th Pittsburgh Conference, Cleveland, Ohio, March 3-7, 1975.
28. (a) R. J. Clerc, A. Hood, and M. J. O'Neal, Jr., Anal. Chem., 27 (1955); (b) H. E. Lumpkin, Anal. Chem., 28, 1946 (1956); (c) M. C. Hamming and N. G. Foster, "Interpretation of Mass Spectra of Organic Compounds", Academic Press, New York, New York, 1972.

29. D. E. Hirsch, R. L. Hopkins, H. J. Coleman, F. D. Cotton, and C. J. Thompson, Anal. Chem., 44, 915 (1972).
30. W. H. McFadden, "Techniques of Combined Gas Chromatography-Mass Spectrometry: Applications in Organic Analysis", Wiley-Interscience, New York, New York, 1973.
31. (a) L. J. Wood, J. Appl. Chem. (Lond.), 11, 130 (1961); (b) F. J. Pinchin and E. Pritchard, Chem. Ind. (Lond.), 1753 (1962); (c) H. D. Sauerland, Brennst. Chem., 44, 37 (1963); (d) E. Proksch, Z. Analyt. Chem., 233, 23 (1966); (e) H. Pichler, P. Hennenberger, and G. Schwarz, Brennst. Chem., 49, 175 (1968); (f) H. Pichler, W. Ripperger, and G. Schwarz, Erdoel Kohle, Erdgas, Petrochem., 23, 91 (1970).
32. G. Schomburg, H. Hushmann, and F. Weeke, J. Chromatogr., 99, 63 (1974).
33. (a) H. C. Anderson and W. R. K. Wu, Bull. U. S. Bur. Mines, No. 66 (1963); (b) Coal Tar Data Book, Coal Tar Research Association, Gomersal, Leeds, 1965; (c) J. L. Schultz, R. A. Friedel, and A. G. Sharkey, Jr., Fuel, 44, 55 (1965); (d) K. F. Lang, Fortschr. Chem. Forsch., 7, 172 (1966); (e) D. McNeil, "Bituminous Materials: Asphalts, Tars and Pitches", Vol. 3, A. J. Hoiberg (Ed.), Interscience Publishers, New York, New York, 1966; (f) K. F. Lang and I. Eigen, Fortschr. Chem. Forsch., 8, 91 (1967); (g) K. D. Bantle, D. W. Jones, T. G. Martin, and W. S. Wise, J. Appl. Chem. (Lond.), 20, 197 (1970).
34. (a) G. F. Crable and N. D. Coggeshall, Anal. Chem., 30, 310 (1958); (b) R. I. Reed, "Application of Mass Spectrometry to Organic Chemistry", Academic Press, London, 1966, Chapt. 6; (c) J. M. Ruth, Anal. Chem., 40, 747 (1968); (d) L. F. Monteiro and R. I. Reed, Int. J. Mass Spectrom. Ion Phys., 2, 265 (1969).
35. D. M. Desiderio, Jr. in "Mass Spectrometry: Techniques and Applications", G. W. A. Milne (Ed.), Wiley-Interscience, New York, New York, 1971, Chapter 2.
36. Private communications with T. Aczel, D. M. Jewell, and H. G. Sharkey, Jr.
37. S. Qader, J. Inst. Pet., 59, 178 (1973).
38. (a) S. Qader, W. H. Wise, and G. R. Hill, I. & E.C. Proc. Design Develop., 7, 390 (1968); (b) E. H. Givens and P. B. Venuto, Preprints, Div. Fuel Chem., Am. Chem. Soc., 15(3), 183 (1970); (c) G. Doyle, Preprints, Div. Fuel Chem., Am. Chem. Soc., 21(7), 165 (1975); (d) L. D. Rollman, Preprints, Div. Fuel Chem., Am. Chem. Soc., 21(7), 59 (1976).

39. We thank H. Ford, G. Keen, and D. Winter at Continental Oil Company, Ponca City, Oklahoma for making available their computer-controlled comparator-microdensitometer and assistance in computer-processing photoplate data.
40. (a) R. E. Dean, E. N. White, and D. McNeil, J. Appl. Chem. (London), 9, 629 (1959); (b) C. Karr, Jr., P. A. Estep, and L. L. Hirst, Jr., Anal. Chem., 32, 463 (1960); (c) S. Friedman, C. Zahn, M. Kaufmann, and I. Wender, Bull. U. S. Bur. Mines, No. 609 (1963); (d) M. Gomez, W. S. Landers, J. L. Shultz, and A. G. Sharkey, Jr., Res. Inv. U. S. Bur. Mines, No. 6586 (1965); (e) J. L. Shultz, T. Kessler, R. A. Friedel, and A. G. Sharkey, Jr., Fuel, 52, 242 (1973).
41. G. K. Hartung, D. M. Jewell, A. O. Larson, and R. A. Flinn, J. Chem. Eng. Data, 6, 477 (1960).
42. (a) D. M. Jewell and G. K. Hartung, J. Chem. Eng. Data, 9, 297 (1964); (b) C. F. Brandenburg and D. R. Latham, J. Chem. Eng. Data, 13, 391 (1968); (c) L. R. Snyder, Anal. Chem., 41, 314 (1969).
43. (a) R. V. Helm, D. R. Latham, C. R. Ferrin, and J. S. Ball, Anal. Chem., 32, 1765 (1960); (b) D. R. Latham, I. Okuno, and W. E. Haines, "Hydrocarbon Analysis", ASTM Special Technical Publication No. 389, American Society for Testing and Materials, 1965, p. 385.
44. (a) A. K. Aboul-Gheit and I. K. Abdou, J. Inst. Petrol., 59, 188 (1973); (b) L. D. Rollmann, Preprints, Div. Fuel Chem., Am. Chem. Soc., 21(7), 59 (1976); (c) B. C. Gates, J. R. Katzer, J. H. Olsen, H. Kwart, and A. B. Stiles, Quarterly Progress Report FE-2028-4 Dist. Category UC-90d, submitted under ERDA Contract E(49-18)-2028.
45. S. Landa, Z. Kafka, V. Galik, and M. Safir, Collect. Czech. Chem. Comm., 34, 3967 (1967).
46. H. A. Smith in "Catalysis", P. H. Emmett (Ed.), Reinhold, New York, New York, 1957, p. 175.
47. We thank Dr. E. J. Eisenbraun for use of the Hewlett-Packard 5750 gas chromatograph.

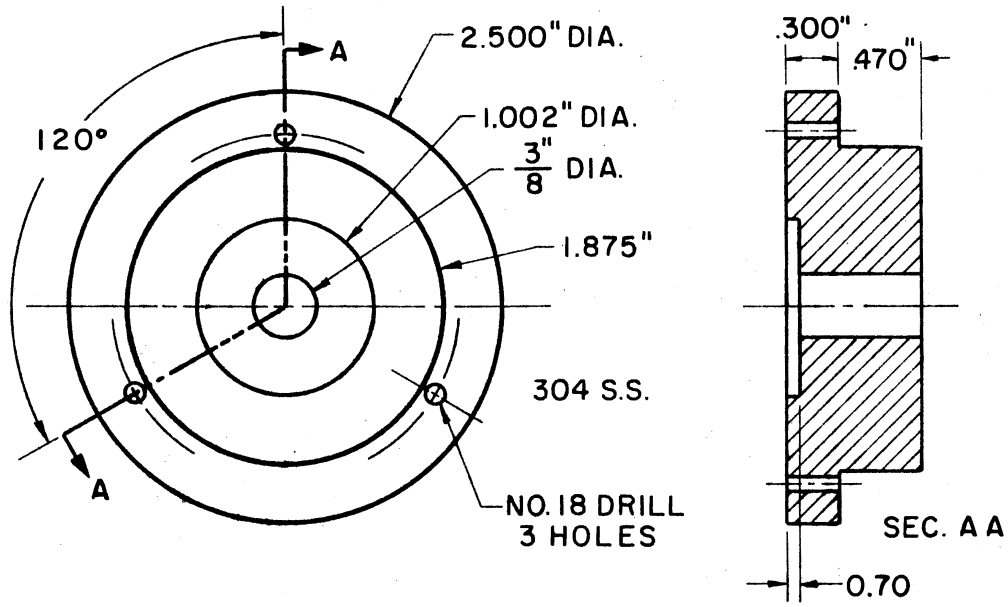
APPENDIX A

PLANS FOR COMBINED FI/EI ION  
SOURCE EQUIPMENT

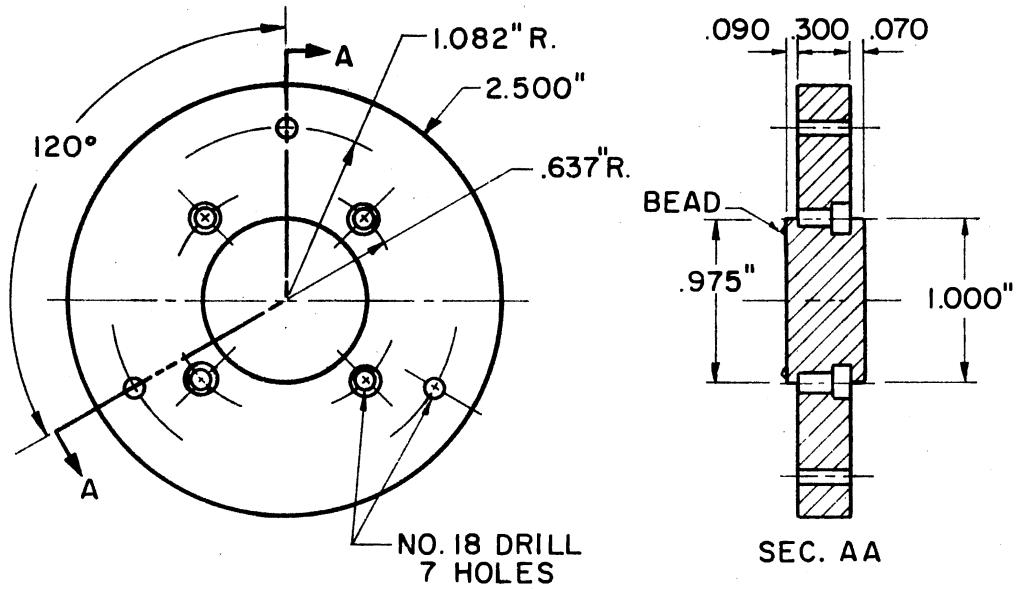


VACUUM SEAL BLOCK - C. R. STEEL

Figure 23. Vacuum Seal Block



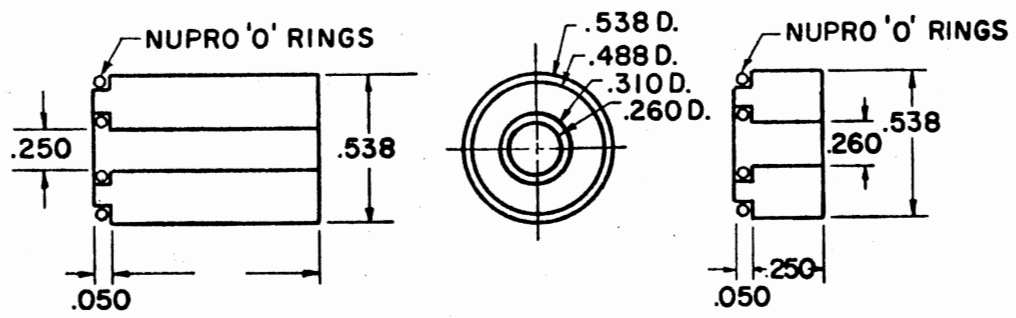
FLANGE - GODDARD VALVE TO SOURCE HOUSING



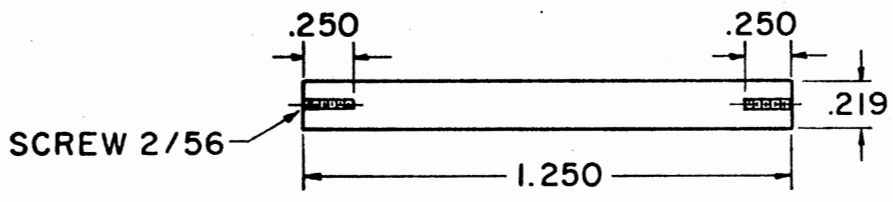
FLANGE - GODDARD VALVE TO SOURCE HOUSING

Figure 24. Goddard Valve to Ion-Source Housing Flange



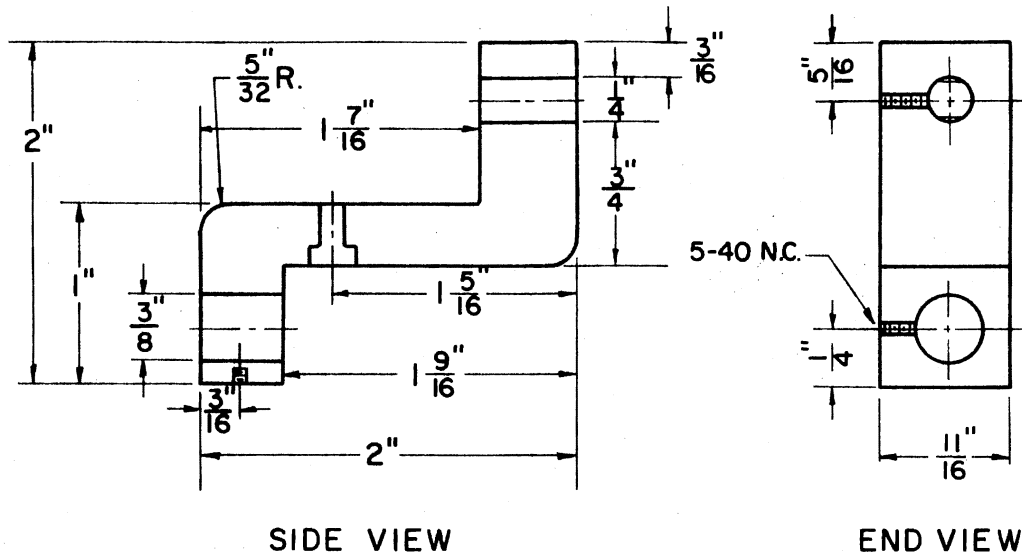


VACUUM SEAL BLOCK SPACERS  
DELFIN

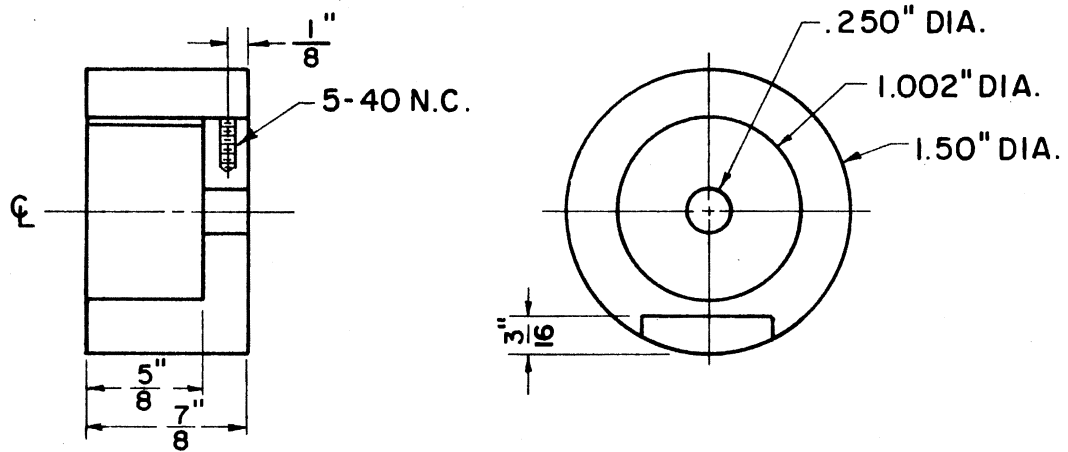


FI CONTROL ROD SPACER  
MACHINABLE CERAMIC

Figure 25. Vacuum Seal Spacers and FI Control Rod Spacer

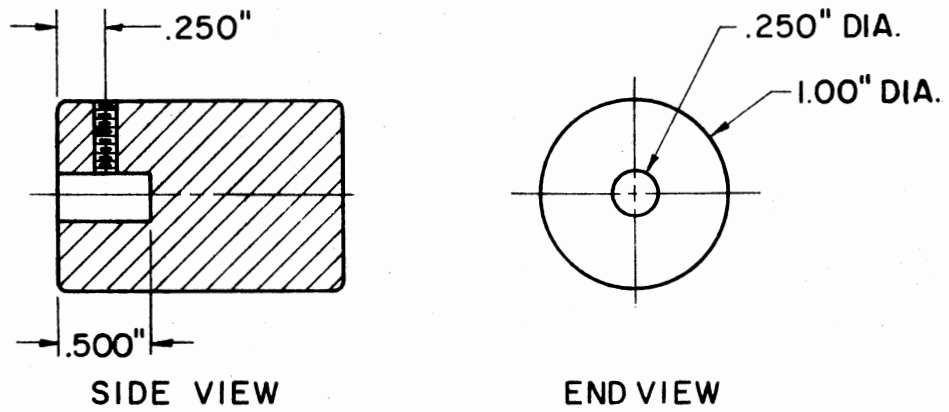


MICROMETER HOLDER  
 $\frac{3}{4}$ " ALUMINUM

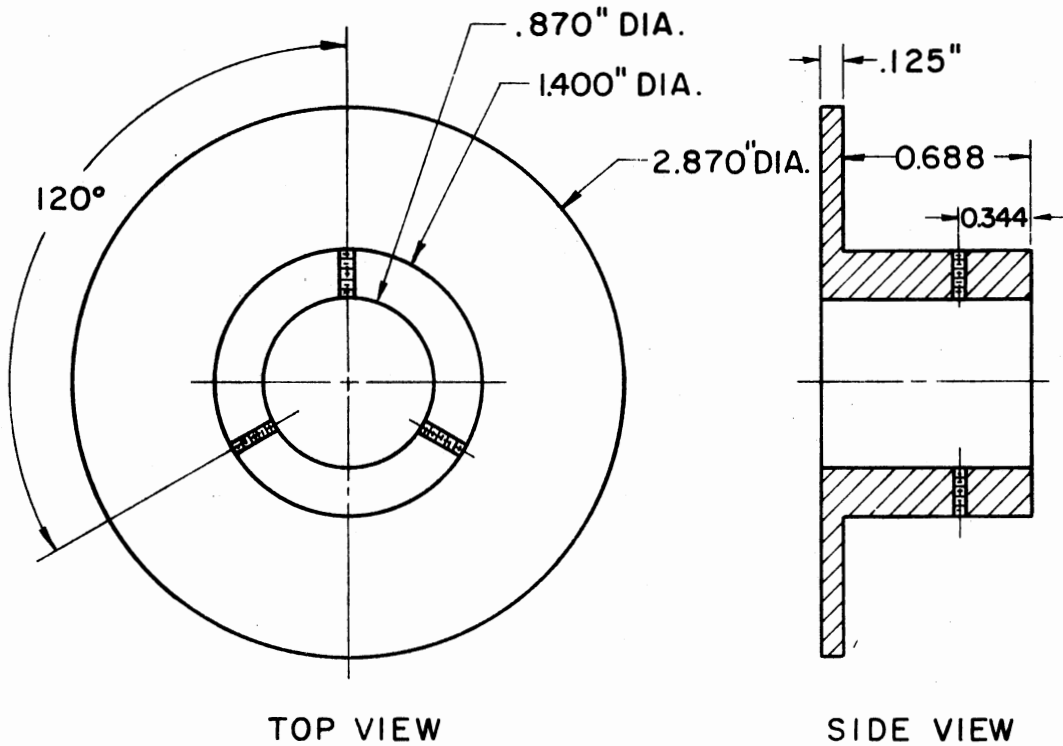


MICROMETER HOLDER  
 DELRIN

Figure 26. Micrometer Holder

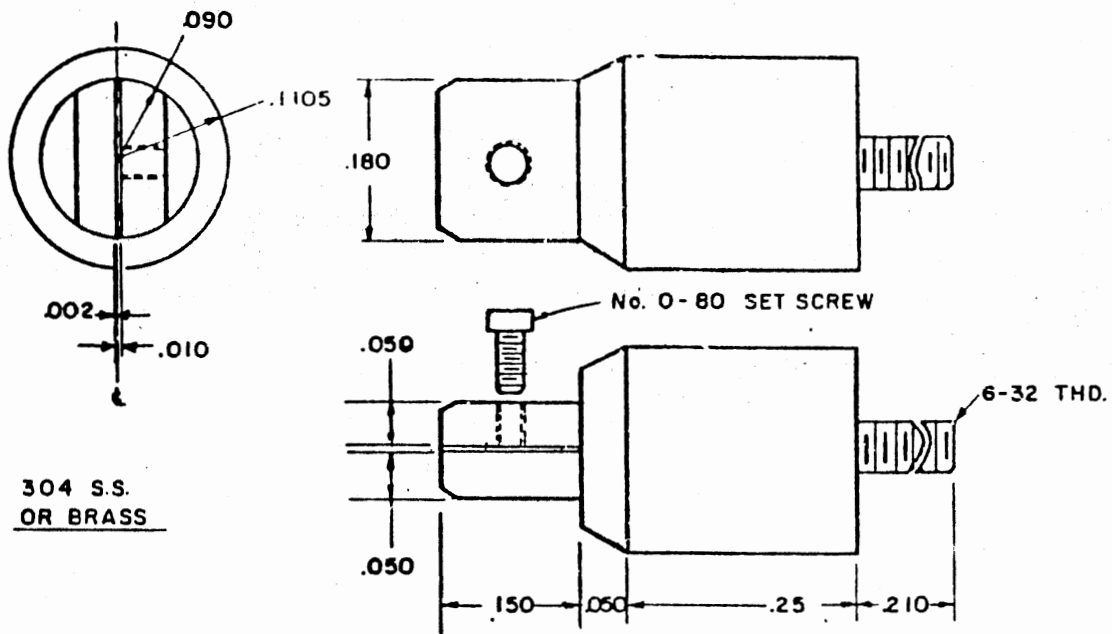


EMITTER ROD HANDLE  
DELFIN

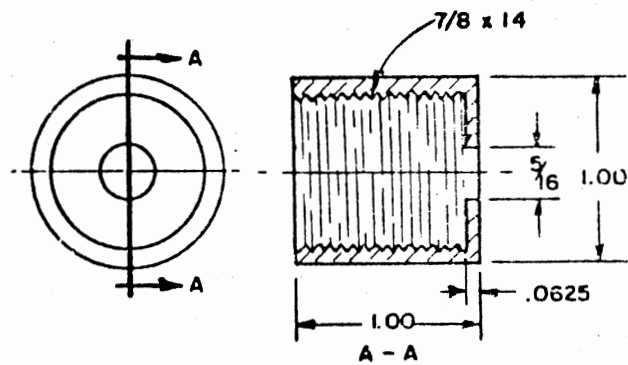


MICROMETER TABLE  
COLD ROLLED STEEL

Figure 27. Emitter Rod Handle and Micrometer Table

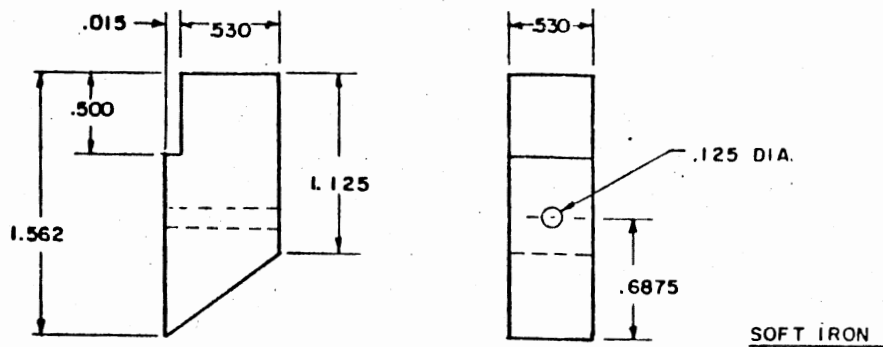


RAZOR BLADE VISE

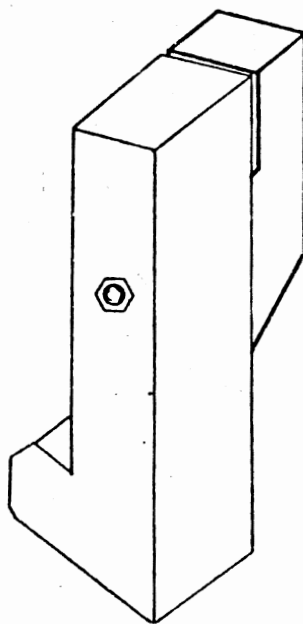


VACUUM SEAL CAP - C.R. STEEL

Figure 28. Razor Blade Vise and Vacuum Seal Cap

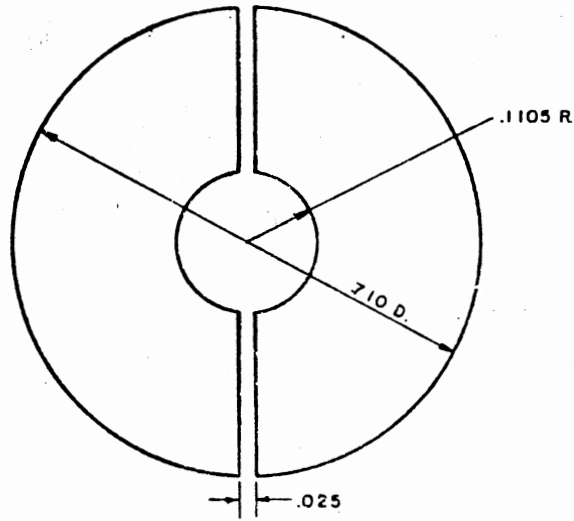
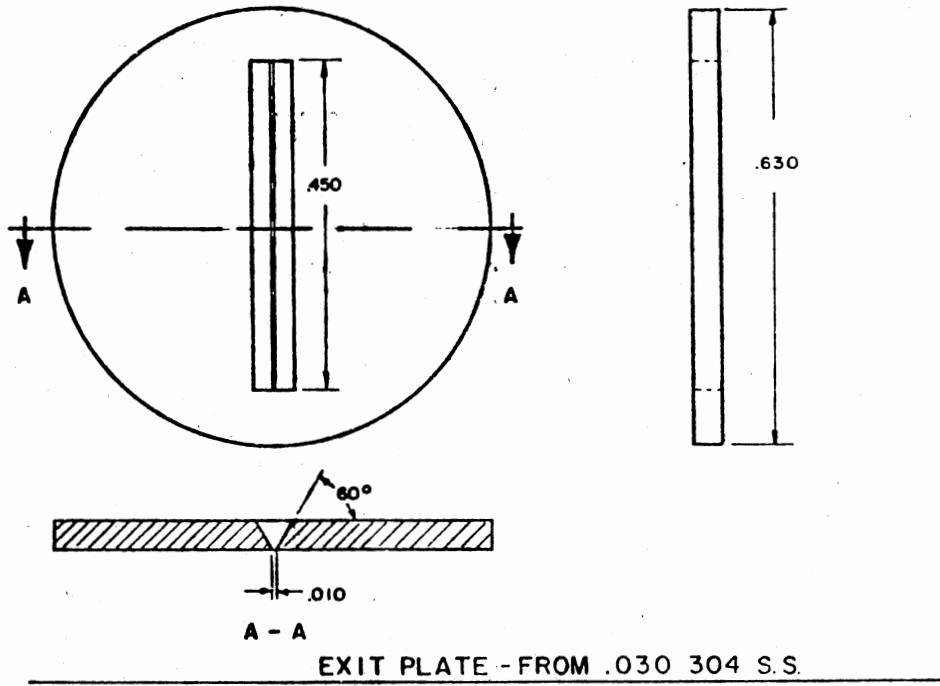


### ION SOURCE MAGNET OFFSET ASSEMBLY



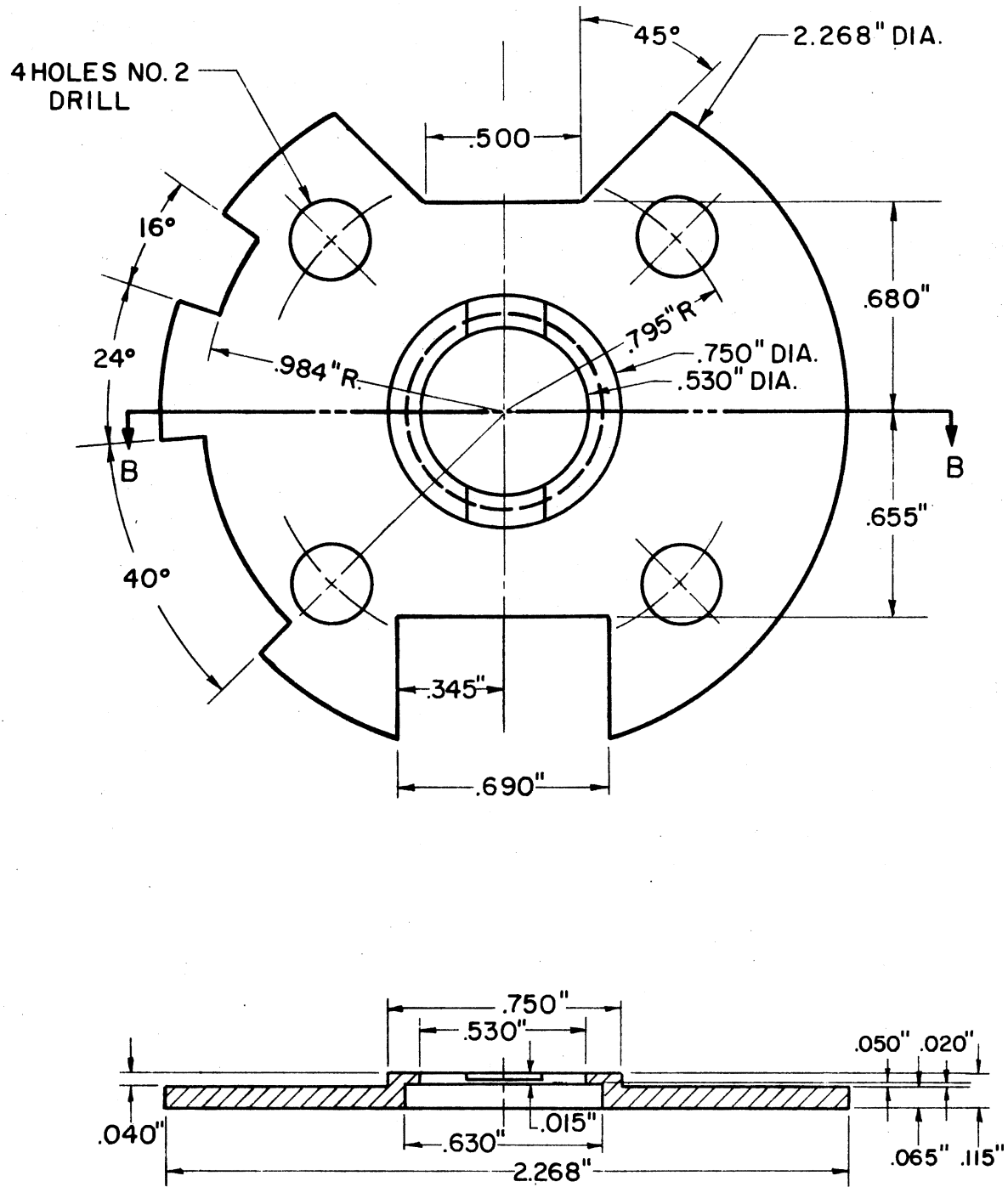
### POLE ASSEMBLY MODIFICATION

Figure 29. Ion-Source Magnet Offsets



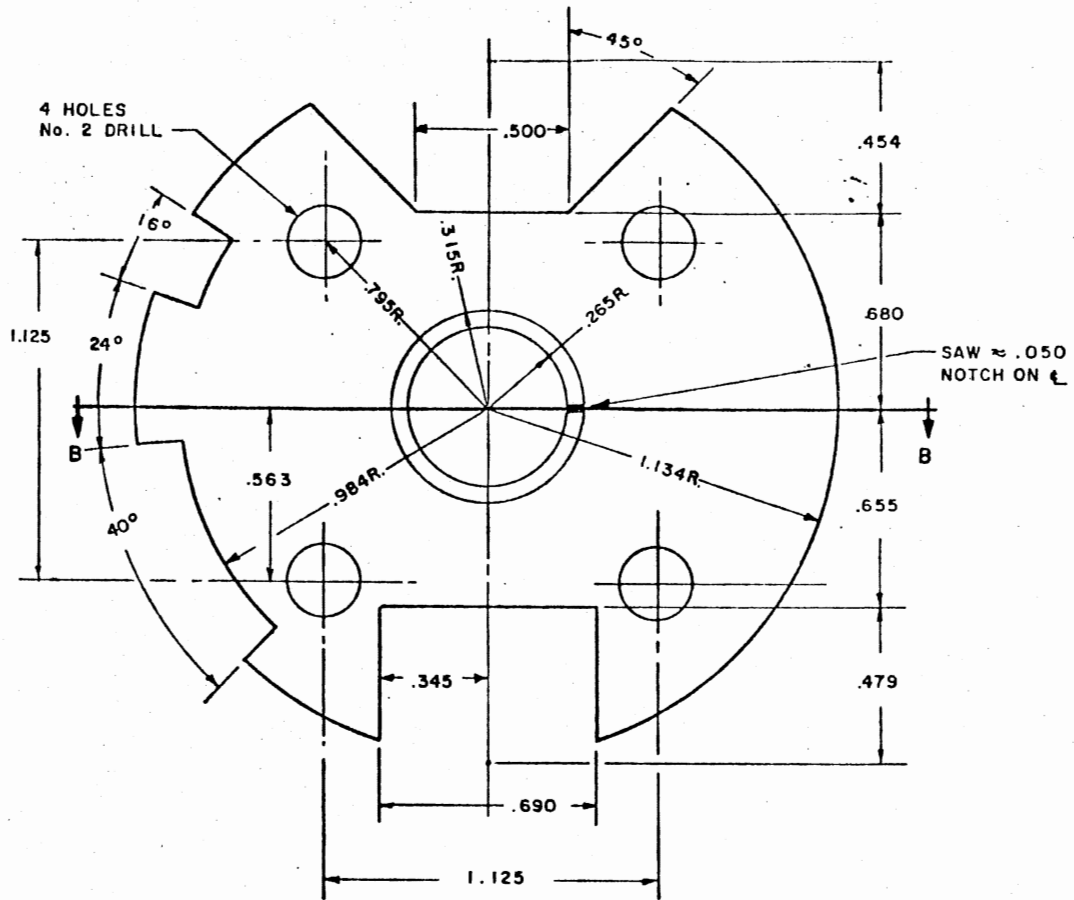
REPELLER MODIFICATION  
FORM .221 D. HOLE WHEN PLATES ARE .025 APART

Figure 30. Cathode and Repellers

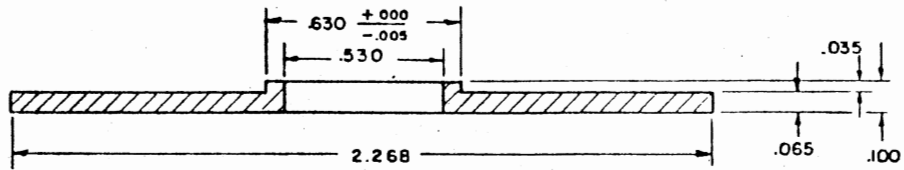


EXIT PLATE INSULATOR  
 MIKROY 750

Figure 31. Cathode Insulator (Top)



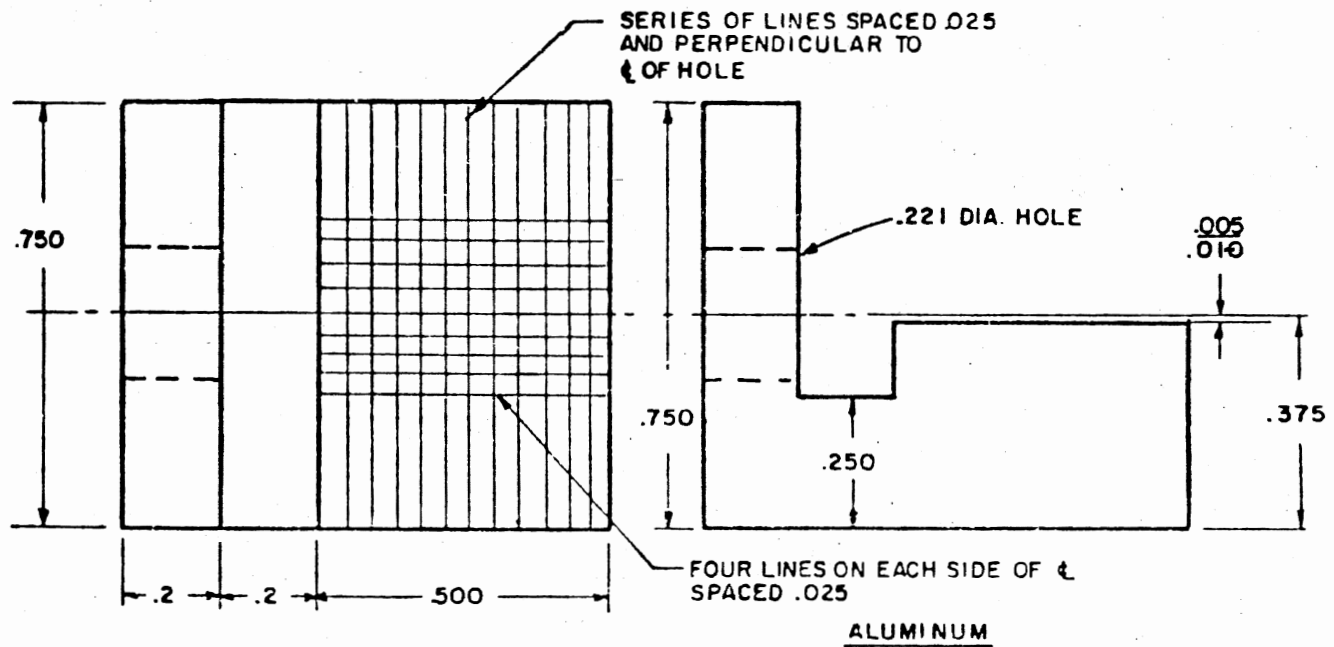
SECTION B - B



EXIT PLATE INSULATOR (MIKROY 750)

Figure 32. Cathode Insulator (Bottom)





BLADE ALIGNMENT JIG

Figure 33. Blade Alignment Jig

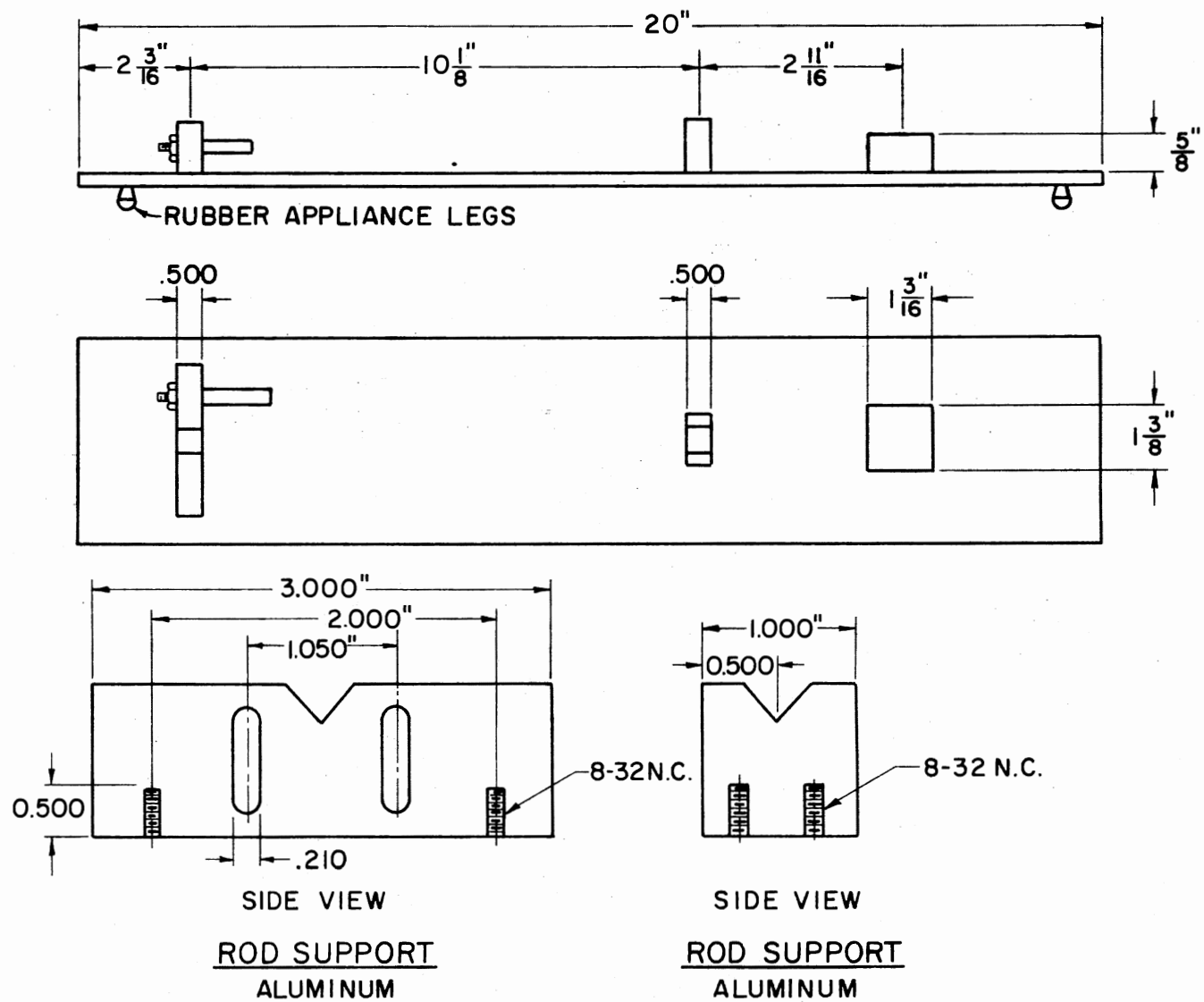
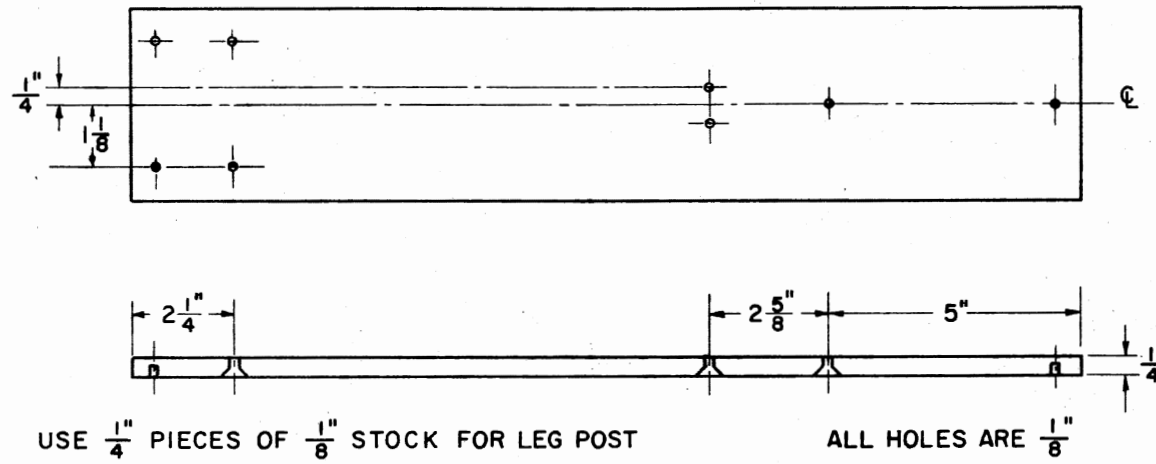
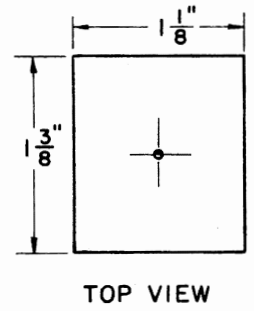


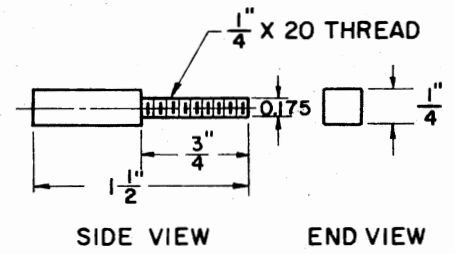
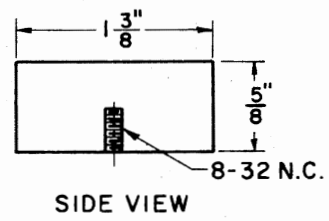
Figure 34. Emitter and Emitter Control Rod Alignment Bench



BASE PLATE  
 $\frac{1}{4}$ " COLD ROLLED STEEL



BLADE VISE PEDESTAL  
 ALUMINUM



MICROMETER SUPPORT ROD  
 ALUMINUM

Figure 35. Emitter and Emitter Control Rod Alignment Bench

APPENDIX B

HIGH RESOLUTION 70-eV MASS SPECTRAL DATA  
FOR ANTHRACENE OIL AND ITS FOUR  
UPGRADED REACTOR SAMPLES

TABLE XXXIII

HIGH-RESOLUTION DATA FOR MAJOR IONS FROM THE FEEDSTOCK  
AND REACTOR SAMPLE HYDROCARBON PLUS ETHER FRACTIONS

Nominal	Mass Experimental <sup>a</sup>	Calculated	$\Delta M \times 10^{+3}$	Assigned Formula
118	118.0758 ± .0018	118.0782	3.6	C <sub>9</sub> H <sub>10</sub>
120	120.0953 ± .0028	120.0939	1.4	C <sub>9</sub> H <sub>12</sub>
128	128.0610 ± .0017	128.0626	1.6	C <sub>10</sub> H <sub>8</sub>
132	132.0937 ± .0027	132.0939	0.2	C <sub>10</sub> H <sub>12</sub>
134	134.0177 ± .0018	134.0190	1.3	C <sub>8</sub> H <sub>6</sub> S
	134.1108 ± .0009	134.1095	1.2	C <sub>10</sub> H <sub>14</sub>
142	142.0760 ± .0023	142.0782	2.5	C <sub>10</sub> H <sub>10</sub>
146	146.0196 <sup>b</sup>	146.0224	2.8	C <sub>6</sub> H <sub>10</sub> S <sub>2</sub>
	146.1087 ± .0027	146.1095	0.8	C <sub>14</sub> H <sub>14</sub>
148	148.0370 <sup>b</sup>	148.0347	2.3	C <sub>9</sub> H <sub>8</sub> S
154	154.0757 ± .0024	154.0782	2.5	C <sub>12</sub> H <sub>10</sub>
156	156.0923 ± .0018	156.0939	1.6	C <sub>12</sub> H <sub>12</sub>
158	158.1102 ± .0025	158.1095	0.7	C <sub>12</sub> H <sub>14</sub>
160	160.1264 ± .0026	160.1252	1.2	C <sub>12</sub> H <sub>16</sub>
162	162.0480 ± .0028	162.0469	1.1	C <sub>13</sub> H <sub>6</sub>
166	166.0768 ± .0036	166.0782	1.4	C <sub>13</sub> H <sub>10</sub>
	168.0574 ± .0017	168.0575	0.1	C <sub>12</sub> H <sub>8</sub> O
168	168.0918 ± .0013	168.0939	1.1	C <sub>13</sub> H <sub>12</sub>
170	170.1091 ± .0025	170.1095	0.4	C <sub>13</sub> H <sub>14</sub>
172	172.1247 ± .0022	172.1252	0.5	C <sub>13</sub> H <sub>16</sub>
174	174.1413 ± .0023	174.1408	0.5	C <sub>13</sub> H <sub>18</sub>

TABLE XXXIII (Continued)

Nominal	Mass Experimental <sup>a</sup>	Calculated	$\Delta M \times 10^{+3}$	Assigned Formula
178	178.0789 ± .0024	178.0782	0.6	C <sub>14</sub> H <sub>10</sub>
180	180.0918 ± .0016	180.0939	2.1	C <sub>14</sub> H <sub>12</sub>
182	182.0721 ± .0022	182.0732	1.1	C <sub>13</sub> H <sub>10</sub> <sup>O</sup>
	182.1093 ± .0037	182.1095	1.1	C <sub>14</sub> H <sub>14</sub>
184	184.0368 ± .0032	184.0347	2.1	C <sub>12</sub> H <sub>8</sub> <sup>S</sup>
	184.1260 ± .0039	184.1252	0.8	C <sub>14</sub> H <sub>16</sub>
186	186.0533 <sup>b</sup>	186.0537	0.4	C <sub>9</sub> H <sub>14</sub> <sup>S</sup>
	186.1411 ± .0032	186.1408	0.3	C <sub>14</sub> H <sub>18</sub>
188	188.0631 ± .0009	188.0626	3.5	C <sub>15</sub> H <sub>8</sub>
190	190.0774 ± .0040	190.9782	0.8	C <sub>15</sub> H <sub>10</sub>
192	192.0931 ± .0016	192.0939	0.8	C <sub>15</sub> H <sub>12</sub>
194	194.0752 ± .0024	194.0732	2.0	C <sub>14</sub> H <sub>10</sub> <sup>O</sup>
	194.1121 ± .0054	194.1095	2.6	C <sub>15</sub> H <sub>14</sub>
196	196.0881 ± .0037	196.0888	0.7	C <sub>14</sub> H <sub>12</sub> <sup>O</sup>
	196.1239 ± .0043	196.1252	1.3	C <sub>15</sub> H <sub>16</sub>
198	198.0533 ± .0053	198.0503	3.0	C <sub>13</sub> H <sub>10</sub> <sup>S</sup>
	198.1422 <sup>c</sup>	198.1408	1.4	C <sub>15</sub> H <sub>18</sub>
200	200.0632 ± .0011	200.0626	0.6	C <sub>16</sub> H <sub>8</sub>
	200.1575 <sup>c,d</sup>	200.1565	1.0	C <sub>15</sub> H <sub>20</sub>
202	202.0783 ± .0031	202.0782	0.1	C <sub>16</sub> H <sub>10</sub>
204	204.0939 ± .0034	204.0939	0.0	C <sub>16</sub> H <sub>12</sub>
206	206.1069 ± .0033	206.1095	4.1	C <sub>16</sub> H <sub>14</sub>
	208.0378 <sup>b</sup>	208.0382	0.4	C <sub>11</sub> H <sub>12</sub> S <sub>2</sub>

TABLE XXXIII (Continued)

Nominal	Mass Experimental <sup>a</sup>	Calculated	$\Delta M \times 10^{+3}$	Assigned Formula
208	208.0889 $\pm$ .0045	208.0888	0.1	C <sub>15</sub> H <sub>12</sub> O
	208.1247 $\pm$ .0036	208.1252	0.7	C <sub>16</sub> H <sub>16</sub>
210	210.1052 $\pm$ .0030	210.1045	0.7	C <sub>15</sub> H <sub>14</sub> O
212	210.1410 $\pm$ .0015	210.1408	0.2	C <sub>16</sub> H <sub>18</sub>
	212.0666 <sup>b</sup>	212.0660	0.6	C <sub>14</sub> H <sub>12</sub> S
	212.1614 $\pm$ .0003	212.1565	4.9	C <sub>16</sub> H <sub>20</sub>
214	214.1696 <sup>c</sup>	214.1721	2.5	C <sub>16</sub> H <sub>22</sub>
216	216.0941 $\pm$ .0014	216.0939	0.2	C <sub>17</sub> H <sub>12</sub>
218	218.0760 $\pm$ .0027	218.0732	2.8	C <sub>16</sub> H <sub>10</sub> O
	218.1133 $\pm$ .0039	218.1095	4.2	C <sub>17</sub> H <sub>14</sub>
220	220.1259 $\pm$ .0033	220.1252	0.7	C <sub>17</sub> H <sub>16</sub>
222	222.1070 $\pm$ .0037	222.1045	2.5	C <sub>16</sub> H <sub>14</sub> O
	222.1420 $\pm$ .0047	222.1408	1.2	C <sub>17</sub> H <sub>18</sub>
224				
226	226.0796 $\pm$ .0032	226.0782	1.4	C <sub>18</sub> H <sub>10</sub>
228	228.0940 $\pm$ .0033	228.0939	0.1	C <sub>18</sub> H <sub>12</sub>
230	230.1102 $\pm$ .0028	230.1095	0.7	C <sub>18</sub> H <sub>14</sub>
232	232.0879 $\pm$ .0021	232.0888	0.9	C <sub>17</sub> H <sub>12</sub> O
	232.1248 $\pm$ .0015	232.1252	0.4	C <sub>18</sub> H <sub>16</sub>
	234.0535 <sup>b</sup>	234.5031	3.1	C <sub>16</sub> H <sub>10</sub> S
234	234.1373 $\pm$ .0009	234.1408	3.5	C <sub>10</sub> H <sub>18</sub>
236	236.1228 $\pm$ .0004 <sup>c, d</sup>	236.1201	2.8	C <sub>17</sub> H <sub>16</sub> O
	236.1589 $\pm$ .0017 <sup>c, d</sup>	236.1565	2.4	C <sub>18</sub> H <sub>20</sub>
240	240.0942 $\pm$ .0020	240.0939	0.3	C <sub>19</sub> H <sub>12</sub>

TABLE XXXIII (Continued)

Nominal	Mass Experimental <sup>a</sup>	Calculated	$\Delta M \times 10^{+3}$	Assigned Formula
242	242.0752 <sup>d</sup>	242.0732	2.0	C <sub>18</sub> H <sub>10</sub> O
	242.1107 ± .0029	242.1095	1.2	C <sub>19</sub> H <sub>14</sub>
244	244.0888 ± .0054	244.0888	0.0	C <sub>18</sub> H <sub>12</sub> O
	244.1248 ± .0025	244.1252	0.4	C <sub>19</sub> H <sub>16</sub>
246	246.1068 ± .0017	246.1045	2.3	C <sub>18</sub> H <sub>14</sub> O
	246.1421 ± .0019	246.1408	1.3	C <sub>19</sub> H <sub>18</sub>
252	252.0915 ± .0030	252.0939	1.4	C <sub>20</sub> H <sub>12</sub>
254	254.1136 <sup>c</sup>	254.1095	4.1	C <sub>20</sub> H <sub>14</sub>
256	256.1280 <sup>c</sup>	256.1252	2.8	C <sub>20</sub> H <sub>16</sub>
258	258.1453 <sup>c</sup>	256.1408	4.6	C <sub>20</sub> H <sub>18</sub>

<sup>a</sup>All deviations are standard deviations. <sup>b</sup>Obs. in MS of feedstock only.

<sup>c</sup>Obs. in MS of Reactor Sample 3. <sup>d</sup>Obs. in MS of Reactor Sample 4.



TABLE XXXIV  
HIGH-RESOLUTION DATA FOR MAJOR IONS FROM THE FEEDSTOCK  
AND REACTOR SAMPLE ACID FRACTIONS

Nominal	Mass <sup>a</sup>		$\Delta m \times 10^3$	Assigned Formula
	Experimental	Calculated		
94	94.0409 ± .0032	94.0419	1.0	C <sub>6</sub> H <sub>6</sub> O
108	108.0570 ± .0032	108.0575	0.5	C <sub>7</sub> H <sub>8</sub> O
117	117.0581 ± .0021	117.0578	0.3	C <sub>8</sub> H <sub>7</sub> N
122	122.0684 ± .0051	122.0732	4.8	C <sub>8</sub> H <sub>10</sub> O
131	131.0732 ± .0042	131.0735	0.3	C <sub>9</sub> H <sub>9</sub> N
134	134.0738 ± .0013	134.0732	0.6	C <sub>9</sub> H <sub>10</sub> O
136	136.0881 ± .0023	136.0888	0.7	C <sub>9</sub> H <sub>12</sub> O
144	144.0561 ± .0015 <sup>b,c</sup>	144.0575	1.4	C <sub>10</sub> H <sub>3</sub> O
145	145.0511	145.0527	1.6	C <sub>9</sub> H <sub>7</sub> NO
146	146.0748 <sup>c</sup>	146.0732	1.6	C <sub>10</sub> H <sub>10</sub> O
148	148.0881 ± .0001	148.0888	0.7	C <sub>10</sub> H <sub>12</sub> O
150	150.1042 ± .0017	150.1045	0.3	C <sub>10</sub> H <sub>14</sub> O
158	158.0713 <sup>c</sup>	158.0732	1.9	C <sub>11</sub> H <sub>10</sub> O
159	159.0695	159.0684	1.1	C <sub>10</sub> H <sub>9</sub> NO
162	162.1037 ± .0025	162.1045	0.8	C <sub>11</sub> H <sub>14</sub> O
164	164.0525 ± .0008	164.0473	5.2	C <sub>9</sub> H <sub>8</sub> O <sub>3</sub>
	164.1212	164.1201	1.1	C <sub>11</sub> H <sub>16</sub> C
167	167.0749 ± .0017	167.0735	1.4	C <sub>12</sub> H <sub>9</sub> N
170	170.0742 ± .0037	170.0732	1.0	C <sub>12</sub> H <sub>10</sub> O
172	172.0886 <sup>b,c</sup>	170.0888	0.2	C <sub>12</sub> H <sub>12</sub> O
173	173.0883 ± .0017 <sup>b</sup>	173.0840	4.3	C <sub>11</sub> H <sub>11</sub> NO
176	176.1223 ± .0029	176.1201	2.2	C <sub>12</sub> H <sub>16</sub> O
178	178.0802 ± .0021	178.0782	2.0	C <sub>14</sub> H <sub>10</sub>
	178.1379	178.1357	2.2	C <sub>12</sub> H <sub>18</sub> O

TABLE XXXIV (Continued)

Nominal	Mass <sup>a</sup>		$\Delta m \times 10^3$	Assigned Formula
	Experimental	Calculated		
181	181.0889 ± .0026	181.0891	0.2	C <sub>13</sub> H <sub>11</sub> N
182	182.0705 ± .0017 <sup>b</sup>	182.0732	2.8	C <sub>13</sub> H <sub>10</sub> O
184	184.0515 ± .0007	184.0524	0.9	C <sub>12</sub> H <sub>8</sub> O <sub>2</sub>
	184.0868 ± .0021	184.0888	2.0	C <sub>13</sub> H <sub>12</sub> O
186	186.1027 ± .0017 <sup>c</sup>	186.1045	1.8	C <sub>13</sub> H <sub>14</sub> O
190	190.1377 ± .0014 <sup>b</sup>	190.1357	2.0	C <sub>13</sub> H <sub>18</sub> O
191	191.0748 ± .0029	191.0735	1.3	C <sub>14</sub> H <sub>9</sub> N
192	192.0775 ± .0023	192.0786	1.1	C <sub>11</sub> H <sub>12</sub> O <sub>3</sub>
193	193.0872 ± .0045	193.0891	1.9	C <sub>14</sub> H <sub>11</sub> N
194	194.0740 ± .0046	194.0732	0.8	C <sub>14</sub> H <sub>10</sub> O
195	195.0692 <sup>c</sup>	195.0684	0.8	C <sub>13</sub> H <sub>9</sub> NO
	195.1086 ± .0038 <sup>d</sup>	195.1048	3.8	C <sub>14</sub> H <sub>13</sub> N
196	196.0885 ± .0013	196.0888	0.3	C <sub>14</sub> H <sub>12</sub> O
198	198.0704 ± .0021	198.0681	2.3	C <sub>13</sub> H <sub>10</sub> O <sub>2</sub>
	198.1071 ± .0019	198.1045	2.6	C <sub>14</sub> H <sub>14</sub> O
204	204.1556 ± .0024	204.1514	4.2	C <sub>14</sub> H <sub>20</sub> O
205	205.0904 ± .0033	205.0891	1.3	C <sub>15</sub> H <sub>11</sub> N
	207.0678 <sup>c</sup>	207.0684	0.6	C <sub>14</sub> H <sub>9</sub> NO
207	207.0762 ± .0006			
	207.1034 ± .0008 <sup>d</sup>	207.1048	1.4	C <sub>15</sub> H <sub>13</sub> N
208	208.0859 ± .0030	208.0888	2.9	C <sub>15</sub> H <sub>12</sub> O
209	209.0824 <sup>c</sup>	209.0840	1.6	C <sub>14</sub> H <sub>11</sub> NO
210	210.0610 <sup>c</sup>	210.0681	7.1	C <sub>14</sub> H <sub>10</sub> O <sub>2</sub>
	210.1039 ± .0028	210.1045	0.6	C <sub>15</sub> H <sub>14</sub> O

TABLE XXXIV (Continued)

Nominal	Mass <sup>a</sup>		$\Delta m \times 10^3$	Assigned Formula
	Experimental	Calculated		
212	212.0451 ± .0007 <sup>c</sup>	212.0473	2.2	C <sub>13</sub> H <sub>8</sub> O <sub>3</sub>
	212.0841 ± .0013	212.0837	0.4	C <sub>14</sub> H <sub>12</sub> O <sub>2</sub>
	212.1189 ± .0020	212.1201	1.2	C <sub>15</sub> H <sub>16</sub> O
217	217.0880 ± .0028	217.0890	1.1	C <sub>16</sub> H <sub>11</sub> N
218	218.0770 ± .0028	218.0732	3.8	C <sub>16</sub> H <sub>10</sub> O
	218.0932 ± .0047	218.0943	1.1	C <sub>13</sub> H <sub>14</sub> O <sub>3</sub>
220	220.0833 ± .0026	220.0888	5.5	C <sub>16</sub> H <sub>12</sub> O
222	222.1083 ± .0035 <sup>b</sup>	222.1045	3.8	C <sub>16</sub> H <sub>14</sub> O
224	224.0873 ± .0041	224.0837	3.6	C <sub>15</sub> H <sub>12</sub> O <sub>2</sub>
	224.1179 ± .0011	224.1201	2.2	C <sub>16</sub> H <sub>16</sub> O
226	226.0651 ± .0010 <sup>b,c</sup>	226.0630	2.1	C <sub>14</sub> H <sub>10</sub> O <sub>3</sub>
	226.1023 ± .0023	226.0994	2.9	C <sub>15</sub> H <sub>14</sub> O <sub>2</sub>
	226.1371 ± .0004	226.1357	1.4	C <sub>16</sub> H <sub>18</sub> O
231	231.1073 ± .0008	231.1048	2.5	C <sub>17</sub> H <sub>13</sub> N
232	232.0915 ± .0046 <sup>b</sup>	232.0888	2.7	C <sub>17</sub> H <sub>12</sub> O
	232.1129 ± .0014	232.1099	3.0	C <sub>14</sub> H <sub>16</sub> O <sub>3</sub>
234	234.0693 ± .0006 <sup>b</sup>	234.0681	1.4	C <sub>16</sub> H <sub>10</sub> O <sub>2</sub>
	234.1077 ± .0021 <sup>b</sup>	234.1045	2.2	C <sub>17</sub> H <sub>14</sub> O
238	238.1378 ± .0040	238.1357	2.1	C <sub>17</sub> H <sub>18</sub> O
240	240.0789	240.0786	0.3	C <sub>15</sub> H <sub>12</sub> O <sub>3</sub>
	240.1178	240.1150	2.8	C <sub>16</sub> H <sub>16</sub> O <sub>2</sub>

TABLE XXXIV (Continued)

Nominal	Mass <sup>a</sup>		$\Delta m \times 10^3$	Assigned Formula
	Experimental	Calculated		
243	243.1072	243.1048	2.4	C <sub>18</sub> H <sub>13</sub> N
246	246.1046	246.1045	0.9	C <sub>18</sub> H <sub>14</sub> O
248	248.0852	258.0837	1.5	C <sub>17</sub> H <sub>12</sub> O <sub>2</sub>
	248.1221 ± .0044	248.1201	2.0	C <sub>18</sub> H <sub>16</sub> O
252	252.1502	252.1514	1.2	C <sub>18</sub> H <sub>20</sub> O
262	262.1335	262.1357	2.2	C <sub>19</sub> H <sub>18</sub> O

<sup>a</sup>All deviations, unless indicated, are standard deviations.

<sup>b</sup>Averaged from two samples.

<sup>c</sup>Obs. in MS of feedstock only.

<sup>d</sup>Obs. in MS of reactor samples only.

TABLE XXXV

HIGH-RESOLUTION DATA FOR MAJOR IONS FROM THE FEEDSTOCK  
AND REACTOR SAMPLE BASE FRACTIONS

Nominal	Mass <sup>a</sup>		$\Delta m \times 10^3$	Assigned Formula
	Experimental	Calculated		
93	93.0583 ± .0008	93.0578	0.5	C <sub>6</sub> H <sub>7</sub> N
107	107.0753 ± .0021	107.0735	1.8	C <sub>7</sub> H <sub>9</sub> N
117	117.0603	117.0578	2.5	C <sub>8</sub> H <sub>7</sub> N
119	119.0754	119.0735	1.9	C <sub>8</sub> H <sub>9</sub> N
121	121.0901 ± .0012	121.0891	1.0	C <sub>8</sub> H <sub>11</sub> N
129	129.0606 ± .0011	129.0578	2.8	C <sub>9</sub> H <sub>7</sub> N
133	133.0844 ± .0022	133.0891	4.7	C <sub>9</sub> H <sub>11</sub> N
135	135.1051 ± .0026	135.1048	0.3	C <sub>9</sub> H <sub>13</sub> N
143	143.0730 ± .0016	143.0735	0.5	C <sub>10</sub> H <sub>9</sub> N
145	145.0890 ± .0034	145.0891	0.1	C <sub>10</sub> H <sub>11</sub> N
147	147.1064 ± .0040 <sup>b</sup>	147.1048	1.6	C <sub>10</sub> H <sub>13</sub> N
149	149.1201 ± .0013	149.1204	0.3	C <sub>10</sub> H <sub>15</sub> N
155	155.0731 ± .0029	155.0735	0.4	C <sub>11</sub> H <sub>9</sub> N
157	157.0876 ± .0028	157.0891	1.5	C <sub>11</sub> H <sub>11</sub> N
159	159.1038 ± .0025	159.1048	1.0	C <sub>11</sub> H <sub>13</sub> N
161	161.0833 ± .0034 <sup>b,c</sup>	161.0840	0.7	C <sub>10</sub> H <sub>11</sub> NO
	161.1187 ± .0017	161.1204	1.7	C <sub>11</sub> H <sub>15</sub> N
163	163.1337 ± .0012	163.1361	2.4	C <sub>11</sub> H <sub>17</sub> N
167	167.0728 ± .0022	167.0735	0.7	C <sub>12</sub> H <sub>9</sub> N
169	169.0533 ± .0007 <sup>b,c</sup>	169.0527	0.5	C <sub>11</sub> H <sub>7</sub> NO
	169.0883 ± .0016	169.0891	0.8	C <sub>12</sub> H <sub>11</sub> N
171	171.1046 ± .0022	171.1048	0.2	C <sub>12</sub> H <sub>13</sub> N
173	173.1193 ± .0009	173.1204	1.1	C <sub>12</sub> H <sub>15</sub> N

TABLE XXXV (Continued)

Nominal	Mass <sup>a</sup>		$\Delta m \times 10^3$	Assigned Formula
	Experimental	Calculated		
175	175.1362 ± .0015	175.1361	0.1	C <sub>12</sub> H <sub>17</sub> N
177	177.1516	177.1517	0.1	C <sub>12</sub> H <sub>19</sub> N
179	179.0737 ± .0014	179.0735	0.2	C <sub>13</sub> H <sub>9</sub> N
181	181.0893 ± .0013	181.0891	0.2	C <sub>13</sub> H <sub>11</sub> N
183	183.0688 ± .0008	183.0684	0.4	C <sub>12</sub> H <sub>9</sub> NO
	183.1039 ± .0013	183.1048	0.9	C <sub>13</sub> H <sub>13</sub> N
185	185.1179 ± .0021	185.1204	2.5	C <sub>13</sub> H <sub>15</sub> N
187	187.1338 ± .0022	187.1361	2.3	C <sub>13</sub> H <sub>17</sub> N
189	189.1522 ± .0010	189.1517	0.5	C <sub>13</sub> H <sub>19</sub> N
191	191.0723 ± .0017	191.0735	1.2	C <sub>14</sub> H <sub>9</sub> N
193	193.0873 ± .0022	193.0891	1.8	C <sub>14</sub> H <sub>11</sub> N
	193.1786 <sup>d</sup>	193.1830	4.4	C <sub>13</sub> H <sub>23</sub> N
195	195.0698 <sup>c</sup>	195.0684	1.4	C <sub>13</sub> H <sub>9</sub> NO
	195.1049 ± .0028 <sup>b</sup>	195.1048	0.1	C <sub>14</sub> H <sub>13</sub> N
197	197.0838 ± .0027	197.0840	0.2	C <sub>13</sub> H <sub>11</sub> NO
	197.1212 ± .0017	197.1204	0.8	C <sub>14</sub> H <sub>15</sub> N
199	199.1395 ± .0037	199.1361	3.4	C <sub>14</sub> H <sub>17</sub> N
201	201.1543 ± .0020	201.1517	2.6	C <sub>14</sub> H <sub>19</sub> N
203	203.0763 ± .0029	203.0735	2.8	C <sub>15</sub> H <sub>9</sub> N
	203.1705 ± .0027 <sup>d</sup>	203.1674	3.1	C <sub>14</sub> H <sub>21</sub> N
205	205.0879 ± .0033	205.0891	2.2	C <sub>15</sub> H <sub>11</sub> N
207	207.1050 ± .0018	207.1048	0.2	C <sub>15</sub> H <sub>13</sub> N
	207.1986	207.1987	0.1	C <sub>14</sub> H <sub>25</sub> N

TABLE XXXV (Continued)

Nominal	Mass <sup>a</sup>		$\Delta m \times 10^3$	Assigned Formula
	Experimental	Calculated		
209	209.0857	209.0840	1.7	C <sub>14</sub> H <sub>11</sub> NO
	209.1220 ± .0033	209.1204	1.6	C <sub>15</sub> H <sub>15</sub> N
211	211.0987 ± .0032	211.0997	1.0	C <sub>14</sub> H <sub>13</sub> NO
	211.1373 ± .0020	211.1361	1.2	C <sub>15</sub> H <sub>17</sub> N
213	213.1512 ± .0043	213.1517	0.5	C <sub>15</sub> H <sub>19</sub> N
215	215.1680 ± .0021	215.2674	0.6	C <sub>15</sub> H <sub>21</sub> N
217	217.0904 ± .0025	217.0891	1.3	C <sub>15</sub> H <sub>11</sub> N
	217.1849 <sup>d</sup>	217.1830	1.9	C <sub>15</sub> H <sub>23</sub> N
219	219.0698 ± .0049	219.0684	1.4	C <sub>15</sub> H <sub>9</sub> NO
	219.1047 ± .0039	219.1048	0.1	C <sub>16</sub> H <sub>13</sub> N
	219.1987 <sup>d</sup>	219.1987	0.0	C <sub>15</sub> H <sub>25</sub> N
221	221.1234	221.1204	3.0	C <sub>16</sub> H <sub>15</sub> N
223	223.1030 ± .0001	223.0997	3.3	C <sub>15</sub> H <sub>13</sub> NO
	223.1414 ± .0029	223.1361	5.3	C <sub>16</sub> H <sub>17</sub> N
225	225.1168 ± .0008	225.1153	1.5	C <sub>15</sub> H <sub>15</sub> NO
	225.1527 ± .0010	225.1517	1.0	C <sub>16</sub> H <sub>19</sub> N
227	227.1659 ± .0016	227.1674	1.5	C <sub>16</sub> H <sub>21</sub> N
229	229.0909 ± .0023	229.0891	1.8	C <sub>17</sub> H <sub>11</sub> N
	229.1827 <sup>d</sup>	229.1830	0.3	C <sub>16</sub> H <sub>23</sub> N
231	231.1029 ± .0014	231.1048	1.9	C <sub>17</sub> H <sub>13</sub> N
233	233.0867 <sup>d</sup>	233.0840	2.7	C <sub>16</sub> H <sub>11</sub> NO
	233.1235 ± .0039	233.1204	3.1	C <sub>17</sub> H <sub>15</sub> N
235	235.1368 ± .0041	235.1361	0.7	C <sub>17</sub> H <sub>17</sub> N

TABLE XXXV (Continued)

Nominal	Mass <sup>a</sup>		$\Delta m \times 10^3$	Assigned Formula
	Experimental	Calculated		
237	237.1159 <sup>d</sup>	237.1153	0.6	C <sub>16</sub> H <sub>15</sub> NO
	237.1540 ± .0037	237.1517	2.3	C <sub>17</sub> H <sub>19</sub> N
241	241.1831 ± .0009	241.1830	0.1	C <sub>17</sub> H <sub>23</sub> N
243	243.1044 ± .0014	243.1048	0.4	C <sub>18</sub> H <sub>13</sub> N
245	245.1192 ± .0047	245.1204	1.2	C <sub>18</sub> H <sub>15</sub> N
247	247.1050 ± .0012 <sup>d</sup>	247.0997	5.3	C <sub>17</sub> H <sub>13</sub> N
	247.1385 ± .0026	247.1361	2.4	C <sub>18</sub> H <sub>17</sub> N
249	249.1520 ± .0032	249.1517	0.3	C <sub>18</sub> H <sub>19</sub> N
251	251.1690 ± .0005	251.1674	1.6	C <sub>18</sub> H <sub>21</sub> N
253	253.0908 ± .0037	253.0891	1.7	C <sub>19</sub> H <sub>11</sub> N
255	255.1047	255.1048	0.1	C <sub>19</sub> H <sub>13</sub> N
257	257.1219 ± .0027	257.1204	1.5	C <sub>19</sub> H <sub>13</sub> N
259	259.1413 ± .0027	259.1361	5.2	C <sub>19</sub> H <sub>17</sub> N

<sup>a</sup>All deviations, unless indicated, are standard deviations.

<sup>b</sup>Averaged from two samples.

<sup>c</sup>Appeared in MS of feedstock only.

<sup>d</sup>Appeared in MS of reactor sample only.



TABLE XXXVI

HIGH-RESOLUTION DATA FOR MAJOR IONS FROM FEEDSTOCK  
AND REACTOR SAMPLE NEUTRAL-NITROGEN FRACTIONS

Nominal	Mass		$\Delta M \times 10^3$	Assigned Formula
	Experimental	Calculated		
117	117.0576 $\pm$ .0002 <sup>a</sup>	117.0578	0.2	C <sub>8</sub> H <sub>7</sub> N
131	131.0731 $\pm$ .0000	131.0735	0.4	C <sub>9</sub> H <sub>9</sub> N
167	167.0740 $\pm$ .0009	167.0735	0.5	C <sub>12</sub> H <sub>9</sub> N
181	181.0870 $\pm$ .0016	181.0891	2.1	C <sub>13</sub> H <sub>11</sub> N
191	191.0726	191.0735	0.9	C <sub>14</sub> H <sub>9</sub> N
193	193.0903	193.0891	0.9	C <sub>14</sub> H <sub>11</sub> N
195	195.1043 $\pm$ .0006	195.1047	0.4	C <sub>14</sub> H <sub>13</sub> N
209	209.1264 $\pm$ .0038	209.1204	6.0	C <sub>15</sub> H <sub>15</sub> N
221	221.1223 $\pm$ .0016	221.1204	2.1	C <sub>16</sub> H <sub>15</sub> N
223	223.1379 $\pm$ .0002	223.1361	1.8	C <sub>16</sub> H <sub>17</sub> N

APPENDIX C

COMPUTER PROGRAM

```

C
C THIS PROGRAM WILL CALCULATE WEIGHT PERCENTS OF COMPCUNDS OCCURING
C AT DIFFERENT NUMINAL MASSES IN A COMPLEX MIXTURE USING PEAK HEIGHT
C OBTAINED FROM FI OR LVEI MASS SPECTRA. THE PROGRAM CAN ALSO APPLY
C SENSITIVITY VALUES IN THE CALCULATION OF WEIGHT PERCENTS. THE OPT-
C ION EXISTS FOR CALCULATION OF MOLE PERCENTS FOR NOMINAL MAS COMP-
C ONENTS FOR DIFFERENT FRACTIONS OF A TOTAL SAMPLE.
C
0001 DIMENSION MW(500),X11(500),X12(500),X13(500),XX1(500),XX2(500),XX3
1(500),XWT1(500),XWT2(500),XWT3(500),AVEWT(500),SIGT(500),NMW(500)
2,CWT1(500),CWT2(500),CWT3(500),XCWT1(500),XCWT2(500),XCWT3(500),SM
3WT1(500),SMWT2(500),SMWT3(500),AVECWT(500),SMCWT1(500),SMCWT2(500)
4,SMCWT3(500),SIGSB(500),TITLE(18),SENS(500),XMW1(500),XMH2(500),XM
5W3(500),TAVEWT(500),AVEMWT(500)
0002 REAL*4 MWTPRC(5,500),NMWTPC(5,500)
C
C THE FIRST CARD OF A DATA SET IS USED FOR TITLES (COL 1-72)
C THE SECOND CARD OF A DATA SET IS THE CONTROL CARD AND CONTAINS THE
C FOLLOWING:
C N(COL 1-3) NUMBER OF CARDS IN ONE FRACTION'S DATA SET
C INT(COL 4-6) AND ISB(COL 7-9) IF IWT=1 AND ISB=0 UNCORRECTED
C WEIGHT PERCENTS FOR THAT DATA SET WILL BE CALCULATED. IF IWT=0 AND
C ISB=1 WEIGHT PERCENTS USING ONLY SENSITIVITIES WILL BE CALCULATED.
C IF IWT=1 AND ISB=1 WEIGHT PERCENTS EXCLUDING AND INCLUDING SENSIT-
C IVITIES WILL BE CALCULATED.
C NN(COL 10-12) NUMBER OF CARDS IN THE SENSITIVITY DECK FOR THE DATA
C IN THIS FRACTION.
C FPERC(COL 13-17) WEIGHT PERCENT FOR THE TOTAL SAMPLE REPRESENTED
C BY THIS FRACTION.
C NOSENS(COL 17-18) IF NOSENS=1 THE PREVIOUS SET OF SENSITIVITIES
C WILL BE USED FOR THE CALCULATION OF WEIGHTS PERCENTS. IF NOSENS=0
C THE NEXT SET OF SENSITIVITIES WILL BE USED FOR THIS CALCULATION.
C
0003 100 CONTINUE
C
C IF ONLY WEIGHT PERCENTS ARE NEEDED THE PROGRAM MAY BE TERMINATED
C AT THIS POINT BY INSERTION OF 2 BLANK CARDS. IF MOLE PERCENTS OF
C COMPONENTS IN ALL FRACTIONS OF A SAMPLE ARE DESIRED THE FOLLOWING
C MUST BE ADDED INSTEAD OF THE 2 BLANK CARDS.
C FIRST CARD TITLE FOR PURPOSES OF IDENTIFICATION(COL 1-72)
C SECOND CARD CONTAINS THE CONTROLS FOR CALCULATION OF MOLE PERCENTS
C NFRAC(COL 19-20) DENOTES THE FRACTION NUMBER OF EACH DATA SET TO
C THE TOTAL SAMPLE.
C MWL AND MWH (COL 21-26) ESTABLISH THE LOWEST AND HIGHEST NOMINAL
C MASS FOR THE PRINTOUT OF MOLE PERCENTS BY FRACTION IN THE TOTAL
C SAMPLE.
C NTFRAC(COL 27-28) THE NUMBER OF SUBFRACTIONS BEING CALCULATED FOR
C MOLE PERCENT.
C 2 BLANK CARDS FOR PROGRAM TERMINATION.
C
0004 READ(5,1) (TITLE(I),I=1,18)
0005 1 FORMAT(18A4)
0006 READ(5,2) N,IWT,ISB,NN,FPERC,NOSENS,NFRAC,MWL,MWH,NTFRAC
0007 2 FORMAT(4I3,F4.4,2I2,3I3)
0008 IF(N.LT.1) GO TO 31
0009 DO 23 LL=1,500
0010 XI1(LL)=0.0
0011 XI2(LL)=0.0

```

```

0012      23 X13(LL)=0.0
0013      NFRAC=NFRAC+1
0014      NTFRAC=NTFRAC+1
0015      DO 71 MM=1,500
0016      MWTPRC(1,MM)=MM
0017      MWTPRC(NFRAC,MM)=0.0
0018      71 CONTINUE
0019      DO 72 I=1,N
0020      READ(5,3) (MW(I),X11(MW(I)),X12(MW(I)),X13(MW(I)),I=1,N)
0021      72 CONTINUE
0022      3 FORMAT(13,3F10.0)
0023      IF(IWT.LT.1) GO TO 20
0024      SUMX1=0.0
0025      SUMX2=0.0
0026      SUMX3=0.0
0027      DO 10 I=1,N
0028      J=MW(I)
0029      XX1(I)=MW(I)*X11(J)
0030      XX2(I)=MW(I)*X12(J)
0031      XX3(I)=MW(I)*X13(J)
0032      SUMX1=SUMX1+XX1(I)
0033      SUMX2=SUMX2+XX2(I)
0034      10 SUMX3=SUMX3+XX3(I)
0035      SUMMWT=0.0
0036      DO 50 I=1,N
0037      XWT1(I)=XX1(I)/SUMX1*100
0038      XWT2(I)=XX2(I)/SUMX2*100
0039      XWT3(I)=XX3(I)/SUMX3*100
0040      AVEWT(I)=(XWT1(I)+XWT2(I)+XWT3(I))/3.0
0041      TAVEWT(I)=AVEWT(I)*FPERC
0042      AVEWT(I)=TAVEWT(I)/MW(I)
0043      82 MWTPRC(NFRAC,MW(I))=AVEWT(I)
0044      SMWT1(I)=(ABS(AVEWT(I)-XWT1(I)))**2.0
0045      SMWT2(I)=(ABS(AVEWT(I)-XWT2(I)))**2.0
0046      SMWT3(I)=(ABS(AVEWT(I)-XWT3(I)))**2.0
0047      50 SIGWT(I)=SQRT((SMWT1(I)+SMWT2(I)+SMWT3(I))/2.0)
0048      WRITE(6,7) TITLE
0049      7 FORMAT(1H1,18A4,/)
0050      WRITE(6,4)
0051      4 FORMAT(' NOMINAL M/E',10X,'SCAN 1',20X,'SCAN 2',20X,'SCAN 3',/,14X
1,'PEAK HEIGHT',2X,'WT PERCENT',2X,'PEAK HEIGHT',2X,'WT PERCENT',2X
2,'PEAK HEIGHT',2X,'WT PERCENT',3X,'AVERAGE WT PERCENT',3X,'STD. DE
1V.',/)
0052      WRITE(6,5) (MW(I),X11(MW(I)),XWT1(I),X12(MW(I)),XWT2(I),X13(MW(I))
1,XWT3(I),AVEWT(I),SIGWT(I),I=1,N)
0053      5 FORMAT(6X,13,6X,F8.3,5X,F8.5,4X,F8.3,5X,F8.5,4X,F8.3,5X,F8.5,9X,F8
1.5,3X,F8.5,/)
0054      IF(FPERC.EQ.0.0) GO TO 20
0055      WRITE(6,7) TITLE
0056      WRITE(6,56)
0057      56 FORMAT(' NOMINAL M/E',5X,'WEIGHT PERCENT OF TOTAL SAMPLE',/)
0058      WRITE(6,57) (MW(I),TAVEWT(I),I=1,N)
0059      57 FORMAT(5X,13,15X,F10.6,/)
0060      20 CONTINUE
0061      IF(ISO.LT.1) GO TO 30
0062      DO 39 L=1,500
0063      CWT1(L)=0.0
0064      CWT2(L)=0.0

```

```

0065      39 CWT3(L)=0.0
0066      DO 75 MG=1,500
0067      NMWTPC(L,MO)=MO
0068      NMWTPC(NFRAC,MO)=0.0
0069      75 CONTINUE
0070      IF(NOSENS.EQ.1) GO TO 24
0071      READ(5,22) (NMW(I),SENS(NMW(I)),I=1,NN)
0072      22 FORMAT(I3,F10.0)
0073      24 CONTINUE
0074      SUMY1=0.0
0075      SUMY2=0.0
0076      SUMY3=0.0
0077      DO 55 I=1,NN
0078      J=NMW(I)
0079      IF(XI1(J).EQ.0) GO TO 47
0080      CWT1(I)=XI1(J)/SENS(J)
0081      47 IF(XI2(J).EQ.0) GO TO 48
0082      CWT2(I)=XI2(J)/SENS(J)
0083      48 IF(XI3(J).EQ.0) GO TO 49
0084      CWT3(I)=XI3(J)/SENS(J)
0085      49 SUMY1=SUMY1+CWT1(I)
0086      SUMY2=SUMY2+CWT2(I)
0087      SUMY3=SUMY3+CWT3(I)
0088      55 CONTINUE
0089      SUMMWT=0.0
0090      DO 70 I=1,NN
0091      XCWT1(I)=CWT1(I)/SUMY1*100
0092      XCWT2(I)=CWT2(I)/SUMY2*100
0093      XCWT3(I)=CWT3(I)/SUMY3*100
0094      AVECWT(I)=(XCWT1(I)+XCWT2(I)+XCWT3(I))/3.0
0095      TAVEWT(I)=AVECWT(I)*FPERC
0096      AVEHWT(I)=TAVEWT(I)/NMW(I)
0097      83 NMWTPC(NFRAC,NMW(I))=AVEHWT(I)
0098      68 SMCWT1(I)=(ABS(AVECWT(I)-XCWT1(I)))**2.0
0099      SMCWT2(I)=(ABS(AVECWT(I)-XCWT2(I)))**2.0
0100      SMCWT3(I)=(ABS(AVECWT(I)-XCWT3(I)))**2.0
0101      SIGSB(I)=SQRT((SMCWT1(I)+SMCWT2(I)+SMCWT3(I))/2.0)
0102      70 CONTINUE
0103      WRITE(6,7) TITLE
0104      WRITE(6,6)
0105      6 FORMAT(40X,'CORRECTED WEIGHT PERCENTS',//,' NOMINAL MASS',10X,'SCAN
IN 1',10X,'SCAN 2',10X,'SCAN 3',10X,'AVERAGE',10X,'STD. DEV.',//)
0106      WRITE(6,8) (NMW(K),XCWT1(K),XCWT2(K),XCWT3(K),AVECWT(K),SIGSB(K),K
I=1,NN)
0107      8 FORMAT(5X,I3,14X,F8.5,8X,F8.5,8X,F8.5,8X,F8.5,10X,F8.5,/)
0108      IF(FPERC.EQ.0.0) GO TO 30
0109      WRITE(6,7) TITLE
0110      WRITE(6,56)
0111      WRITE(6,57) (NMW(I),TAVEWT(I),I=1,NN)
0112      30 CONTINUE
0113      GO TO 100
0114      31 CONTINUE
0115      IF(MWH.EQ.0) GO TO 1000
0116      SUMMOL=0.0
0117      DO 86 MO=1,500
0118      SUMMOL=SUMMOL+NMWTPC(2,MO)
0119      DO 86 LN=3,5
0120      86 SUMMOL=SUMMOL+MWTPRC(LN,MO)

```

```
0121      DO 77 MO=1,500
0122          NMWTPC(2,MO)=(NMWTPC(2,MO)/SUMMOL)*100
0123      DO 77 LN=3,5
0124          77 NMWTPC(LN,MO)=(MWTPRC(LN,MO)/SUMMOL)*100
0125          WRITE(6,7) TITLE
0126          WRITE(6,58) (NMWTPC(1,I),NMWTPC(2,I),NMWTPC(3,I),NMWTPC(4,I),NMWTP
            IC(5,I),I=MWL,MWH)
0127          58 FORMAT(1X,F4.0,10X,F10.6,10X,F10.6,10X,F10.6,10X,F10.6,/)
0128      1000 CONTINUE
0129          WRITE(6,11)
0130          11 FORMAT(1H1)
0131          STOP
0132          END
```

VITA <sup>2</sup>

Gil Jay Greenwood

Candidate for the Degree of

Doctor of Philosophy

Thesis: CHARACTERIZATION OF COAL-DERIVED LIQUIDS USING MASS  
SPECTROMETRY

Major Field: Chemistry

Biographical:

Personal Data: Born in Lincoln, Nebraska, on January 10, 1949,  
the son of Mr. and Mrs. K. R. Greenwood, Tulsa, Oklahoma.

Education: Graduate from Tulsa Edison High School, Tulsa,  
Oklahoma in June, 1967; received Bachelor of Science degree  
in Chemistry from Oklahoma State University, Stillwater,  
Oklahoma, July, 1971; completed requirements for the Doctor  
of Philosophy degree at Oklahoma State University in  
May, 1977.

Professional Experience: Graduate Teaching Assistant, Oklahoma  
State University, 1971-1974; Dow Chemical Summer Fellow,  
Summer, 1973; Conoco Oil Company Summer Fellow, Summer,  
1974; Graduate Research Assistant, 1974-1977.

Membership in Honorary and Professional Societies: Phi Lambda  
Upsilon, Honorary Chemical Society; American Chemical  
Society.